



#### DISCLAIMER

This report was prepared as an account of work sponsored by an agency of the United States Government. Neither the United States Government nor any agency thereof, nor any of their employees, makes any warranty, expressed or implied, or assumes any legal liability or responsibility for the accuracy, completeness, or usefulness of any information, apparatus, product, or process disclosed, or represents that its use would not infringe privately owned rights. Reference herein to any specific commercial product, process, or service by trade name, trademark, manufacturer, or otherwise does not necessarily constitute or imply its endorsement, recommendation, or favoring by the United States Government or any agency thereof. The views and opinions of authors expressed herein do not necessarily state or reflect those of the United States Government.

This report has been reproduced directly from the best available copy.

Available to DOE and DOE contractors from the Office of Scientific and Technical Information, P.O. Box 62, Oak Ridge, TN 37831; prices available from (615) 576-8401.

Available to the public from the National Technical Information Service, U.S. Department of Commerce, 5285 Port Royal Rd., Springfield VA 22161

DOE/BC/14936-10  
Distribution Category UC-122

Geologic And Engineering Characterization Of Geraldine Ford Field, Reeves And  
Culberson Counties, Texas

Topical Report  
1997

By  
Shirley P. Dutton  
Mohammad A. Malik  
George B. Asquith  
Mark D. Barton  
Andrew G. Cole  
John Gogas  
Sigrid J. Cliff  
Jose I Guzman

April 1998

Work Performed Under Contract No. DE-FC22-95BC14936

Prepared for  
U.S. Department of Energy  
Assistant Secretary for Fossil Energy

Jerry Casteel, Project Manager  
National Petroleum Technology Office  
P.O. Box 3628  
Tulsa, OK 74101

Prepared by:  
Bureau of Economic Geology  
The University of Texas at Austin  
University Station, Box X  
Austin, TX 78713-7508

## CONTENTS

ABSTRACT .....	1
INTRODUCTION .....	2
General Information .....	3
Project Description .....	3
Summary Field History .....	8
THREE-DIMENSIONAL DESCRIPTION OF RESERVOIR .....	13
Areal and Vertical Description .....	13
Porosity Distribution .....	17
Saturation Distribution .....	17
Permeability Distribution .....	22
Structure .....	27
Net Pay .....	27
Vertical Porosity and Permeability Profiles .....	29
Natural Water Influx .....	33
Geologic Characteristics .....	33
Lithology .....	33
Geologic Age .....	35
Facies Analysis of Ramsey Sandstone .....	35
Mapping of Genetic Units .....	36
Upper Ford Siltstone .....	38
Ramsey 1 Sandstone .....	38
SH1 Siltstone .....	41
Ramsey 2 Sandstone .....	43
Lower Trap Siltstone .....	43
Distribution of Facies .....	45

Channel Facies .....	50
Levee Facies .....	51
Lobe Facies .....	51
Laminated Siltstone Facies .....	52
Lutite Facies .....	52
Proposed Depositional Model for Ford Geraldine Unit .....	53
Characterization of Diagenetic Heterogeneity .....	55
Petrography of Ramsey Sandstones .....	56
Diagenetic Controls on Reservoir Quality .....	58
Evaluation of Reservoir Heterogeneity .....	61
Geophysical Interpretation of the Ramsey Reservoir Using 3-D Seismic Data .....	63
Synthetic Seismograms and Wavelet Extraction .....	66
Structure, Amplitude, and Coherency Cube Maps .....	67
Correlation Coefficients and Cross Plots .....	68
Conclusions .....	70
Fluid Characteristics .....	70
FIELD DEVELOPMENT HISTORY .....	74
Primary Recovery .....	74
Secondary Recovery .....	74
Tertiary Recovery .....	74
FIELD PRODUCTION CONSTRAINTS AND DESIGN LOGIC .....	78
Review of Reservoir Description and Development History .....	78
Constraints on Further Producibility .....	85
Method of Problem Detection .....	86
Proposed Solution for Reduction of Constraints .....	86
Evaluation .....	87
EVALUATION OF COST-SHARE PROJECT RESULTS .....	87

Type of Project.....	87
Simulation Study .....	87
Geostatistical Permeability Modeling .....	88
Data Evaluation .....	88
Autocorrelation .....	88
Permeability Scale-Up .....	93
Estimate of Tertiary Recovery from Production Data .....	94
Simulations of Tertiary Recovery .....	98
Simulation Results .....	101
ENVIRONMENTAL INFORMATION .....	103
CONCLUSIONS .....	105
ACKNOWLEDGMENTS .....	106
REFERENCES .....	107
APPENDIX A .....	113
Summary of electronic data .....	113
Summary of hard-copy data .....	115

### Figures

1. Location of Geraldine Ford and Ford West (4100') fields in Reeves and Culberson Counties, Texas .....	4
2. Status of wells in the Ford Geraldine unit and distribution of core control .....	9
3. Stratigraphic nomenclature of the Delaware Mountain Group in the Delaware Basin subsurface and outcrop areas and time-equivalent formations on the surrounding shelves .....	10
4. Waterflooding of the Ford Geraldine unit took place in five stages, in the areas shown ...	12
5. Typical log from the Ford Geraldine unit well No. 108 .....	15
6. Distribution of geophysical log suites available in Ford Geraldine unit .....	16
7. Distribution of porosity in Ramsey sandstone from 4900 core analyses .....	18

8.	Map of average porosity for the Ramsey sandstone in the Ford Geraldine unit .....	19
9.	Distribution of water saturation in Ramsey sandstone from 4900 core analyses .....	20
10.	Map of water saturation for the Ramsey sandstone in the Ford Geraldine unit .....	21
11.	Map of mobile oil saturation for the Ramsey sandstone in the Ford Geraldine unit.....	23
12.	Distribution of permeability in Ramsey sandstone from 4900 core analyses .....	24
13.	Cross plot of core porosity versus core permeability for the Ramsey sandstone in the Ford Geraldine unit .....	25
14.	Map of geometric mean permeability for the Ramsey sandstone interval, calculated from porosity data from geophysical logs and the core-porosity versus core-permeability transform.....	26
15.	Structure contours on the top of the Lamar limestone dip to the east and northeast .....	28
16.	Map of net pay for the Ramsey sandstone in the Ford Geraldine unit .....	30
17.	Map of thickness of the total Ramsey sandstone interval .....	31
18.	Vertical permeability profiles from core-analysis data for 5 wells in the Ford Geraldine unit .....	32
19.	Vertical porosity profiles from core-analysis data for 5 wells in the Ford Geraldine unit .....	34
20.	Dip cross section A–A' down the length of Geraldine Ford field .....	37
21.	Isopach map of the upper Ford laminated siltstone .....	39
22.	Isopach map of the Ramsey 1 sandstone .....	40
23.	Isopach map of the SH1 laminated siltstone .....	42
24.	Isopach map of the Ramsey 2 sandstone .....	44
25.	Isopach of the lower Trap laminated siltstone .....	46
26.	Cross section B–B' through the northern end of Geraldine Ford field.....	47
27.	Cross section C–C' through the southern part of Geraldine Ford field .....	48
28.	Representative cores of the Ramsey sandstone and bounding Trap and Ford laminated siltstones .....	49
29.	Diagram illustrating depositional model for upper Bell Canyon Formation.....	54
30.	Ramsey sandstones at Geraldine Ford field are arkoses having an average composition of Q <sub>63</sub> F <sub>32</sub> R <sub>5</sub> .....	57

31.	Distribution of porosity and permeability in channel, levee, and lobe facies .....	59
32.	The main controls on porosity and permeability in the Ramsey sandstones are authigenic cements, particularly calcite, and, to a lesser extent, chlorite .....	60
33.	No significant differences exist in the porosity versus permeability relationship in channel, levee, and lobe facies .....	62
34.	Capillary pressure curves and calculated radii of pore throats for Ramsey sandstones .....	64
35.	Outline of the area in which the 3-D seismic survey was acquired .....	65
36.	Plot of average reservoir pressure through time for Geraldine Ford field during the period of primary recovery .....	73
37.	Plots of primary, secondary, and tertiary production in the Ford Geraldine unit, and volumes of water and CO <sub>2</sub> injected .....	75
38.	Map of primary recovery for the Ramsey sandstone in the Ford Geraldine unit .....	76
39.	Map of secondary production resulting from the waterflood conducted from 1969 to 1980 .....	77
40.	Map of tertiary production through 1995 resulting from the CO <sub>2</sub> flood that started in 1981 .....	79
41.	Map of total production from the Ford Geraldine unit through 1995 .....	80
42.	Map of the percentage of water produced during initial potential tests .....	82
43.	Map of water cut at the end of primary production in 1969 .....	83
44.	Cumulative distribution function of core-analysis permeability for 21 wells in the demonstration area .....	89
45.	Vertical semivariograms for core-analysis permeability for wells FGU 6, 7, and 15 in the demonstration area, and the average for all three wells .....	91
46.	Map of demonstration area and location of wells used to generate the 3-D permeability distribution .....	92
47.	Cumulative distribution functions of permeability from fine-scale permeability distribution, scaled-up permeability distribution, and permeability data from core analyses .....	95
48.	Original oil in place in waterflood areas 1 through 5 .....	96
49.	Primary, secondary, primary + secondary, tertiary, and total recovery through December, 1995 as a percentage of original oil in place in areas 1 through 5 .....	97
50.	Primary, secondary, and tertiary recovery for all Ford Geraldine unit except area 5 .....	99
51.	Primary and secondary recovery and project tertiary recovery for area 5 .....	100

52.	Results of simulation of a CO <sub>2</sub> flood in a quarter five-spot injection pattern in the demonstration area oil recovery as a fraction of remaining oil in place, and surface oil production rates .....	102
53.	Results of simulation of a CO <sub>2</sub> flood in a quarter five-spot injection pattern in the demonstration area: surface water/oil ratio and surface gas/oil ratio .....	104

#### Tables

1.	General information about Geraldine Ford field .....	5
2.	Areal and vertical description of reservoir .....	14
3.	Highest correlation coefficients calculated from the data set of seismic attributes cross plotted with various rock properties .....	69
4.	Fluid characteristics of reservoir .....	71
5.	Reservoir pressure and fluid properties .....	72
6.	Highest correlation coefficients calculated from the data set of petrophysical parameters cross plotted with total recovery from Ford Geraldine unit wells through 1995 .....	84

## ABSTRACT

The objective of this Class III project is to demonstrate that detailed reservoir characterization of clastic reservoirs in basinal sandstones of the Delaware Mountain Group in the Delaware Basin of West Texas and New Mexico is a cost-effective way to recover more of the original oil in place by strategic infill-well placement and geologically based field development. The study focused on Geraldine Ford field, which produces from the upper Bell Canyon Formation (Ramsey sandstone). Geraldine Ford field is located in Reeves and Culberson Counties, Texas. The field was unitized in 1968 and is operated by Conoco, Inc., as the Ford Geraldine unit; it contains an estimated 99 million barrels (MMbbl) of original oil in place.

Petrophysical characterization of the Ford Geraldine unit was accomplished by integrating core and log data and quantifying petrophysical properties from wireline logs. Core-porosity to log-data transforms and core-porosity to core-permeability transforms were derived for the reservoir. The petrophysical data were used to map porosity, permeability, net pay, water saturation, mobile oil saturation, and other reservoir properties.

Core descriptions, subsurface mapping, and study of an outcrop analog indicate that reservoir sandstones at the Ford Geraldine unit were deposited in a channel-levee and lobe system. Ramsey sandstone channels are about 1,200 ft wide and 15 to 35 ft thick, and they are flanked by levee deposits. Lobe facies were deposited at the mouth of channels. Uniform grain size in the sediment source area resulted in channel, levee, and lobe facies having similar porosity and permeability relationships. The main control on reservoir quality in these sandstones is the volume of authigenic calcite and chlorite. Calcite cement occurs in all facies but is more abundant near the top and base of sandstones.

Interpretation of the 3-D seismic volume indicates that Ramsey sandstone thickness in the Ford Geraldine unit is  $\leq 1/4$  wavelength of the seismic data. The coherency cube is effective in delineating the field outline, and a residual map of the top of the Lamar Limestone identified a

residual high that is associated with Ramsey sandstone thickness. The amplitude family of attributes had the highest correlations with the reservoir properties of average porosity and porosity  $\times$  thickness.

Once the reservoir-characterization study was completed, a demonstration area of approximately 1 mi<sup>2</sup> in the northern part of the unit was chosen for reservoir modeling/simulation. To estimate the tertiary recovery potential of the demonstration area, flow simulations were performed for a CO<sub>2</sub> flood. A quarter of a five-spot injection pattern in the demonstration area was selected for flow simulations, and two cases of permeability distribution were considered, one using stochastic permeability distribution generated by conditional simulation and the other using layered permeabilities. Flow simulations were performed using UTCOMP, an isothermal, three-dimensional, compositional simulator for miscible gas flooding. Results indicate that 10 to 30 percent (1 to 3 MMbbl) of remaining oil in place in the demonstration area can be produced by CO<sub>2</sub> injection.

## INTRODUCTION

This report summarizes information developed about Geraldine Ford field during the first phase of a study sponsored by the U.S. Department of Energy. The objective of this DOE Class III project is to demonstrate that detailed reservoir characterization of clastic reservoirs in basinal sandstones of the Delaware Mountain Group in the Delaware Basin of West Texas and New Mexico is a cost-effective way to recover more of the original oil in place by strategic infill-well placement and geologically based field development. Reservoirs in Geraldine Ford and other Delaware Mountain Group fields have low producibility (average recovery <14 percent of the original oil in place) because of a high degree of vertical and lateral heterogeneity caused by depositional processes and post-depositional diagenetic modification.

The study characterized Geraldine Ford field, which produces from the upper Bell Canyon Formation (Ramsey sandstone), and compared it with Ford West field, which produces from the Cherry Canyon Formation. Geraldine Ford field was the main focus of the project because it has

more data available and a higher volume of oil in place than Ford West field, making it the more attractive target for enhanced recovery. This report summarizes the reservoir characterization and production history of Geraldine Ford field.

### General Information

Geraldine Ford field is located 2 mi south of the Texas-New Mexico state line in Reeves and Culberson Counties, Texas (fig. 1). The field, which was discovered in 1956, is in Railroad Commission of Texas District 8. The field was unitized in 1968 and is operated by Conoco, Inc. as the Ford Geraldine unit (table 1). The unit contains an estimated 99 million barrels (MMbbl) of original oil in place (Pittaway and Rosato, 1991).

### Project Description

The goal of the study is to demonstrate that reservoir characterization, utilizing 3-D seismic data and other techniques, and integrated with reservoir simulation can optimize infill drilling and Enhanced Oil Recovery (CO<sub>2</sub> flood) projects. The project will thus increase production and prevent premature abandonment of slope and basin clastic reservoirs in mature fields in the Delaware Basin, West Texas.

Geraldine Ford and Ford West fields produce from slope and basin clastic reservoirs in the Delaware Basin, which is part of the Permian Basin of West Texas. Geraldine Ford field, which produces from the Bell Canyon Formation, has undergone primary, secondary (waterflood), and tertiary (CO<sub>2</sub> flood) recovery in part of the field. Field development was designed without benefit of a detailed reservoir characterization study, and thus an understanding of geologically controlled reservoir heterogeneity was not incorporated into previous production practices. Because of serious producibility problems—inadequate reservoir characterization, poor sweep efficiency, and reservoir heterogeneity—recovery efficiency at Geraldine Ford field is only 26 percent. Unless new ideas and approaches that incorporate an understanding of the geologic complexity of slope

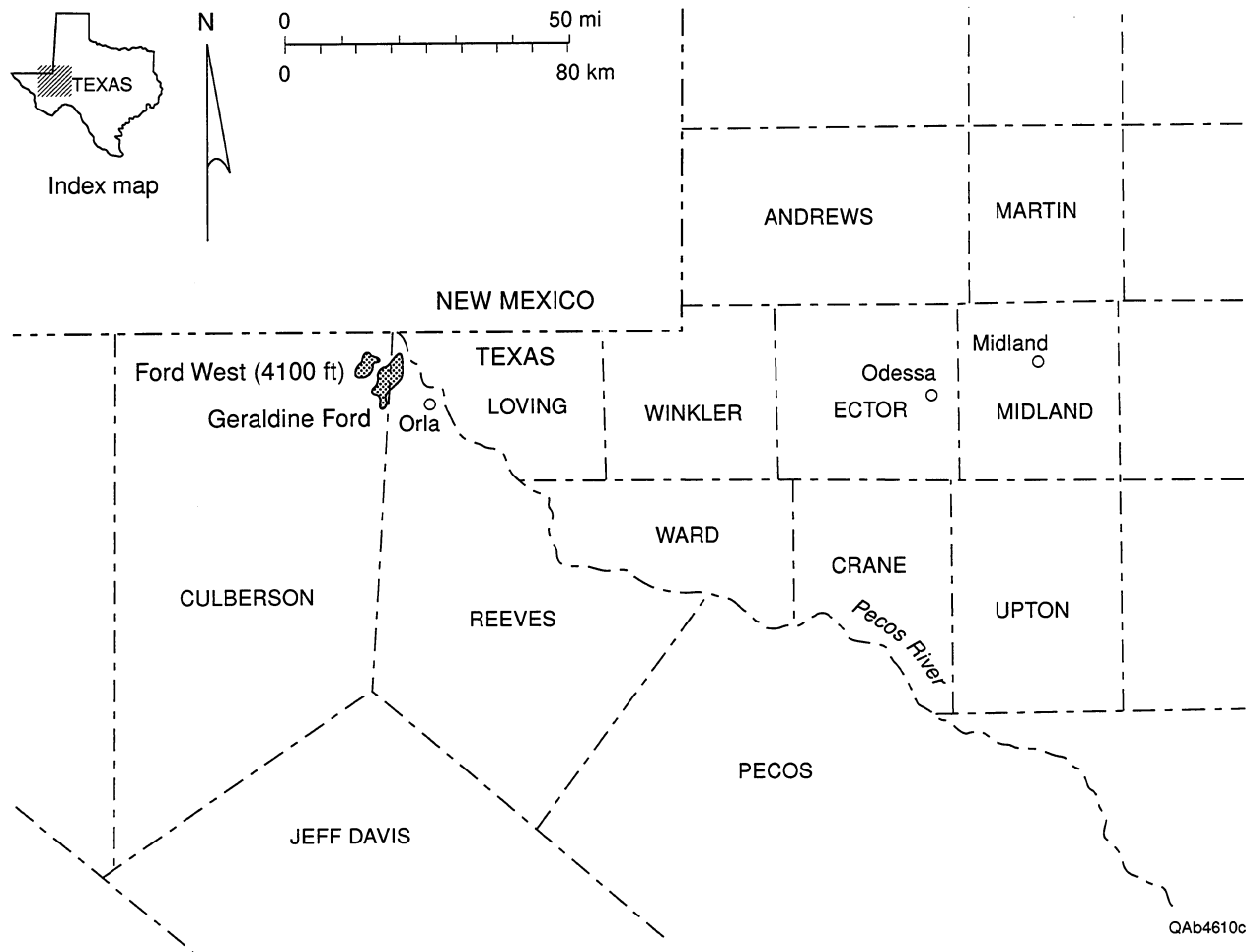


Figure 1. Location of Geraldine Ford and Ford West (4100') fields in Reeves and Culberson Counties, Texas.

Table 1. General information about Geraldine Ford field

Field Name  
Geraldine Ford

Unit Name  
Ford Geraldine

Reservoir Name  
Ramsey sandstone

State  
Texas

Counties  
Culberson and Reeves

Formation  
Bell Canyon

Railroad Commission District of Texas  
8

Field Discovery Date  
April 14, 1956

Current Operator  
Conoco, Inc.

Current working interest ownership (>10%)  
Continental Oil Company (45.006%)  
Humble Oil and Refining Company (10.008%)  
Sun Oil Company (13.967%)  
Texaco Inc. (21.0385%)

Project Team Members  
Bureau of Economic Geology  
The University of Texas at Austin  
University Station, Box X  
Austin, TX 78713

Conoco, Inc.  
10 Desta Drive  
Suite 100 West  
Midland, TX 79701

Technical Contact  
Dr. Shirley P. Dutton  
Bureau of Economic Geology  
The University of Texas at Austin  
University Station, Box X  
Austin, TX 78713  
(512) 471-0329

Primary Drive Mechanism  
Pressure depletion (solution gas drive) assisted by natural water drive

Estimated primary recovery factor  
18%

Estimated incremental secondary recovery factor  
4.5

Estimated total of primary and secondary recovery (%)  
22.5%

Date of first production  
April 29, 1956

Number of wells drilled in field  
340

Well patterns  
5-spot

Number of wells penetrating reservoir  
340

Total completions to date in field  
334

Total current completions  
210

Total current producers  
122

Total current injection wells  
88

Number of flowing wells  
None

Project location

Within Culberson County, Texas, T&P Block 58, T-1, all or parts of sections 26, 34, 35, 38, 39, 46, and 47; T-2, parts of sections 2 and 3.

Within Reeves County, Texas, T&P Block 57, T-1, all or parts of sections 13, 17, 18, 19, 24, 25, 26, 30, 31, 35, 36, 37, and 38 (see fig. 2).

and basin clastic reservoirs are applied to this large field, much of the remaining oil will not be recovered.

Phase I of this project involved integrated reservoir characterization studies of both Geraldine Ford field and the smaller Ford West field, which produces from the Cherry Canyon Formation and is still under primary recovery. This comparative study will provide a detailed understanding of the architecture and heterogeneity of each field and allow comparison of Bell Canyon and Cherry Canyon reservoirs. Geraldine Ford and Ford West fields produce from the most prolific horizons in the Bell and Cherry Canyon Formations, and the proposed reservoir characterization study will provide insights that are applicable to these zones in other fields in the basin.

The following technologies were used for reservoir characterization:

- 3-D seismic
- Subsurface log, core, and petrophysical study
- High resolution sequence stratigraphy
- Mapping and petrophysical study of nearby outcrops
- Petrography
- Analysis of production history
- Geostatistical analysis of interwell heterogeneity

Once the comparative reservoir-characterization study of both fields was completed, a pilot area of approximately 1 mi<sup>2</sup> in Geraldine Ford field was chosen for reservoir modeling/simulation. On the basis of the results of the reservoir characterization and simulation, the economic and technical feasibility of conducting the Phase II demonstration activities in the pilot area will be assessed.

Phase II will apply the knowledge gained from reservoir-characterization and simulation studies to increase recovery from the pilot area. A geologically designed, enhanced-recovery program (CO<sub>2</sub> flood, waterflood, or polymer flood) and well-completion program will be developed, and one to three infill wells will be drilled and cored. The infill well(s) will be drilled into untapped reservoir compartments in an area that also has deeper pool potential, most likely along the field margins. The Phase I studies will guide the drilling program design, so that

borehole connectivity with prospective sandstone lenses will be optimized. The goal of the infill drilling program is to demonstrate that economically significant unrecovered oil remains in geologically resolvable untapped compartments. The infill well(s) will also be part of a new geologically designed enhanced recovery project (most likely a CO<sub>2</sub> flood) to be installed in the pilot area. Design of this new flood will be guided by the results of Phase I, and detailed comparison will be made between production from the pilot area during the CO<sub>2</sub> flood and the predictions that were made during Phase I based on flow-model simulations. This comparison will provide an important opportunity to test the accuracy of reservoir-characterization and flow-simulation studies as predictive tools in resource preservation of mature fields.

Through technology transfer, the knowledge gained in the comparative study of these two fields, with 89 MMbbl of remaining oil in place, can then be applied to increase production from the more than 100 other Delaware Mountain Group reservoirs in West Texas and New Mexico, which together contain 1,558 MMbbl of remaining oil. In addition, the development and transfer of advanced reservoir characterization techniques provide an opportunity for increasing oil recovery from two other major slope and basin clastic plays in the Permian Basin. The volume of oil to which these technologies can be extended exceeds 10 billion stock-tank barrels of mobile and residual oil.

### Summary Field History

Geraldine Ford field is located in Reeves and Culberson Counties, Texas (fig. 1). It contains an estimated 99 million barrels (MMbbl) of original oil in place (Pittaway and Rosato, 1991). There are currently 122 producer and 88 injector wells in the field (fig. 2; table 1). Cumulative production to date is 28.0 MMbbl. Oil gravity is 40° (API), and viscosity is 0.77 cp at 82° F and 1,380 psi. Average current reservoir pressure is 1500 psi. There is no field-wide oil-water contact (Ruggiero, 1985).

Geraldine Ford field was discovered in 1956 from reservoirs in the upper Bell Canyon Formation (fig. 3). Well completions typically included hydraulic fracturing and acidizing. By the

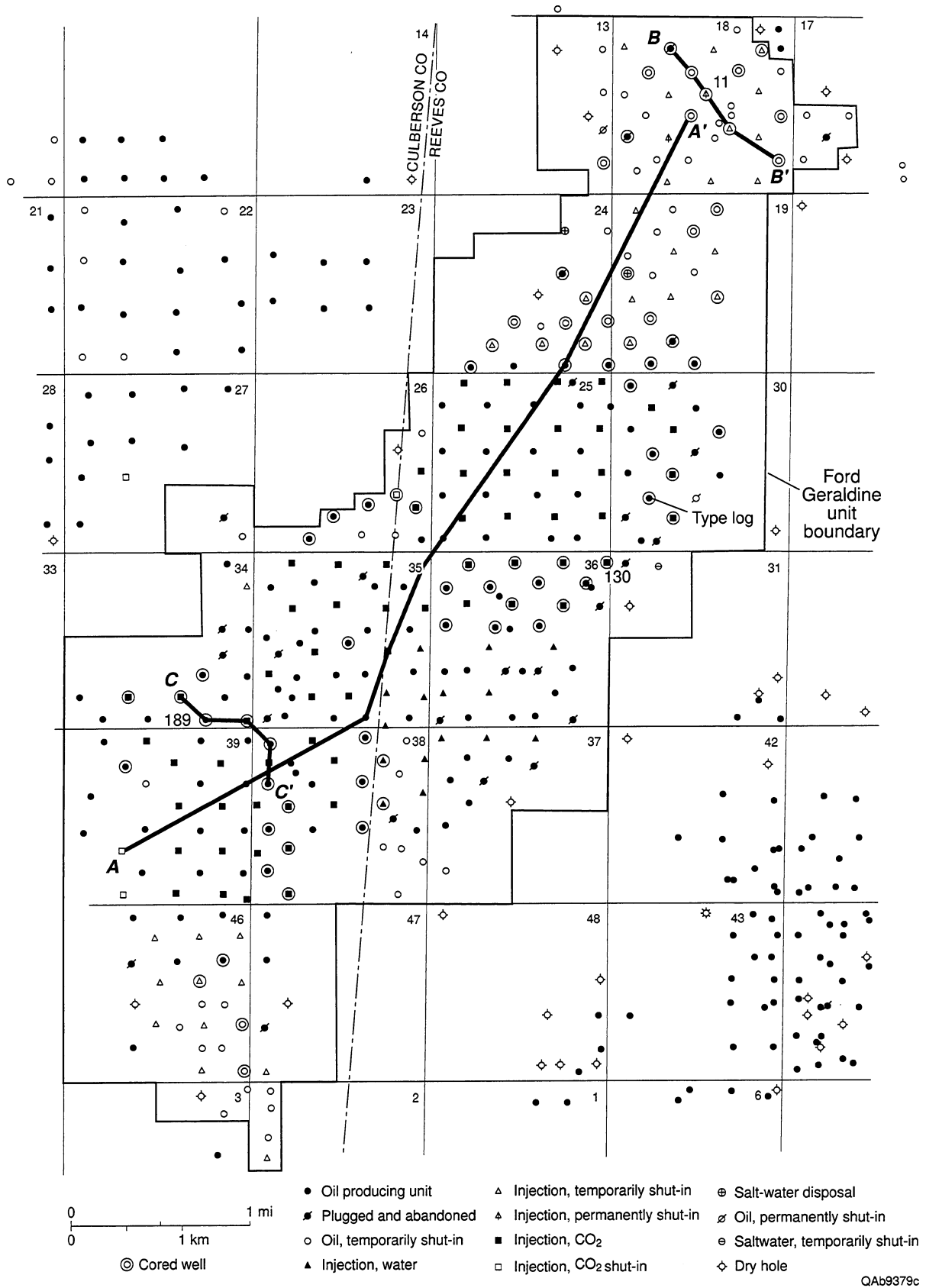


Figure 2. Status of wells in the Ford Geraldine unit and distribution of core control. Type log is shown in figure 5, cross section A–A' in figure 20, cross section B–B' in figure 26, and C–C' in figure 27. Core descriptions of the three wells identified by number (11, 130, and 189) are shown in figure 28.



end of 1959 most of the field had been developed on a 20-acre spacing, and reservoir pressure had declined to bubble point (1383 psi), resulting in a sharp increase in gas-oil ratio and water production (Ruggiero, 1985, 1993). Reduced pressures initially aided high production rates as gases dissolved in the oil came out of solution, but also produced local gas caps within compartments in the reservoir. By 1968, reservoir pressure had dropped to 300 to 500 psi. The solution-gas drive was assisted by a natural water drive prior to waterflooding (Conoco, 1979). The field was unitized (into the Ford Geraldine unit) for secondary development after primary cumulative production of 13.2 MMbbl.

Secondary development was initiated in 1969, with reservoir pressure increased to nearly 1400 psi for a planned five-stage waterflood (Ruggiero, 1985, 1993). A pilot waterflood was started in 1969 in area 1 (fig. 4). Injection patterns were geometric 5-spots. The waterflood was then extended to the entire field in the five stages marked in figure 4. The proposed demonstration area for the Class III project was waterflooded in stage 5 for a very short time in 1980. Secondary recovery of 2,875 bopd peaked in 1975. By 1981, recovery rates dropped to 569 bopd, and water cuts had risen to 95 percent of production. An additional 6.8 MMbbl of oil was produced after unitization, but only 3.5 MMbbl was attributed to the waterflood, significantly less than the amount predicted from reservoir simulation. By the end of secondary development, recovery efficiency had increased to only 22.5 percent. Of that, 18 percent is attributed to primary recovery and 4.5 percent to secondary recovery (Pittaway and Rosato, 1991).

In 1981, tertiary recovery by CO<sub>2</sub> injection began in the central part of the reservoir and was gradually expanded to include most of the unit. The same patterns used in the waterflood were used in the CO<sub>2</sub> flood. However CO<sub>2</sub> flooding was never implemented in the proposed demonstration area (area 5 of figure 4). The CO<sub>2</sub> supply was erratic until the end of 1985. Production response occurred in 1986 after increased and constant CO<sub>2</sub> injection began in December 1985 (Pittaway and Rosato, 1991). Before CO<sub>2</sub> flooding, production was down to 300 bopd; by 1991 production had increased to nearly 2,000 bopd.

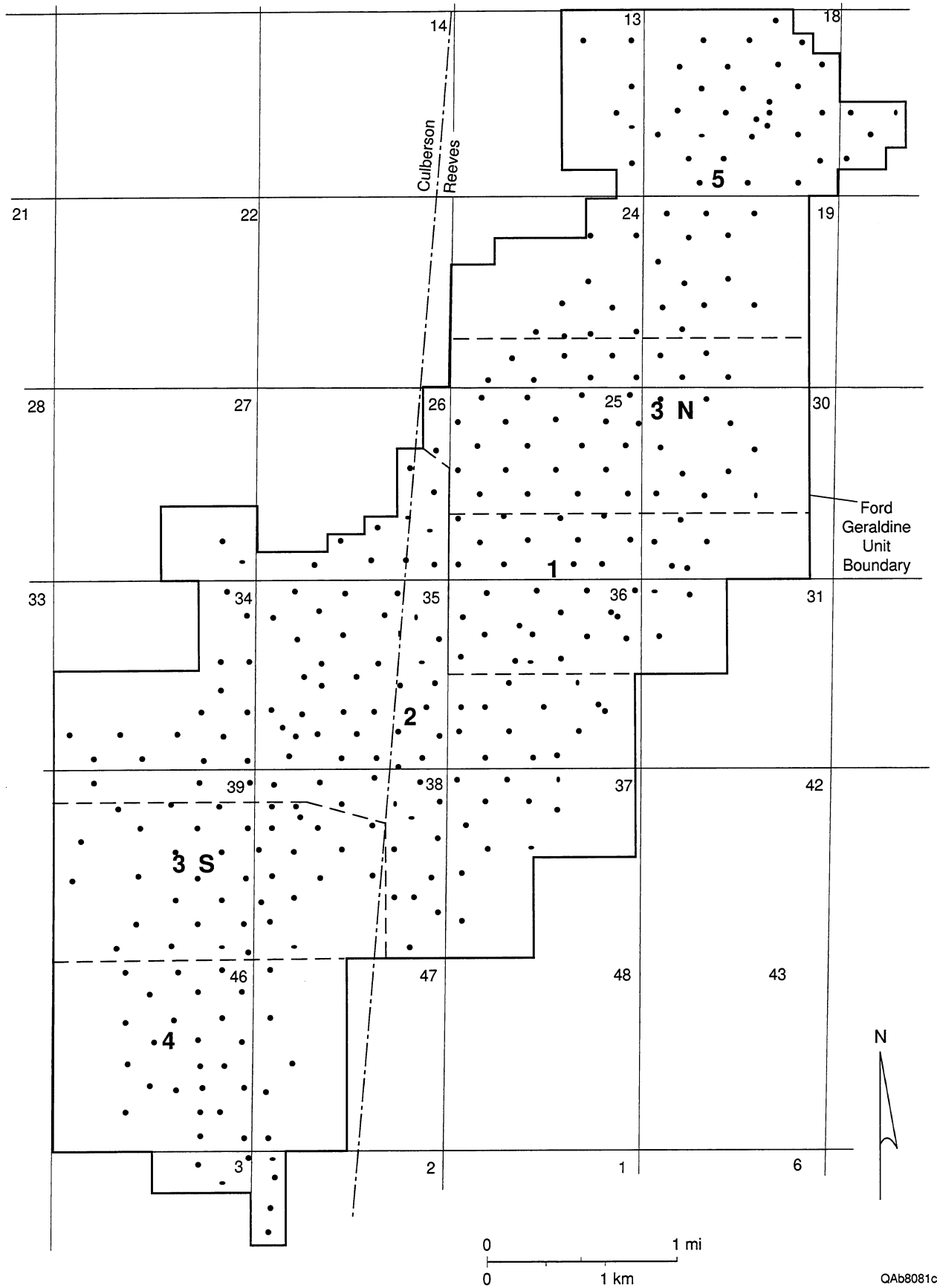


Figure 4. Waterflooding of the Ford Geraldine unit took place in five stages, in the areas shown.

Effective reservoir sweep was reduced by early CO<sub>2</sub> breakthrough. Injected CO<sub>2</sub> ponded near the structural axis of the field, with CO<sub>2</sub> ineffective at mobilizing oil from more heterogeneous strata along the flanks (Ruggiero, 1985, 1993). To alleviate early CO<sub>2</sub> breakthrough, production rates were balanced and reservoir pressures were maintained above 900 psi, the minimum pressure needed for miscibility. Average reservoir pressure on January 1, 1997 was 1500 psi. Cumulative tertiary production to date has been 5.7 million barrels, and tertiary recovery efficiency is 5.8 percent (K. R. Pittaway, written communication, 1997). Estimated ultimate tertiary recovery is 9.0 percent.

### THREE-DIMENSIONAL DESCRIPTION OF RESERVOIR

#### Areal and Vertical Description

Ford Geraldine unit includes 8,540 acres (table 2). The main reservoir at Geraldine Ford field is the Ramsey sandstone, but there is also some production from the underlying Olds sandstone (fig. 5). Ramsey sandstone is a 0- to 60-ft-thick sandstone that is bounded by the Ford and Trap laminated siltstones. In the northern part of the Ford Geraldine unit, the Ramsey is divided into two sandstones (Ramsey 1 and Ramsey 2) separated by a 1- to 3-ft-thick laminated siltstone (SH1) (Ruggiero, 1985). In the southern part of the Ford Geraldine unit, only the Ramsey 1 sandstone is present.

An excellent subsurface data base for reservoir characterization is available for the Ford Geraldine unit. Logs were available from 305 of the 340 wells in the field, most commonly gamma ray or gamma ray and neutron logs (fig. 6). Porosity logs were available from 182 wells, but only 38 wells have both porosity and resistivity logs (fig. 6). A total of 3,615 ft of core from the Ramsey sandstone and adjacent siltstones from 70 wells was available for the project, and these data were supplemented by Ruggiero's descriptions (1985) of 681 ft of core from 13 additional wells. Core analyses (permeability, porosity, water saturation, and oil saturation) from 4,900 samples from 152 wells throughout the Ford Geraldine unit were entered into a spreadsheet.

## Table 2. Areal and vertical description of reservoir

### Areal extent

Ford Geraldine Unit is 8540 acres

### Porosity mean

22.0%

### Original saturation mean at discovery

Oil 52.3%

Water 47.7%

### Current saturation mean

Average fieldwide oil saturation after waterflood = 38%

Average fieldwide water saturation after waterflood = 62%

### Permeability mean

38.4 md (arithmetic average)

16.2 md (geometric mean)

### Directional permeability (Kv/Kh)

0.01

### Reservoir dip

0.7° to the northeast

### Average net pay thickness

25 ft

### Average gross pay thickness

31 ft

### Number of reservoir layers

Two: Ramsey 1 and Ramsey 2

Ford Geraldine Unit No. 108

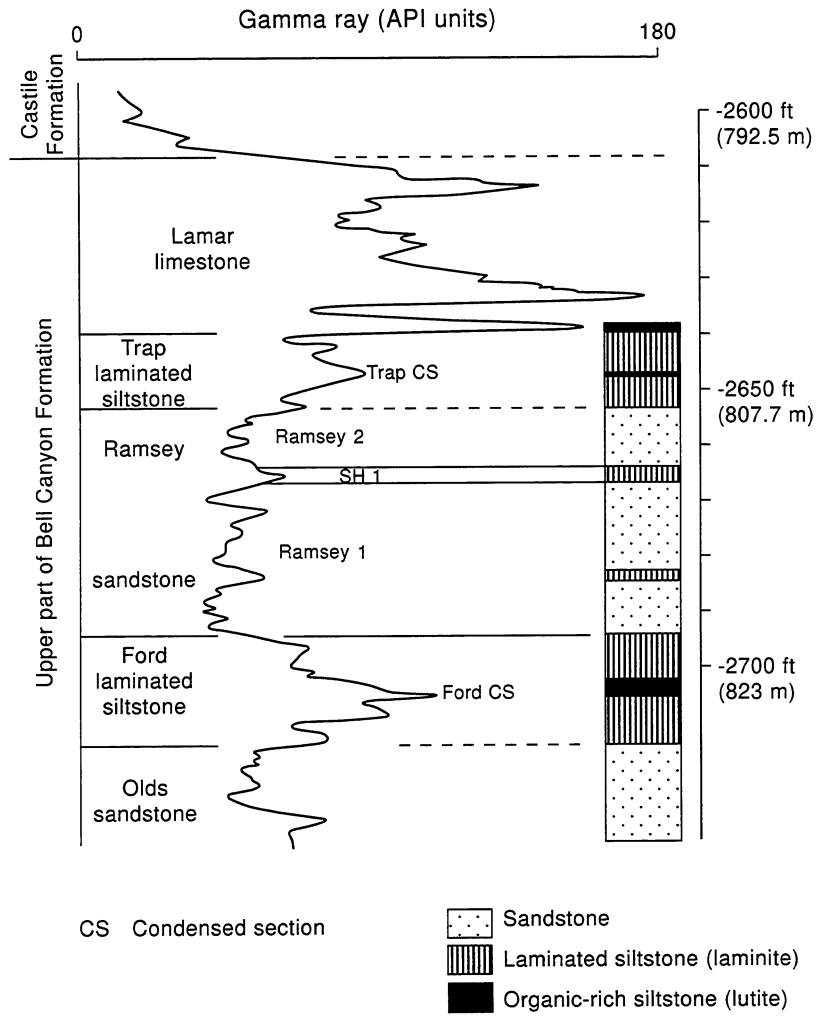


Figure 5. Typical log from the Ford Geraldine unit well No. 108 (modified from Ruggiero, 1985). Well location is shown in figure 2.

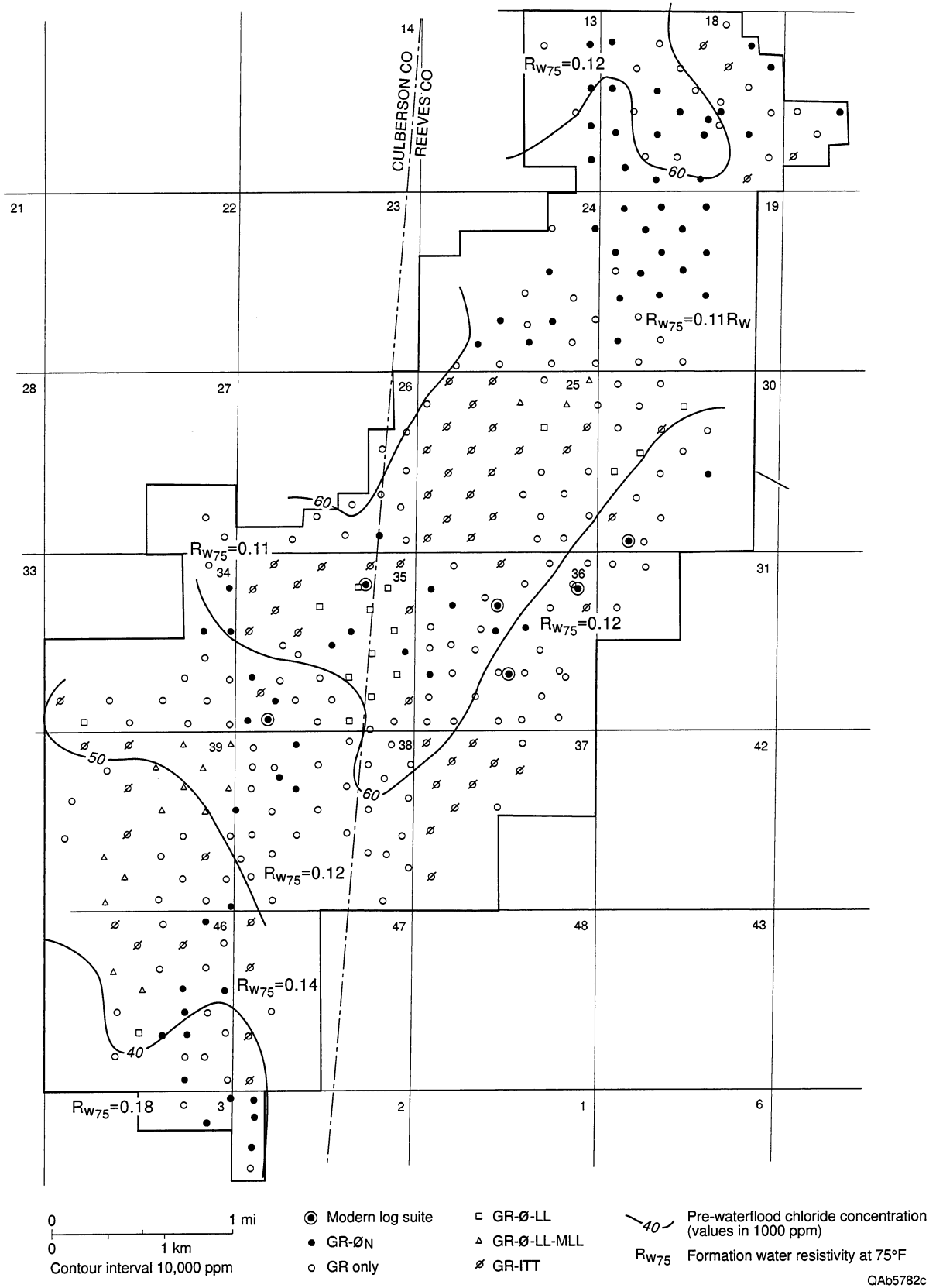


Figure 6. Distribution of geophysical log suites available in Ford Geraldine unit. Map also shows prewaterflood water-salinity distribution and formation-water resistivities ( $R_w$ ) at 75°F for the Ford Geraldine unit. Water-salinity distribution from Ruggiero, 1985.

Areal mapping of reservoir properties across the field was accomplished using geophysical logs and core-porosity to log-data transforms and core-porosity to core-permeability transforms.

### Porosity Distribution

Average porosity in the Ramsey interval (Ramsey 1 and Ramsey 2 sandstone and the SH1 siltstone) is 22.0 percent (fig. 7, table 2), as determined by 4900 core analyses. Standard deviation is 4.1 percent. Areal distribution of porosity was mapped from geophysical log data using core-log porosity transforms (Asquith and others, in press; Dutton and others, 1997). The map of average porosity (fig. 8) for the Ramsey sandstone in the Ford Geraldine unit exhibits a general northeast-southwest trend of high porosity, but the areas of highest porosity values are broken up.

### Saturation Distribution

Water saturation ( $S_w$ ) at field discovery averaged 47.7 percent, well above the irreducible water saturation of 35 percent (Pittaway and Rosato, 1991). Most wells produced some water at discovery. Average  $S_w$ , measured in 4900 core analyses of the Ramsey interval, was 46.4 percent (fig. 9); standard deviation was 10.1 percent. Areal distribution of  $S_w$  was mapped from geophysical log data (Dutton and others, 1997). Average  $S_w$  calculated from log data was 52 percent and standard deviation was 10 percent. A map of average bulk volume water (BVW) was constructed in order to determine  $S_w$  northeast of sections 25 and 30, where no resistivity logs were run (fig. 6). To obtain  $S_w$  in the northeast part of the unit, average BVW values were extrapolated to the northeast, and BVW values assigned to wells with porosity logs. After water saturations were calculated in these wells by the formula  $S_w = BVW_{ave}/\phi$ , these  $S_w$  values were averaged and mapped (fig. 10). The  $S_w$  map shows an increase to the northeast, which is to be expected because that direction is structurally downdip.

No gas cap was originally present in the field, so oil saturation at field discovery was  $1.0 - S_w$ . For an average  $S_w$  of 47.7 percent, average oil saturation was 52.3 percent. Mobile oil

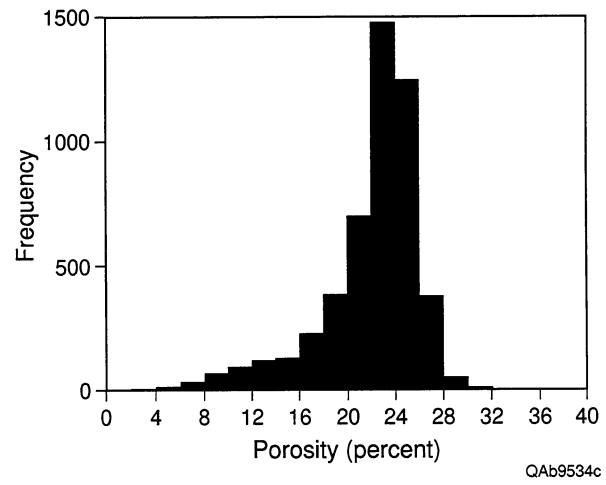
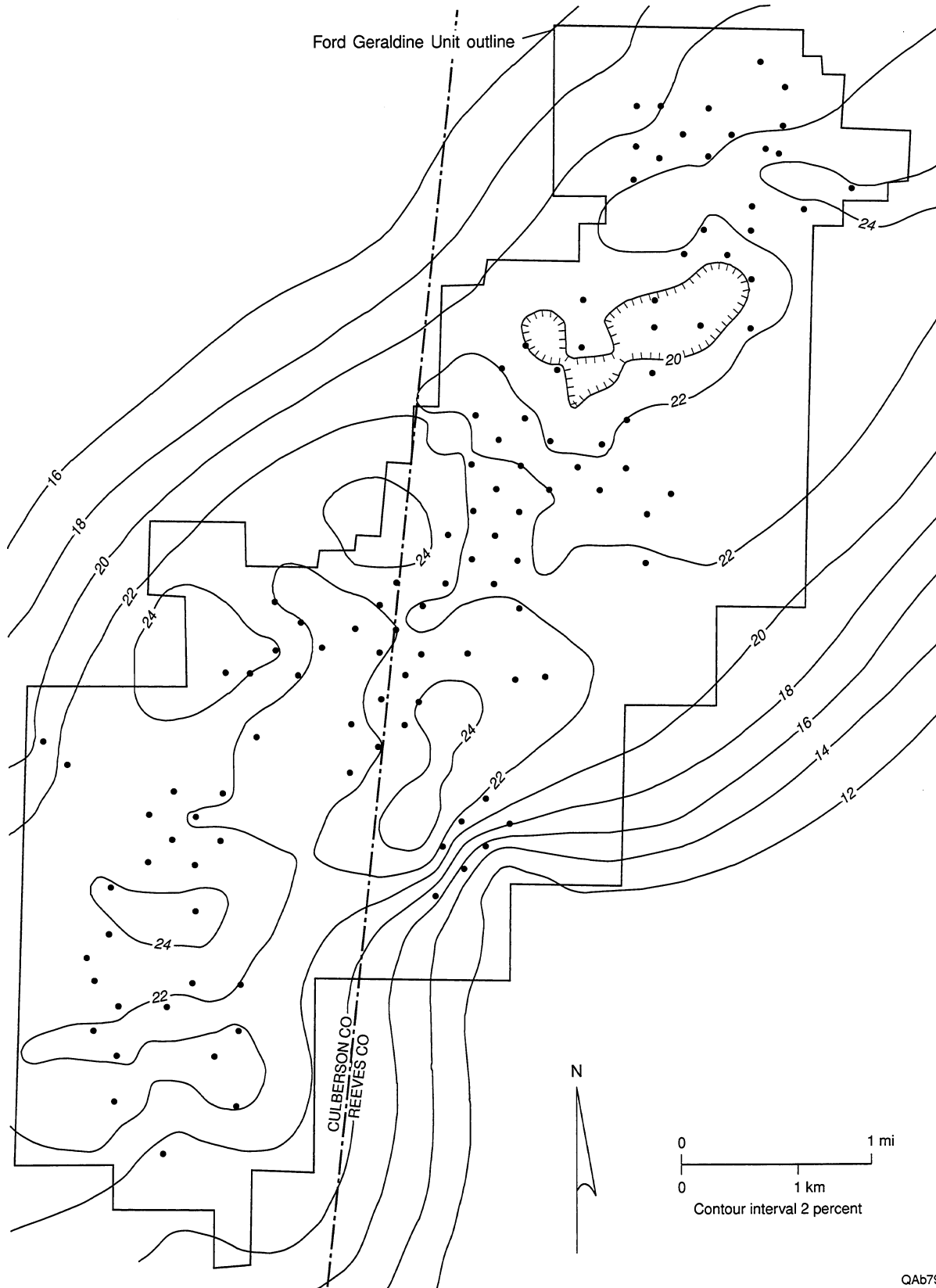


Figure 7. Distribution of porosity in Ramsey sandstone from 4900 core analyses.



QAb7922c

Figure 8. Map of average porosity for the Ramsey sandstone in the Ford Geraldine unit, Reeves and Culberson Counties, Texas. The porosities were determined by core-log porosity transforms (Asquith and others, in press; Dutton and others, 1997).

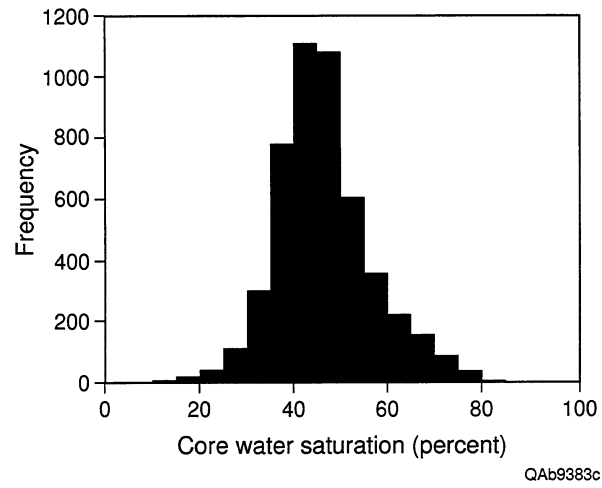
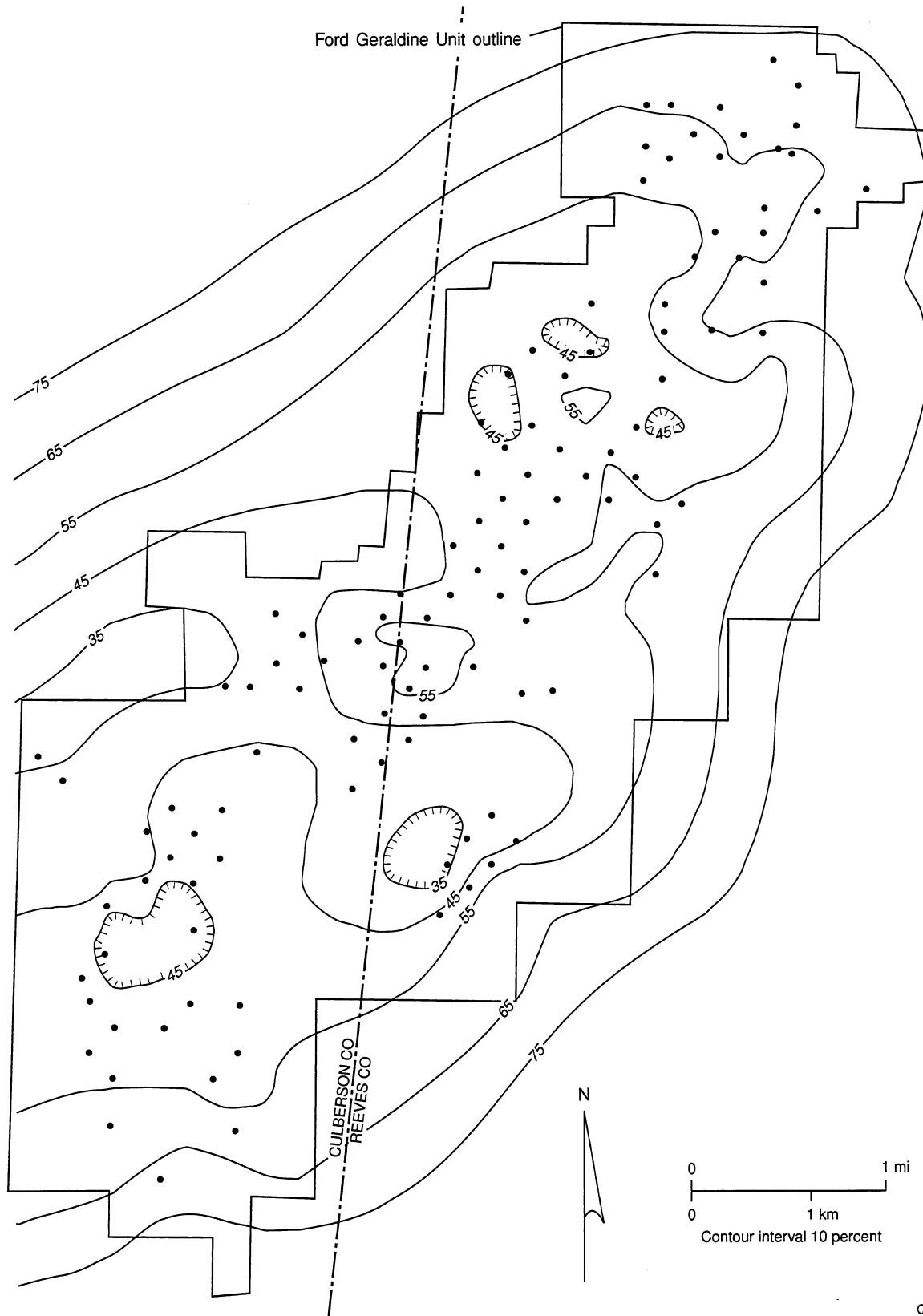


Figure 9. Distribution of water saturation in Ramsey sandstone from 4900 core analyses.



QA7515c

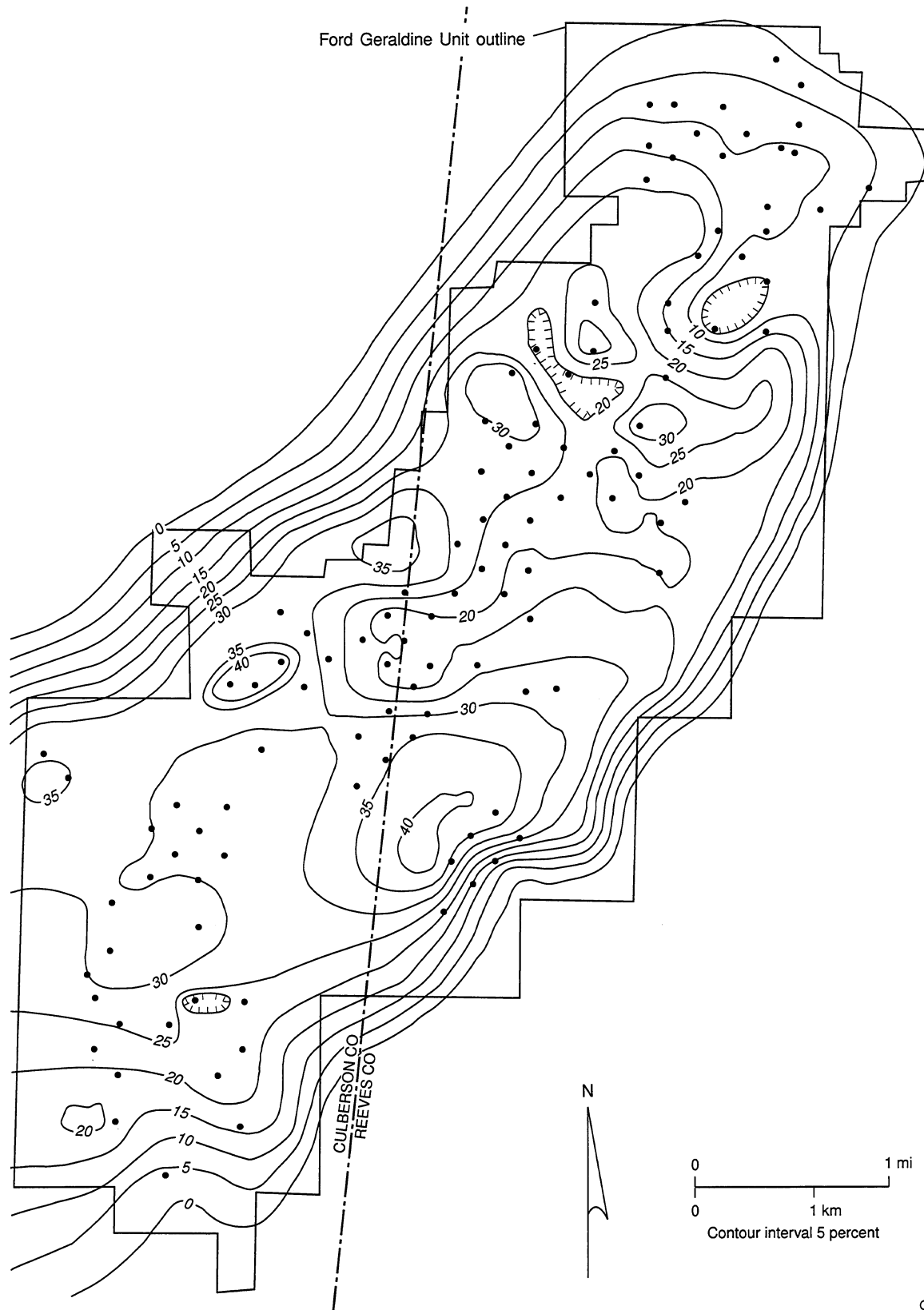
Figure 10. Map of water saturation ( $S_w$ ) for the Ramsey sandstone in the Ford Geraldine unit, Reeves and Culberson Counties, Texas. The water saturations ( $S_w$ ) in the northeast part of the unit were calculated from the average bulk volume water (BVW) values by the formula  $S_w = BVW_{avg}/\phi$ .

saturations (MOS) were calculated from log data by the formula  $MOS = (1.0 - S_w) - ROS$ . The values for residual oil saturation (ROS) were calculated using the following porosity–ROS transform:  $ROS = -0.74 (\text{porosity}) + 41.41$  (Dutton and others, 1997). Average MOS calculated from log data was 22 percent and standard deviation was 10 percent. Average ROS calculated from log data was 25 percent and standard deviation was 1 percent. The MOS map has high MOS values concentrated to the southwest (updip) and in the central portions of the Ford Geraldine unit (fig. 11).

Average fieldwide oil saturation after waterflood was 38 percent, and average fieldwide water saturation was 62 percent (Conoco, 1979). These averages are the best estimates available of saturation distribution at the inception of the DOE cost-share project in the stage 5 area at the northern end of the Ford Geraldine unit. Data are not available to map current saturation distribution.

### Permeability Distribution

Arithmetic average permeability in the Ramsey interval (Ramsey 1 and Ramsey 2 sandstone and the SH1 siltstone) is 38.4 md (table 2), as determined by 4900 core analyses. Standard deviation is 43.5 md. Geometric mean permeability of the Ramsey interval is 16.2 md, with a standard deviation of 6.3 md (fig. 12). The ratio of vertical to horizontal permeability ( $K_v/K_h$ ) is 0.01. Areal distribution of permeability was mapped from geophysical log data using a core-porosity-to-permeability transform together with core-porosity-to-log-porosity transforms (Asquith and others, in press; Dutton and others, 1997). A subset of the total core data, consisting of 1,146 core analyses from wells with porosity logs, was used for the core-porosity-to-permeability transform (fig. 13). The map of geometric mean permeability determined from log data (fig. 14) for the Ramsey sandstone in the Ford Geraldine unit shows that some of the highest average permeability occurs along the margins of the field, in what is interpreted to be a levee facies (see section on Distribution of Facies). Some areas of lower permeability occur near the center of the field.



QAb7919c

Figure 11. Map of mobile oil saturation (MOS) for the Ramsey sandstone in the Ford Geraldine unit, Reeves and Culberson Counties, Texas. Higher values of MOS occur in the southwest part of the unit, which is structurally high.

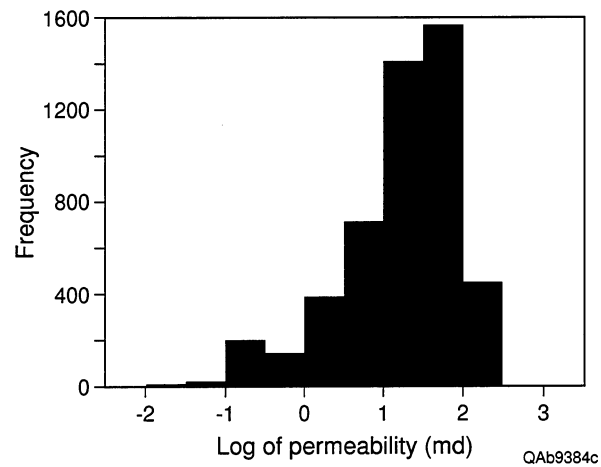


Figure 12. Distribution of permeability in Ramsey sandstone from 4900 core analyses. The mean of the log-permeability values is 1.21, thus the geometric mean permeability of the Ramsey sandstone is 16.2 md ( $10^{1.21} = 16.2$ ).

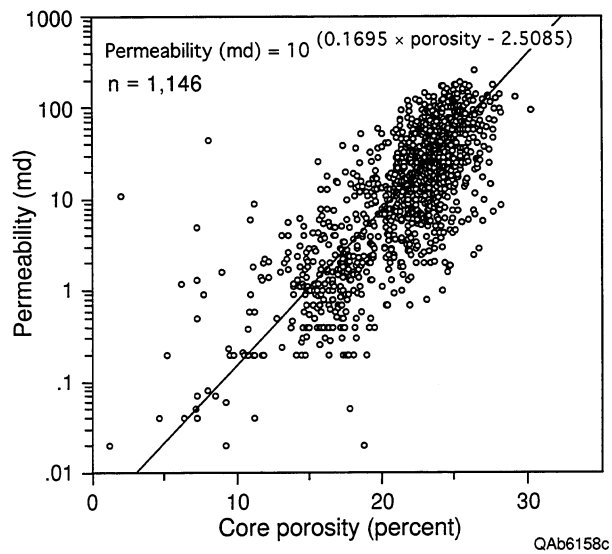


Figure 13. Cross plot of core porosity versus core permeability for the Ramsey sandstone in the Ford Geraldine unit, Reeves and Culberson Counties, Texas. A subset of the total core data, consisting of 1,146 core analyses from wells with porosity logs, was used in this plot and for the core-porosity versus core-permeability transform.



## Structure

The Ramsey sandstone at Ford Geraldine unit dips  $0.7^\circ$  to the northeast (fig. 15, table 2), almost directly opposite original depositional dip because Late Cretaceous movement associated with the Laramide Orogeny tilted the Delaware Basin eastward (Hills, 1984). No faults are interpreted to cut the Ramsey sandstone at the Ford Geraldine unit. Production from Geraldine Ford field and other upper Bell Canyon fields in the Delaware Basin occurs from the distal (southwest) ends of east-dipping, northeast-oriented linear trends of thick Ramsey sandstone deposits. Most hydrocarbons in these fields are trapped by stratigraphic traps formed by an updip lateral facies change from high-permeability reservoir sandstones to low-permeability siltstones. Several of the fields, including Geraldine Ford, show minor structural closure because linear trends of thick sandstones formed compactional anticlines by differential compaction during burial (Ruggiero, 1985).

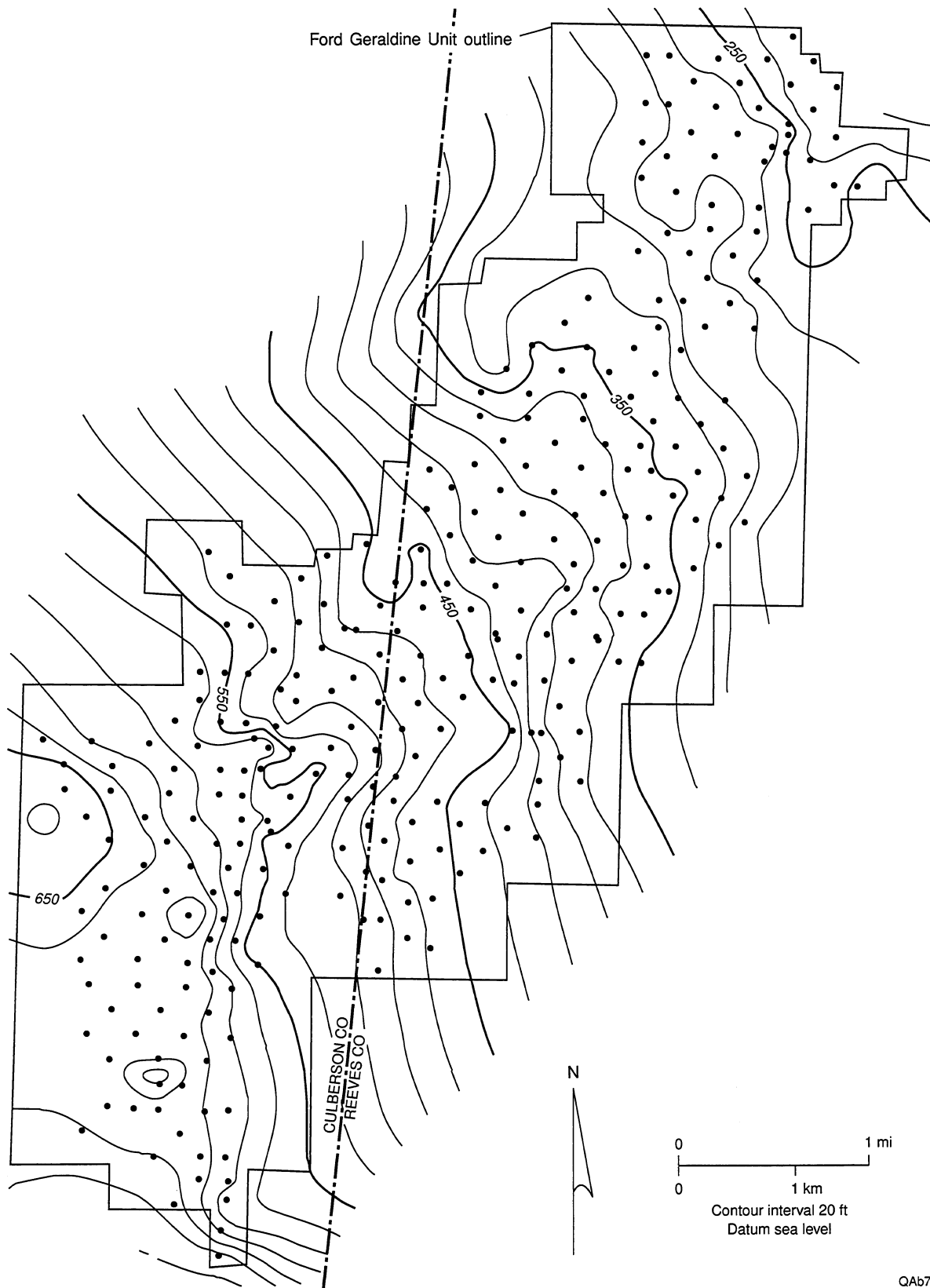
## Net Pay

Net pay in the Ramsey reservoir was calculated from geophysical logs, using cut-offs for volume of clay ( $V_{cl}$ ), porosity ( $\emptyset$ ), and water saturation ( $S_w$ ). Accurate values for  $V_{cl}$  are difficult to determine for the Delaware sandstones due to the lack of adjacent shales. Therefore the selection of a  $V_{cl}$  cut-off was based on the work of Dewan (1984), which suggests a  $V_{cl}$  cut-off of 15 percent for reservoirs with dispersed authigenic clay. The dispersed authigenic clay cut-off was used because of the common occurrence of authigenic clay in the Delaware sandstones (Williamson, 1978; Thomerson, 1992; Walling, 1992; Asquith and others, 1995; and Green and others, 1996).

Examination of the core porosity versus core permeability cross plot (fig. 13) for the Ramsey sandstone in the Ford Geraldine unit resulted in the selection of the following porosity cut-offs:

$\emptyset \leq 15$  percent for a permeability of 1.0 md

$\emptyset \leq 20$  percent for a permeability of 5.0 md



QAb7508c

Figure 15. Structure contours on the top of the Lamar limestone dip to the east and northeast. The trap at Geraldine Ford field is formed by pinchout of permeable sandstone into low-permeability siltstone structurally updip. The field has minor structural closure because of differential compaction over the reservoir sandstone body.

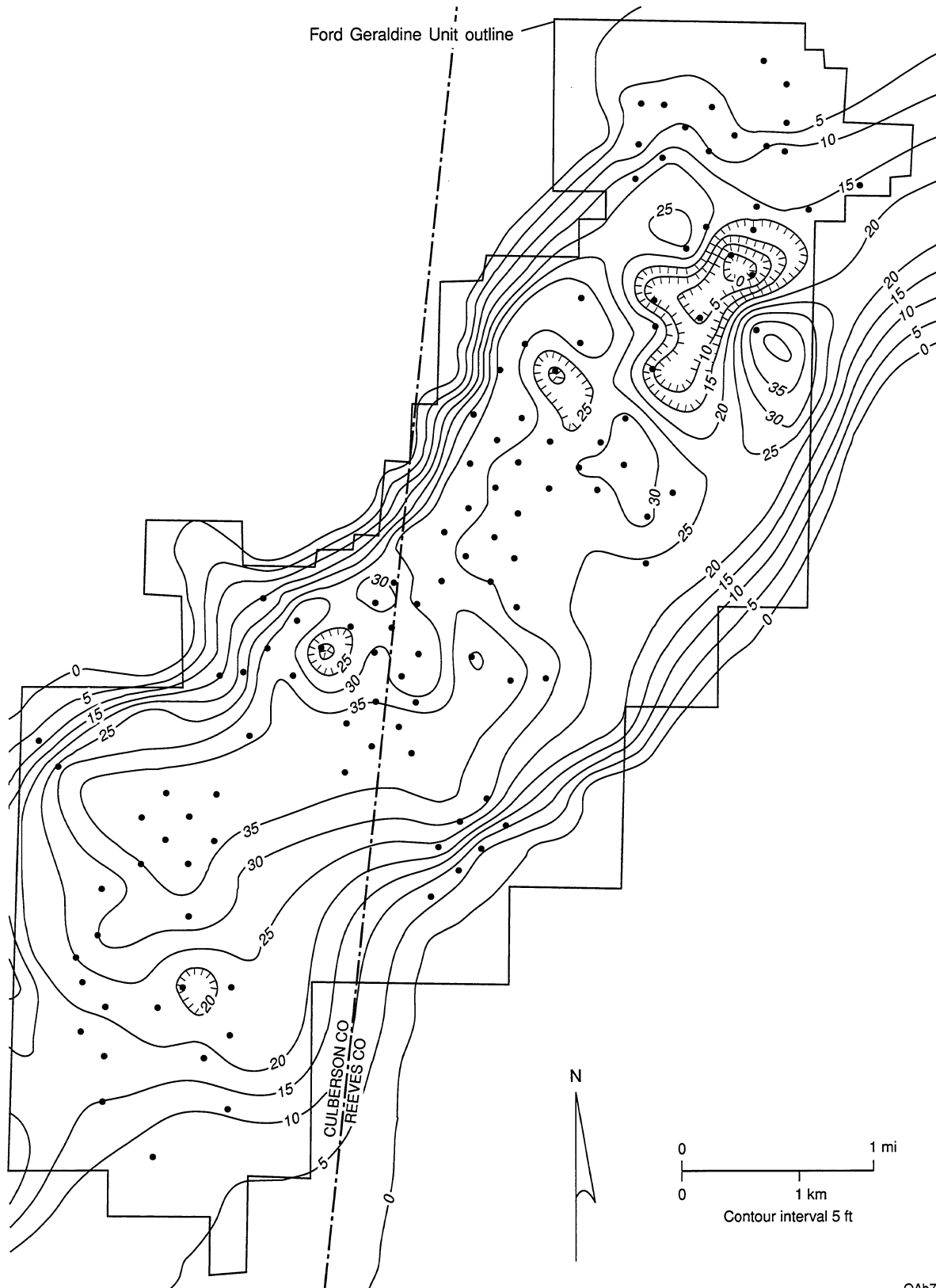
Five relative permeability curves from the FGU-156 well were used to establish the water saturation ( $S_w$ ) cut-off. The normalized relative permeability curves indicated that at a water saturation ( $S_w$ ) of 60 percent, the relative permeability to oil ( $K_{ro}$ ) is approximately 8 times the relative permeability to water ( $K_{rw}$ ) (Asquith and others, in press; Dutton and others, 1997). Therefore a water saturation cut-off of 60 percent was selected for the Ramsey sandstone in the Ford Geraldine unit.

The average net pay of the Ramsey sandstone calculated from geophysical logs using these cutoffs is 23.1 ft, with a standard deviation of 11.4 ft. This value is close to the average net pay cited by Pittaway and Rosato (1991) of 25 ft. Net pay is greatest to the southwest (structurally updip) and in the central part of the unit (fig. 16). When a 20 percent porosity cutoff is used (corresponding to 5 md permeability), average net pay is 20.8 ft, with standard deviation of 11.0 ft.

Gross pay was calculated as the thickness of the total Ramsey sandstone interval (Ramsey 1 sandstone, SH1, and Ramsey 2 sandstone). Average gross pay thickness is 31.3 ft, with a standard deviation of 11.8 ft. The trend of gross pay thickness follows the northeast-southwest elongate outline of the Ford Geraldine unit (fig. 17).

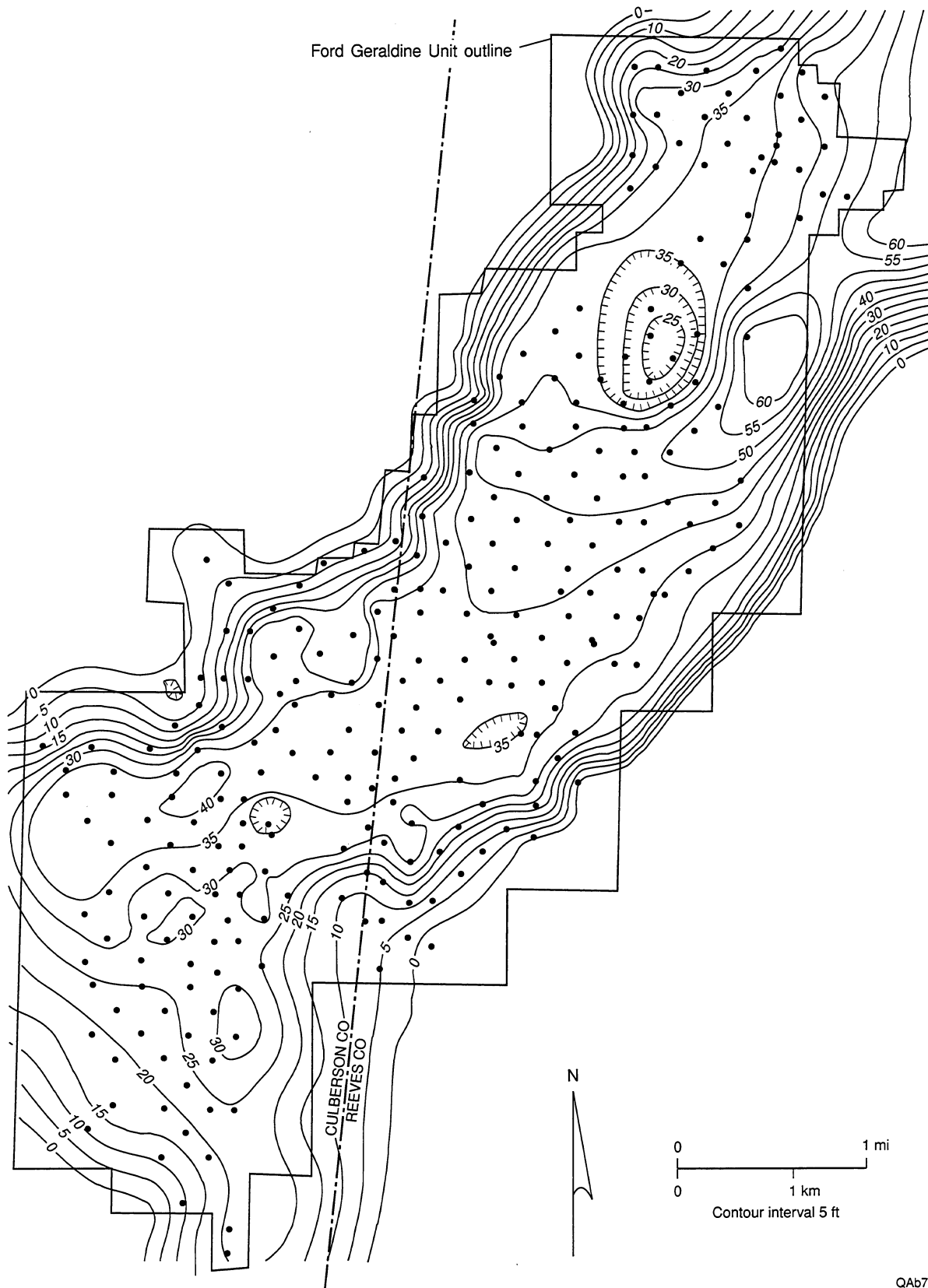
#### Vertical Porosity and Permeability Profiles

Vertical permeability profiles through the Ramsey sandstone are quite variable (fig. 18). In the northern part of the unit, where the Ramsey is divided by the SH1 siltstone, the higher permeabilities of the Ramsey 1 and 2 sandstones are separated by the low-permeability SH1 siltstone (see wells FGU-17 and FGU-70 on figure 18). Even within the Ramsey 1 and 2 sandstones, permeability is highly variable, with numerous spikes of high and low permeability. In many, but not all, wells, the highest permeability streaks occur at the top of the Ramsey sandstone, in either the Ramsey 1 or Ramsey 2 sandstone, whichever is at the top of the interval at that location (see wells FGU-70, FGU-193, and FGU-241 on figure 18). Low permeability commonly occurs immediately below these high-permeability streaks at the top of the Ramsey. The low-



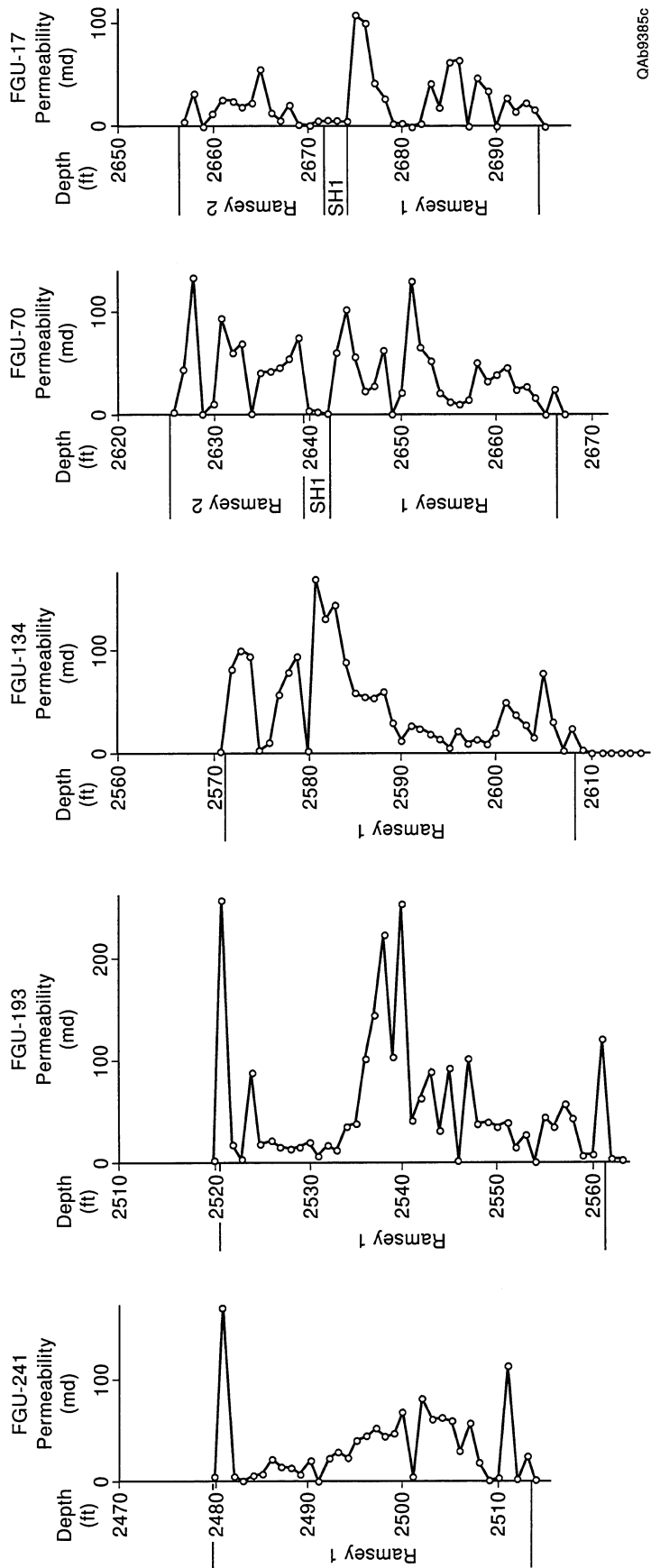
QA7526c

Figure 16. Map of net pay for the Ramsey sandstone in the Ford Geraldine unit, Reeves and Culberson Counties, Texas. The cut-offs for net pay were  $V_{cl} \leq 15$  percent,  $\phi \geq 15$  percent, and  $S_w < 60$  percent.



QA67920c

Figure 17. Map of thickness of the total Ramsey sandstone interval, from the top of the Ford siltstone to the base of the Trap siltstone, which is equivalent to gross pay thickness. Average Ramsey sandstone (gross-pay) thickness is 31.3 ft, with a standard deviation of 11.8 ft.



GAb9385c

Figure 18. Vertical permeability profiles from core-analysis data for 5 wells in the Ford Geraldine unit. Well locations correspond to cross section A-A', shown in Figure 20.

permeability zones correspond to calcite-cemented nodules (see section on Characterization of Diagenetic Heterogeneity), and the high-permeability streaks may result from leaching of carbonate cement (Dutton and others, 1996).

Vertical porosity profiles show a similar irregular distribution of porosity (fig. 19), with numerous low-porosity streaks throughout Ramsey 1 and 2 sandstones. Low-porosity zones are interpreted as corresponding to the low-permeability, calcite-cemented nodules.

### Natural Water Influx

Natural water influx into the field is suggested by the increase in produced water cuts prior to waterflooding and by the general trend of fresher water up-structure than down-structure (fig. 6). The salinity trend is interpreted to indicate that water less saline than the initial formation water entered the reservoir from the southwest. The Delaware Mountains, which are southwest of Geraldine Ford field, are the most likely fresh-water recharge area for the Delaware Basin (Hiss, 1975).

Few resistivity logs were run in the field (fig. 6), making it difficult to identify an oil-water contact. Ruggiero (1985) reported that the Ramsey sandstone has multiple oil-water contacts in the field. An oil-water contact was tentatively identified in areas 1 and 3N (fig. 4) from oil and water saturations in core analyses (Conoco, 1979). That oil-water contact apparently dips to the east-northeast at 75 to 80 ft/mi, almost the same angle as the structure on the top of the Ramsey.

## Geologic Characteristics

### Lithology

Three major rock types are present in Geraldine Ford field: very fine-grained sandstone, laminated siltstone (laminite), and organic-rich siltstone (lutite) (Ruggiero, 1985, 1993). The sandstone facies which forms the reservoir is a silty, very fine grained, well-sorted arkose. The laminite facies consists of parallel-laminated siltstone with alternating laminae (0.2 to 2 mm thick)

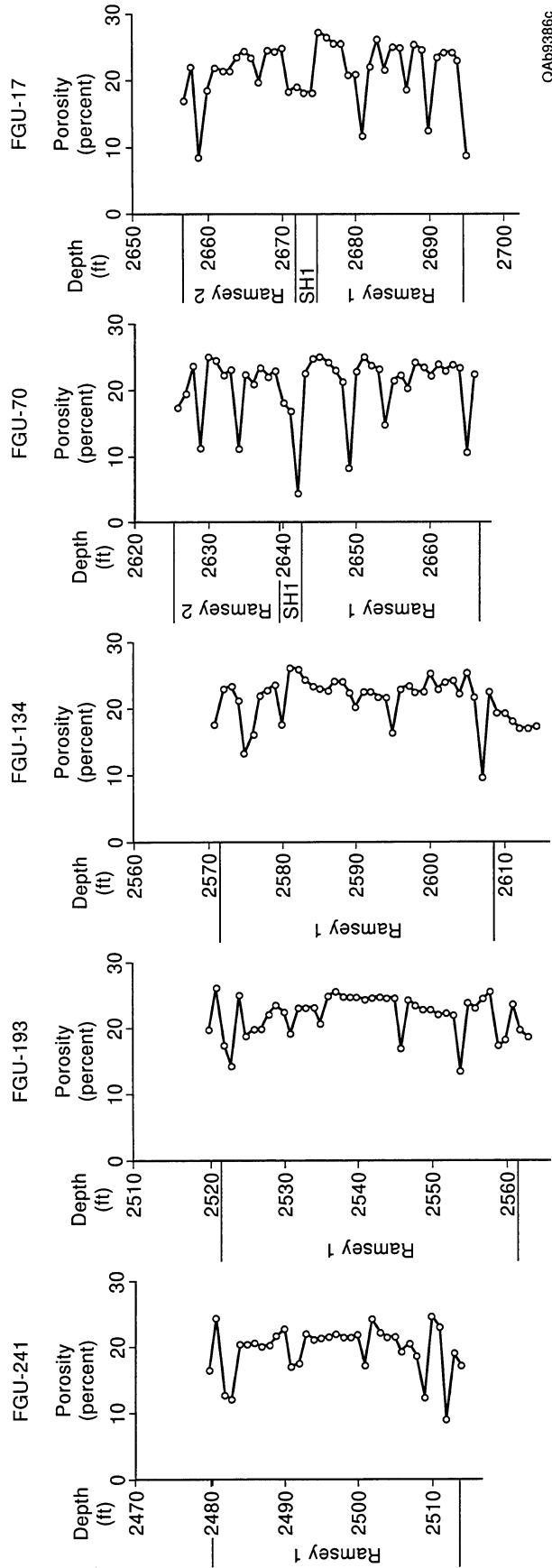


Figure 19. Vertical porosity profiles from core-analysis data for 5 wells in the Ford Geraldine unit. Well locations correspond to cross section A-A', shown in Figure 20.

of organics and silt (Ruggiero, 1985, 1993). This laminated siltstone forms the seal of the stratigraphic trap. Lutite is a dark, fissile, organic-rich siltstone containing little detrital clay (Ruggiero, 1985, 1993) that also contributes to the seal.

Ramsey sandstones in the Ford Geraldine unit have a very narrow range of grain sizes. The average grain size in sandstone samples is 0.092 mm (3.44  $\phi$ ), and the range is 0.069 to 0.103 mm. The proportion of silt-size grains in the sandstones ranges from 0 to 28 percent. The sandstones are mostly well sorted, having an average standard deviation of 0.42  $\phi$ . Sorting ranges from 0.35 to 0.51  $\phi$ . Clay minerals in Ramsey sandstone are interpreted as authigenic. Thus, as has been noted by previous workers (for example, Williamson, 1978; Berg, 1979), the Ramsey sandstones are unusual in their lack of detrital clay.

Five laminated siltstone samples have an average grain size of 0.062 mm (4.01  $\phi$ ), and they contain 28 to 62 percent silt grains. A lutite sample near the base of the Lamar has an average grain size of 0.033 mm (4.94  $\phi$ ), and it contains 46 percent silt, 46 percent organic matter, and 8 percent sand.

## Geologic Age

The Ramsey sandstone is part of the Bell Canyon Formation in the Permian Guadalupian series (fig. 3). The age of the Guadalupian series is 255 to 270 my (Hills and Kottlowski, 1983).

## Facies Analysis of Ramsey Sandstone

Interpretation of the processes that deposited the reservoir sandstones at Geraldine Ford field was based strongly on the outcrop characterization of analogous reservoir sandstones in the upper Bell Canyon (Barton, 1997; Dutton and others, 1997). Five of the six facies identified in upper Bell Canyon sandstones in outcrop were observed in the 70 Ramsey sandstone cores from Geraldine Ford field (fig. 2). These facies were also observed by Ruggiero (1985) in the 13 cores he described. The five facies were (1) massive, organic-rich siltstone (lutite), (2) laminated

siltstone (laminite), (3) sandstones that are graded or display partial Bouma sequences, (4) structureless or convoluted sandstone, and (5) cross-stratified sandstone. Massive sandstones are volumetrically the most abundant sandstone facies in the core, although that may be in part a result of the narrow range in grain sizes, which makes sedimentary structures indistinct and difficult to see in core. On outcrop, weathering processes may help to accentuate the sedimentary structures and make them more visible. Thus, some sandstones described as massive in the core may actually contain sedimentary structures that could not be distinguished.

The Ramsey sandstone is a 0- to 60-ft thick sandstone that is bounded by the Ford and Trap laminated siltstones. Lutites in the underlying Ford siltstone and the overlying Trap siltstone (fig. 5) are interpreted to be condensed sections that mark the top and base of a genetic unit, equivalent to a high-order cycle (Gardner, 1992; Kerans and others, 1992). In the northern part of the Ford Geraldine unit, the Ramsey is divided into two sandstones (Ramsey 1 and Ramsey 2) separated by a 1- to 3-ft-thick laminated siltstone (SH1) (fig. 20) (Ruggiero, 1985). In the southern part of the Ford Geraldine unit, only the Ramsey 1 sandstone is present. Thus, the Ramsey high-order cycle is subdivided into the following five units, from oldest to youngest: (1) upper Ford siltstone, from the Ford condensed section to the top of the Ford siltstone, (2) Ramsey 1 sandstone, (3) SH1 siltstone, (4) Ramsey 2 sandstone, and (5) lower Trap siltstone, from the base of the Trap siltstone to the Trap condensed section (fig. 5).

### Mapping of Genetic Units

Key stratigraphic horizons were correlated using digitized logs from 304 wells in the unit. An 8-layer, three-dimensional deterministic geologic model was constructed using stratigraphic-interpretation computer software.

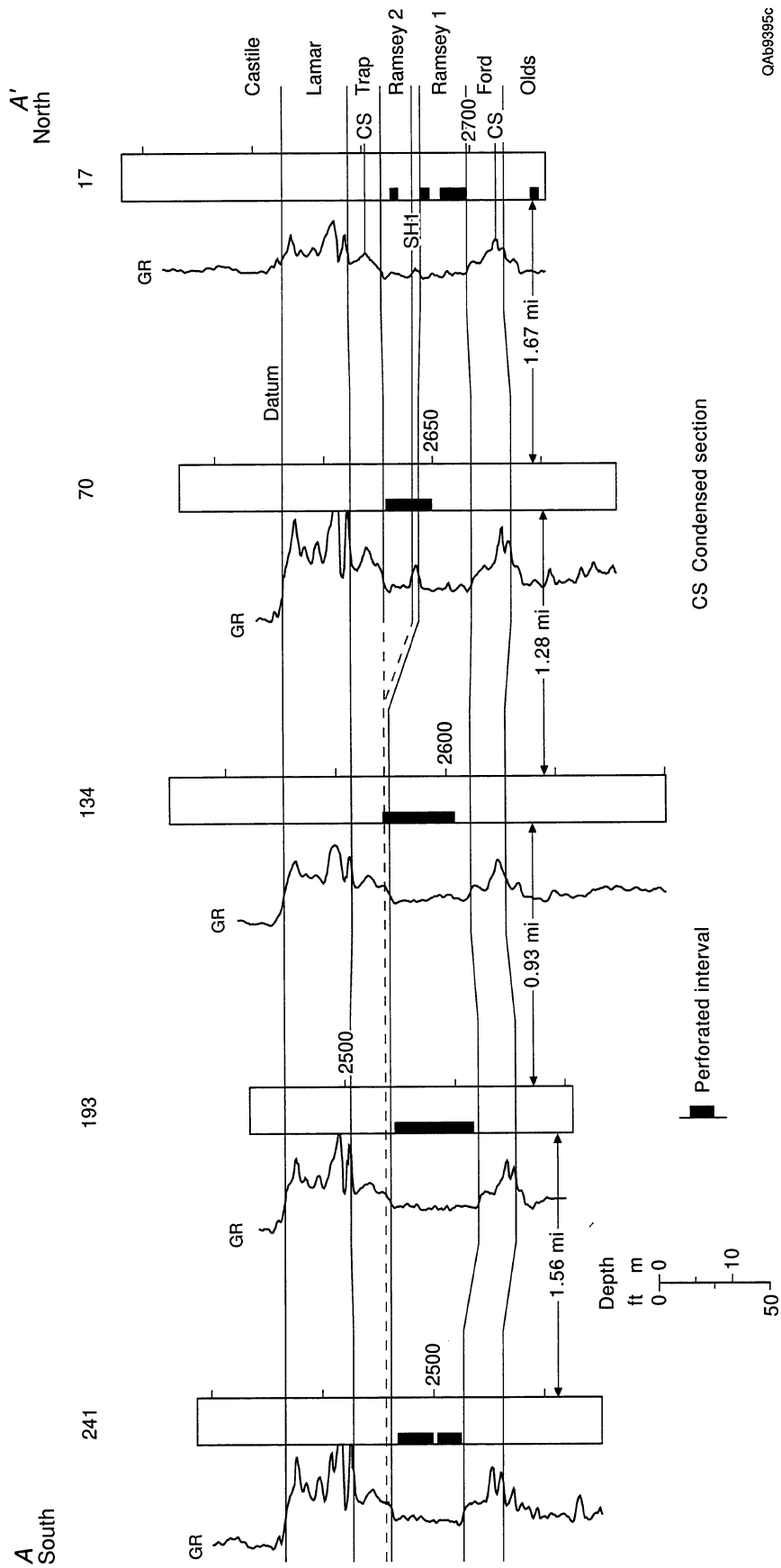


Figure 20. Dip cross section A-A' down the length of Geraldine Ford field. In the northern part of the field the SH1 laminated siltstone separates the reservoir into Ramsey 1 and Ramsey 2 sandstones. Only Ramsey 1 sandstone is present in the southern part of the field. Location of cross section is shown in figure 2.

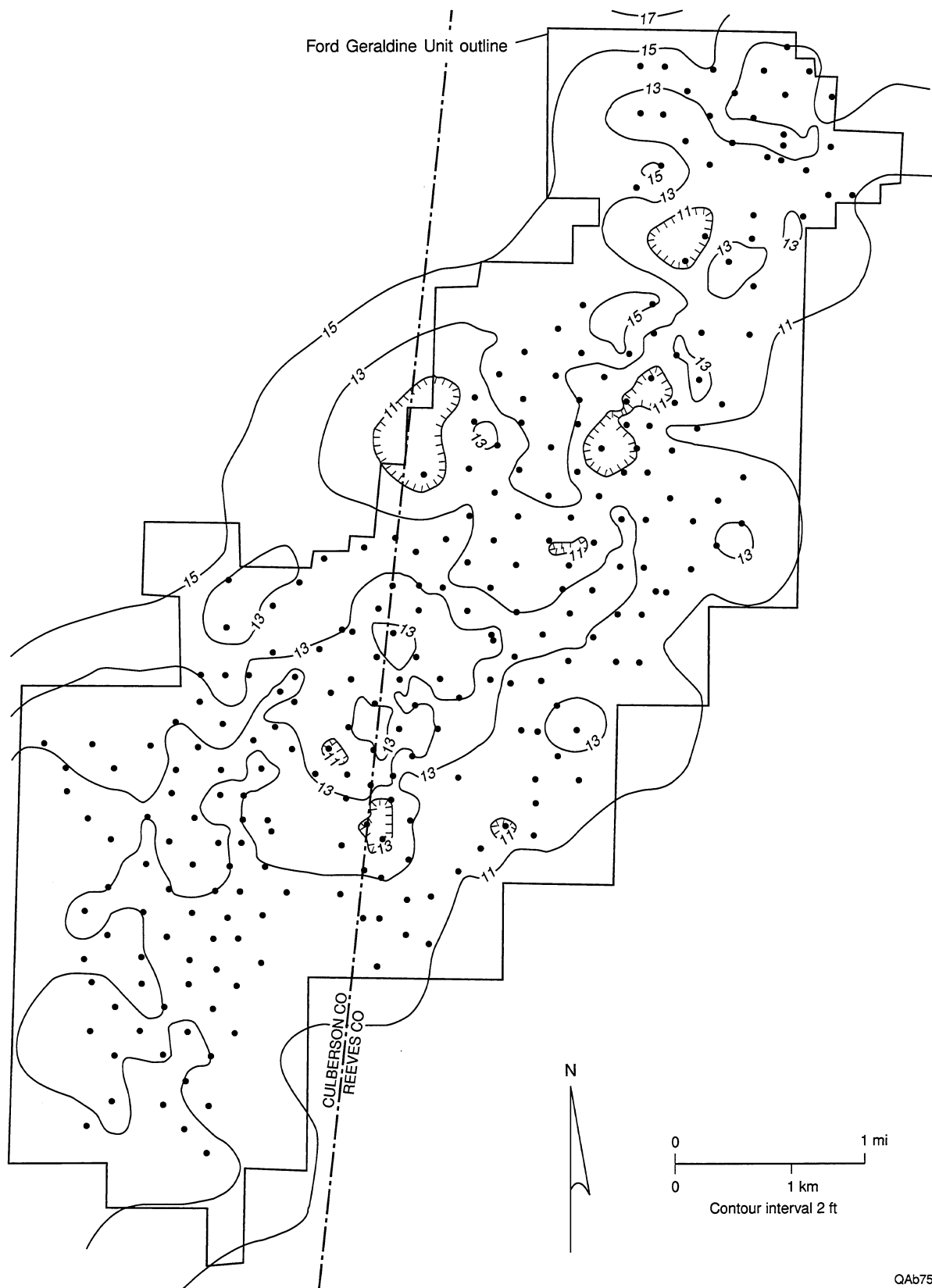
### *Upper Ford Siltstone*

The upper Ford is composed of organic-rich siltstone laminae interbedded on a millimeter scale with organic-poor siltstone laminae. The average grain size of the silt coarsens upward from the Ford condensed section to the top of the Ford, and the percentage of sand, amount of burrowing, and thickness of organic-poor laminae all increase toward the sandstone. Ripples and truncated laminae occur within the upper Ford siltstone. Gamma-ray response decreases over this interval, probably because much of the radioactivity is contained in organic matter within the organic-rich layers. The upper Ford thins from the northwestern side of the field (13 to 15 ft) to the southeast (11 to 13 ft) (fig. 21). Porosity in the Ford siltstone ranges from 1.1 to 20.3 percent and averages 16.9 percent. Permeability ranges from 1 to 33 md, and geometric mean permeability is 2 md.

### *Ramsey 1 Sandstone*

The Ramsey 1 sandstone occurs across all of Ford Geraldine unit (fig. 22). It pinches out at the northwest and southeast margins of the field and reaches a maximum thickness of >35 ft along a curving northeast-southwest trend. At the southwest end of the field, the single trend of thick sandstone splits into several smaller trends (fig. 22). The Ramsey 1 sandstone interval is 83 to 100 percent sandstone, with some thin interbeds of laminated siltstone and lutite. The average grain size of Ramsey 1 sandstones is 0.091 mm (3.47 Ø), which is near the boundary between upper and lower very fine sandstone. The range of average grain sizes is quite narrow, from 0.056 to 0.103 mm (3.28 to 4.16 Ø).

Core descriptions show that sandstones from all three sandstone facies occur in the Ramsey 1. Massive sandstones are common in all parts of the interval and throughout the field. Cross-bedded sandstones are most common along the trend of thickest sandstone through the center of the field. Sandstones with partial Bouma sequences, particularly rippled sandstones, and siltstone interbeds occur most commonly in the sandstone wedge that follows the margins of the thick



QA67509c

Figure 21. Isopach map of the upper Ford laminated siltstone, measured from the Ford condensed section to the top of the Ford. The relatively uniform thickness of the Ford interval suggests it was deposited either as widespread windblown silt or in a broad lobe that extends beyond the margins of the field.

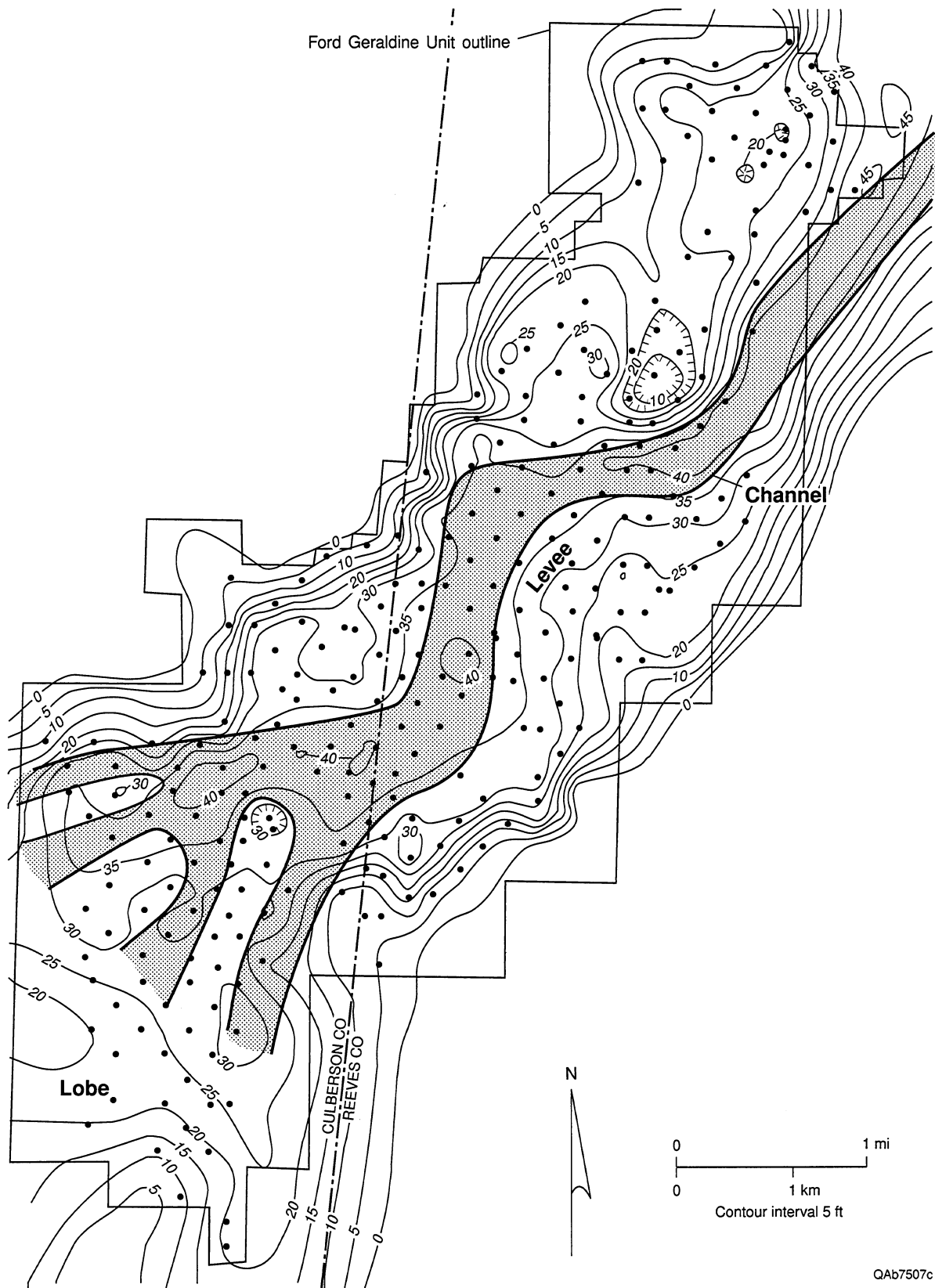


Figure 22. Isopach map of the Ramsey 1 sandstone, the main reservoir interval at Geraldine Ford field. It is interpreted as a channel-levee system that progrades over an elongate lobe. At the southwestern end of the field, the channel apparently breaks up into many smaller branches with attached lobes.

sandstone and pinches out at the edges of the field. Massive and contorted sandstones with abundant dewatering structures occur commonly in the lower Ramsey 1 interval.

Ruggiero (1985, 1993) subdivided the Ramsey 1 interval into three sandstones that he correlated across most of the field. In this study, the siltstones within the Ramsey 1 that Ruggiero used to correlate were determined to have only local distribution, so fieldwide subdivision of the Ramsey 1 was not deemed appropriate.

In most wells the gamma-ray response is distinctly lower in the Ramsey 1 sandstone than in the underlying Ford siltstone; in some wells the gamma response continues to decrease upward in the lower Ramsey 1 interval. Porosity in the Ramsey 1 sandstone ranges from 2.9 to 29.9 percent and averages 21.8 percent. Permeability ranges from 0.01 to 400 md, and geometric mean permeability is 19 md; arithmetic average permeability is 39 md.

### *SH1 Siltstone*

The SH1 siltstone represents a break in sandstone deposition within the Ramsey interval, when laminated siltstone was deposited (fig. 23). The SH1 siltstone can be differentiated from the Trap siltstone only at the northern end of the field, where the two are separated by the Ramsey 2 sandstone (fig. 5), but it is interpreted to be of widespread extent. Where it can be mapped separately, it is mostly 2 to 4 ft thick, increasing to >6 ft at the northwestern edge of the unit (fig. 23). The SH1 siltstone is composed of laminated siltstone similar to the Ford; burrows are common. Some ripples and truncated laminae occur in the siltstone, and, in a few wells, a lutite occurs at the base of the SH1 interval. Porosity in the SH1 siltstone ranges from 3.8 to 26.8 percent and averages 18.0 percent. Permeability ranges from 0.1 to 26 md, and geometric mean permeability is 2 md.

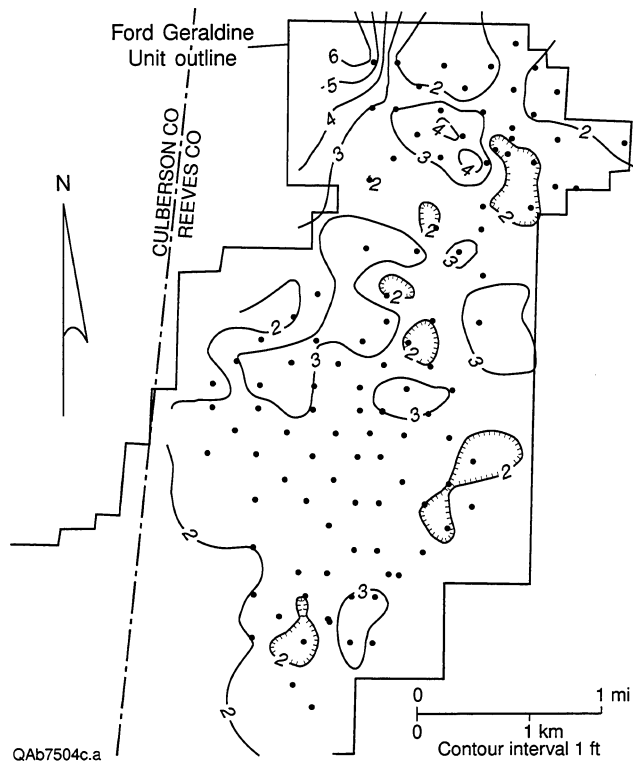


Figure 23. Isopach map of the SH1 laminated siltstone, which was deposited during a break in sandstone deposition. It can be differentiated from the Trap siltstone only at the northern end of the field, where it is overlain by the Ramsey 2 sandstone, but is thought to be of wide extent. Like the Ford and Trap laminites, the SH1 siltstone was probably deposited by windblown silt settling out of suspension or as a distal fan lobe.

### *Ramsey 2 Sandstone*

The younger sandstone in the Ramsey cycle, called the Ramsey 2 (Ruggiero, 1985), occurs only at the northern end of the unit (fig. 24). This sandstone is thinner than the Ramsey 1, having a maximum thickness of >14 ft along a sinuous, bifurcating northeast-southwest trend. The Ramsey 2 sandstone did not prograde as far into the basin in the Ford Geraldine area as the Ramsey 1 sandstone; the main area of Ramsey 2 sandstone deposition was in the Sullivan-Screwbean area, another linear Ramsey sandstone trend to the east and south (Ruggiero, 1985). The Ramsey 2 sandstone interval is 86 to 100 percent sandstone, with some thin interbeds of laminated siltstone and lutite. The average grain size of Ramsey 2 sandstones is 0.091 mm (3.46 Ø), almost exactly the same as the average grain size of Ramsey 1 sandstones. The range of average grain sizes is similarly narrow, from 0.085 to 0.099 mm (3.34 to 3.56 Ø).

As was true of the Ramsey 1, core descriptions show that sandstones from all three sandstone facies occur in the Ramsey 2. Cross-bedded sandstones are most common along the trend of thickest sandstone. Sandstones with partial Bouma sequences, particularly rippled sandstones and sandstones with contorted ripples, occur adjacent to the margins of the thick Ramsey 2 sandstone. Massive and contorted sandstones with dewatering structures occur commonly in the areas of thinner Ramsey 2 sandstone, particularly at the northwest edge of the unit (fig. 24). Many of the thickest areas of Ramsey 2 sandstone correspond to areas of thin Ramsey 1 sandstone, suggesting that Ramsey 2 sandstones were deposited in the adjacent topographic depressions created by deposition of the preceding Ramsey 1 beds. Porosity in the Ramsey 2 sandstone ranges from 10.2 to 25.3 percent and averages 20.5 percent. Permeability ranges from 2 to 230 md, and geometric mean permeability is 17 md; arithmetic average permeability is 41 md.

### *Lower Trap Siltstone*

The Ramsey cycle is capped by the Trap laminated siltstone. An isopach map of the lower Trap siltstone, measured from the top of the Ramsey sandstone (1 or 2, depending on location in

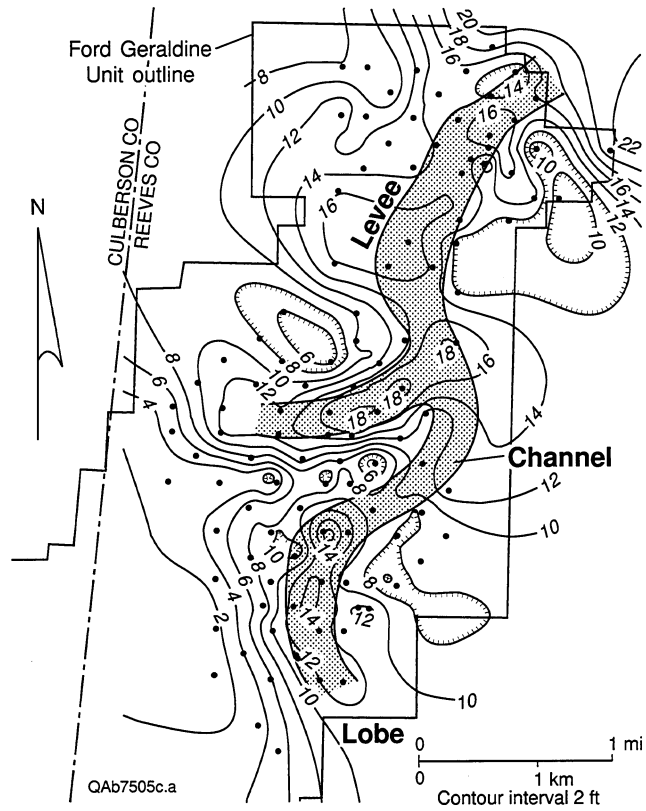


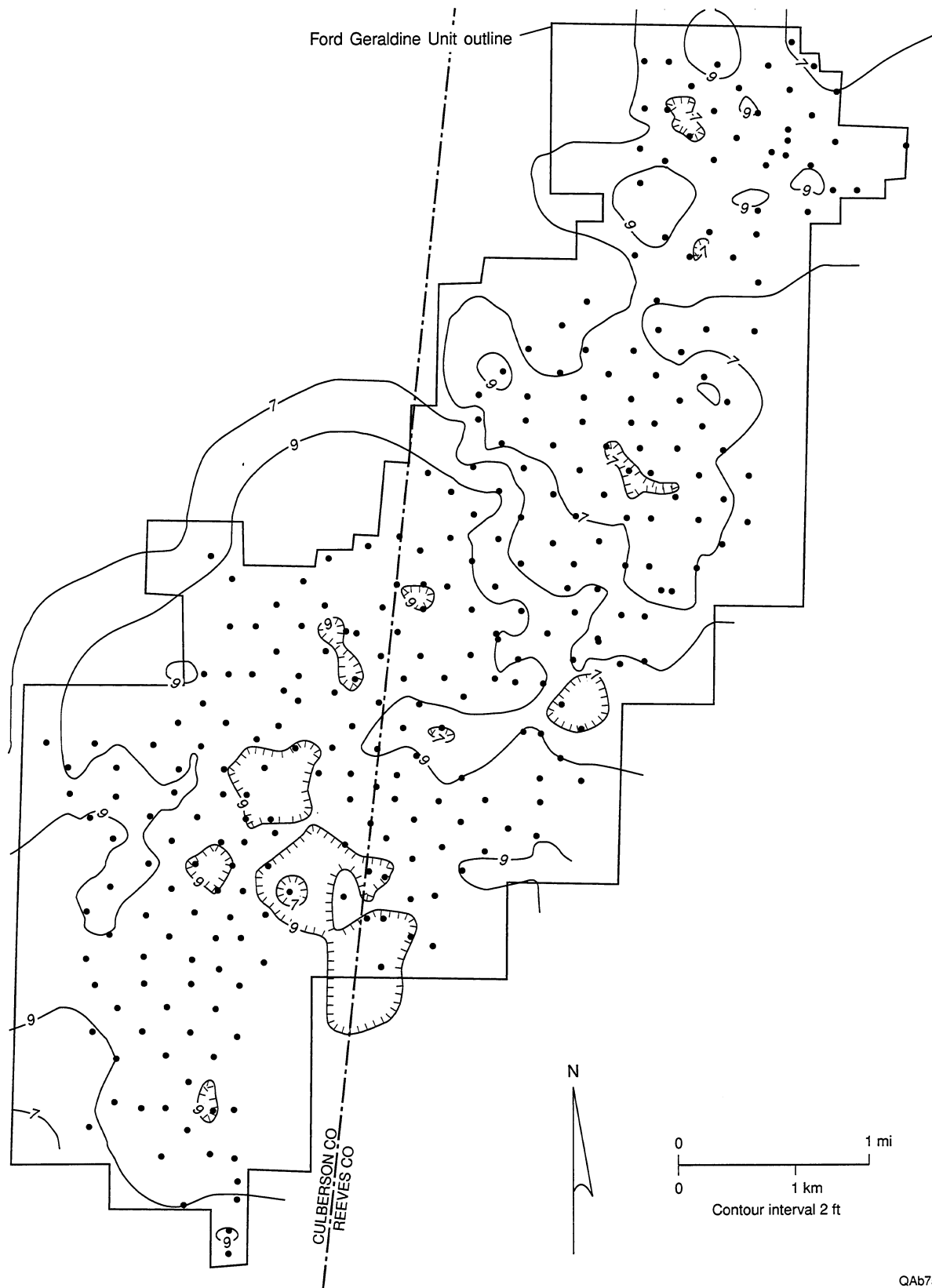
Figure 24. Isopach map of the Ramsey 2 sandstone. This sandstone is also interpreted as a channel-levee system that prograded over lobe deposits, but it did not prograde as far into the basin as did the Ramsey 1 sandstone. Many of the thickest areas of Ramsey 2 sandstone correspond to thin Ramsey 1, suggesting that Ramsey 2 sandstones were deposited in the adjacent topographic depressions created by deposition of the preceding Ramsey 1 beds.

the field) to the Trap condensed section (fig. 5), shows a distinct thickness change between the north and south parts of the unit (fig. 25). The lower Trap siltstone is thicker at the south end of the field (mostly 8 to 10 ft, compared with 6 to 8 ft at the north end) because the SH1 siltstone cannot be differentiated there and thus its thickness is added to the Trap thickness. Like the Ford siltstone, the Trap is composed of organic-rich siltstone laminae interbedded on a millimeter scale with organic-poor siltstone laminae. The average grain size of the silt decreases upward from the base of the Trap to the Trap condensed section, whereas the percentage of sand, amount of burrowing, and the thickness of organic-poor laminae all decrease away from the sandstone. Ripples and truncated laminae occur within the lower Trap siltstone. Gamma-ray response increases over this interval as the amount of organic matter increases toward the condensed section. Porosity in the Trap siltstone ranges from 4.3 to 21.7 percent and averages 12.7 percent. Permeability ranges from 0.01 to 45 md, and geometric mean permeability is 0.4 md.

#### Distribution of Facies

Vertical and lateral distribution of facies described in cores is illustrated on representative cross sections through cored wells from the northern and central parts of the Ford Geraldine unit (figs. 26, 27). As mentioned previously, much of the core appears massive, but sandstones with graded beds or partial Bouma sequences, sandstones with dewatering structures and convoluted bedding, and cross-laminated sandstones all occur in the Ramsey 1 and 2 sandstones (fig. 28). Laminated siltstones and lutites occur within the Ramsey sandstone interval and in the adjacent Ford and Trap units (fig. 28).

On the basis of facies distribution in the widely spaced subsurface cores (figs. 2, 28), combined with information on facies distribution of Bell Canyon sandstones mapped in continuous outcrops (Barton, 1997; Dutton and others, 1997 and in press), the Ramsey sandstone at Ford Geraldine unit is interpreted as consisting of channel, levee, and lobe deposits (figs. 26, 27).



QAb7506c

Figure 25. Isopach of the lower Trap laminated siltstone, measured from the top of the Ramsey sandstone (1 or 2, depending on location in the field) to the Trap condensed section. The lower Trap is thicker at the southern end of the field because the SH1 siltstone cannot be differentiated. Thus its thickness is added to the Trap thickness.

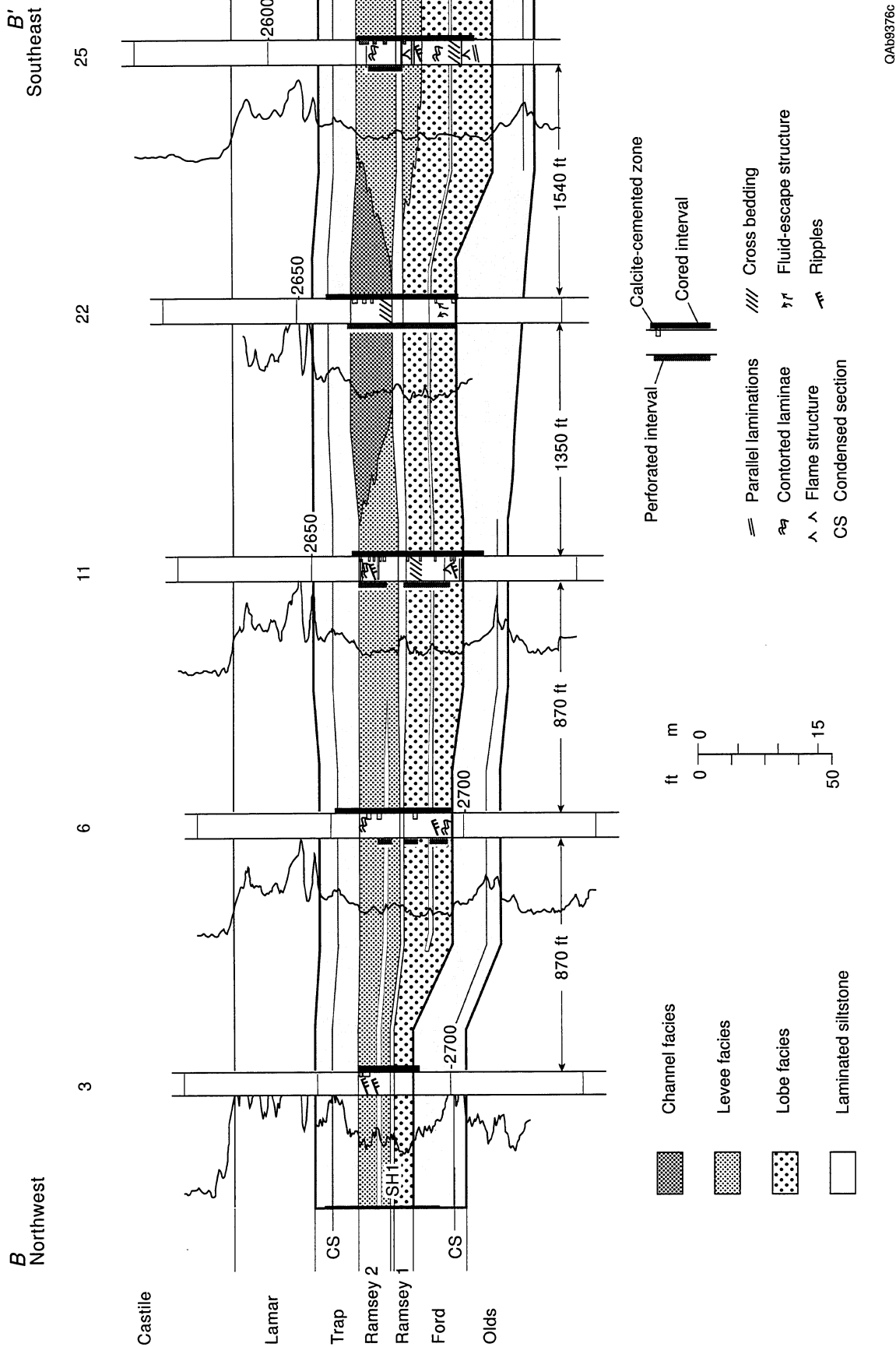


Figure 26. Cross section B–B' through the northern end of Geraldine Ford field, where the SH1 laminated siltstone separates the reservoir into Ramsey 1 and Ramsey 2 sandstones. Deposition of Ramsey sandstones is interpreted to have occurred by sandy high- and low-density turbidity currents that carried a narrow range of sediment size, mostly very fine sand to coarse silt. On the basis of core descriptions and study of the outcrop analog, Ramsey sandstones are interpreted to have been deposited on the basin floor in a sand-rich, channel-levee system with attached lobes. Location of cross section is shown in figure 2.

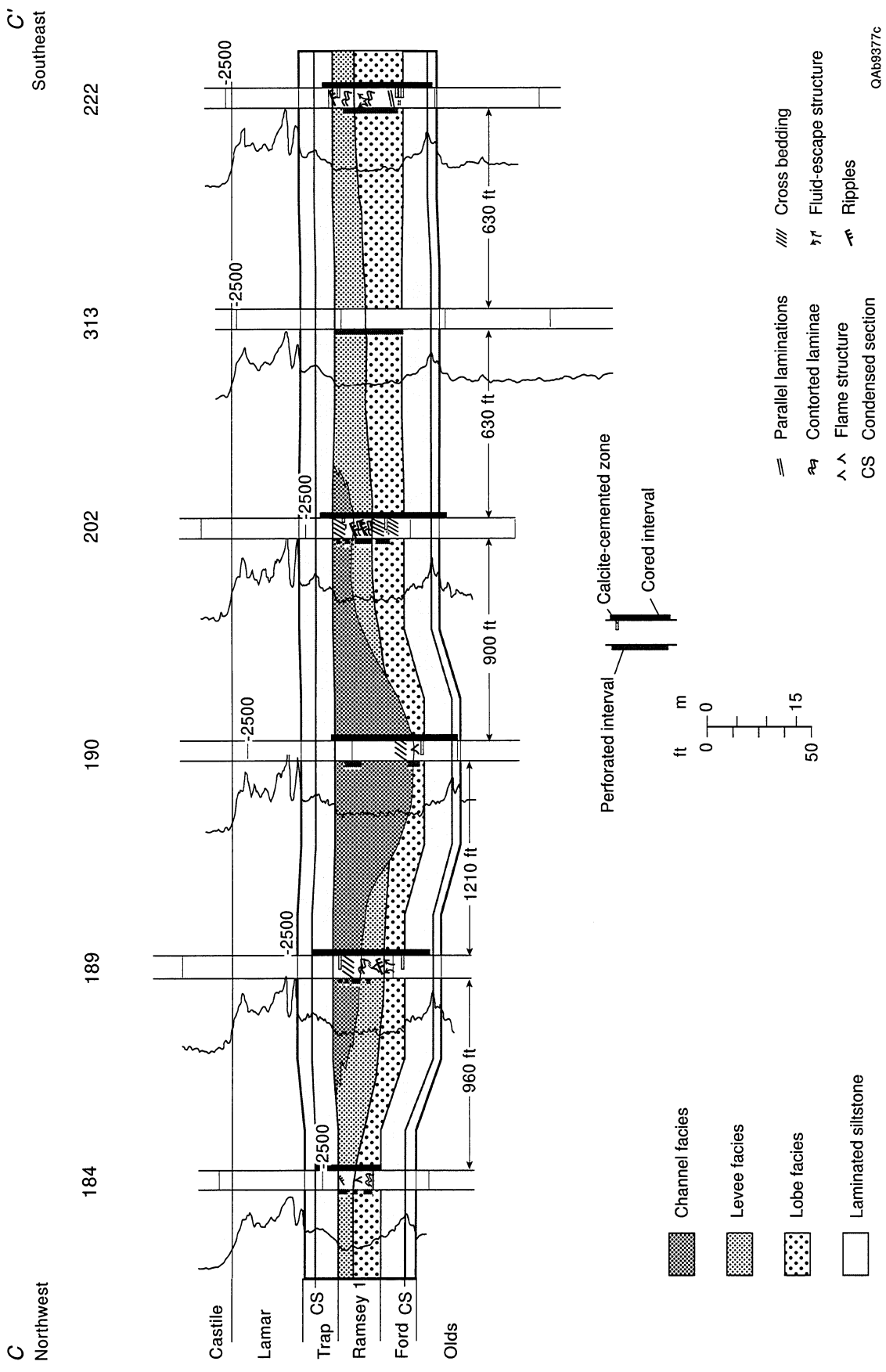


Figure 27. Cross section C–C' through the southern part of Geraldine Ford field, where only the Ramsey 1 sandstone is present. Channel, levee, and lobe facies are similar to those in cross section B–B' (fig. 26). Location of cross section is shown in figure 2.

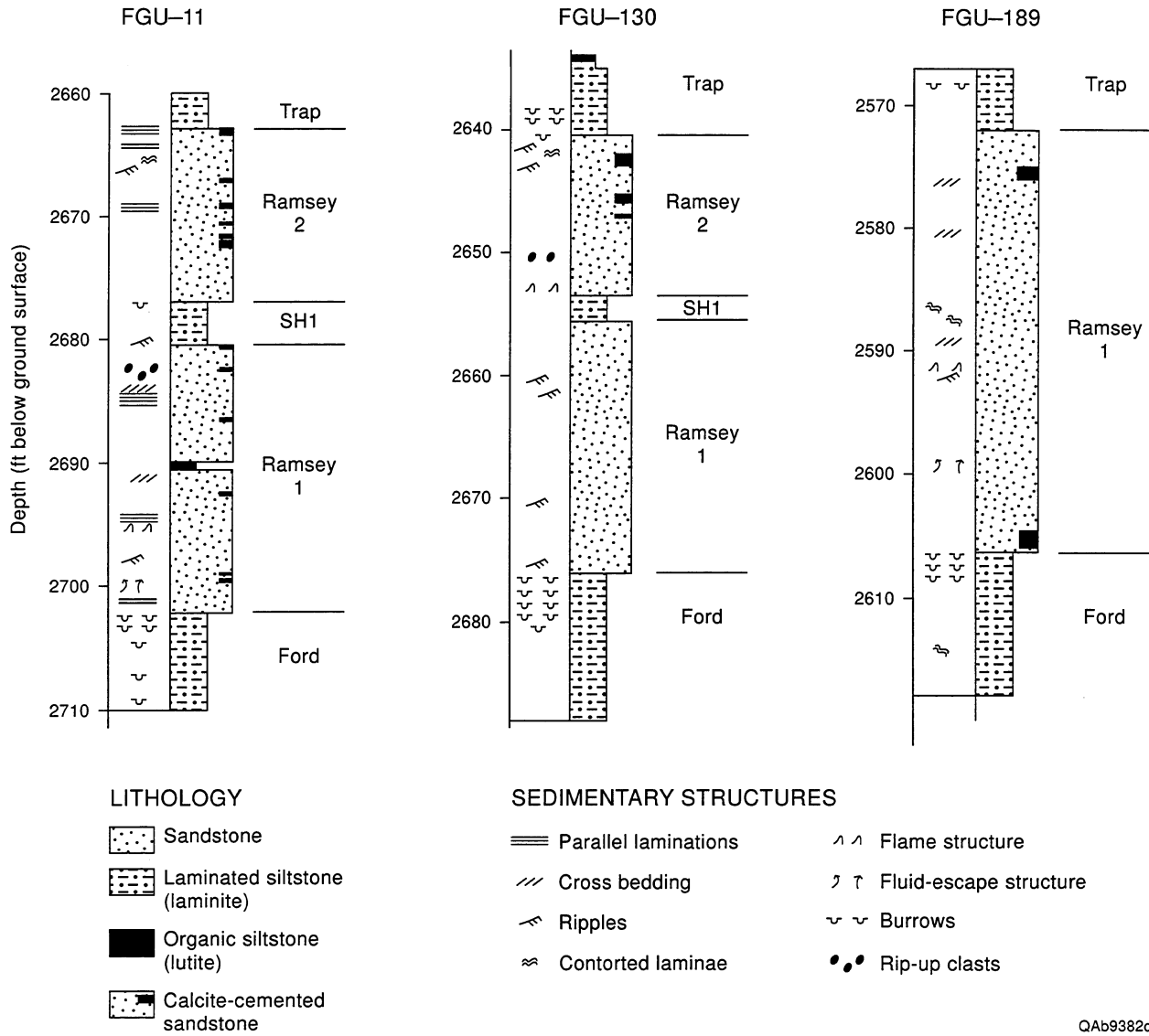


Figure 28. Representative cores of the Ramsey sandstone and bounding Trap and Ford laminated siltstones. Location of wells FGU-11, FGU-130, and FGU-189 is shown in figure 2.

## *Channel Facies*

Channels facies consist of massive and crossbedded sandstones interpreted to have been deposited from high-density turbidity currents (Lowe, 1982). Massive sandstones were probably deposited rapidly from suspension, whereas the crossbedded sandstones may result from a lower fall-out rate from suspension (Kneller, 1996). Crossbedded Bell Canyon sandstones in outcrop are interpreted as the product of infilling of scoured zones, not migrating bedforms. This may have occurred during the first phase of sediment deposition from a high-density turbidity current (Lowe, 1982), when the current was locally erosive, and deposits show scours and lenticularity. During this stage, bedforms can form, including dune-like features, but flow unsteadiness “prevents the evolution of highly organized dunes” (Lowe, 1982, p. 283). Kneller (personal communication, 1996) reports that traction structures, including climbing dunes, can form from high-density turbidity currents when the suspended load fall-out rate is relatively low.

As interpreted from the cross sections and isopach map, channels in the Ramsey 1 sandstone are 30 to 35 ft thick and 1,200 ft across (fig. 22, 27) (Dutton and others, in press). Ramsey 2 channels are thinner, mostly 15 to 20 ft thick, but also about 1,200 ft wide (fig. 24, 26) (Dutton and others, in press). In outcrop, many channels were nested and laterally offset from each other (Barton, 1997; Dutton and others, 1997). Similar nesting of multiple channels may occur in the Ford Geraldine unit, but the core control is not sufficiently close to distinguish separate channels. The aspect ratio (width:thickness) of Ramsey 1 channel deposits is 40:1 to 34:1, and in Ramsey 2, 80:1 to 60:1. Within channels, the ratio of net-to-gross sandstone is 100 percent. Log response is generally blocky (for example, fig. 27, well 190). The main Ramsey 1 channel thins and bifurcates into about 4 channels at the southwest part of the unit (fig. 22). The Ramsey 2 channel bifurcates farther updip, at the north end of the unit (fig. 24), reflecting the backstepping of the younger sandstone in this area. The average porosity in 272 channel sandstone samples is 22.1 percent. Geometric mean permeability is 16 md, and median permeability is 21 md. From core-analysis data, average water saturation is 41.9 percent and average residual oil saturation is 12.4 percent.

### *Levee Facies*

Levee facies occur as a sediment wedge along the margins of the channels (figs. 22, 24, 26, 27). These channel-margin deposits consist of sandstones with partial Bouma sequences, particularly ripples and convoluted ripples, and interbedded siltstones. They are interpreted as channel levees formed by overbanking of low-density turbidity currents. Thickness of the levee facies decreases away from the channels, and the volume of interbedded siltstones increases. Log response is more serrated than in the channels because of the presence of interbedded siltstones (for example, fig. 26, well 6). The average porosity in 318 levee sandstones is 22.3 percent. Geometric mean permeability is 19 md, and median permeability is 29 md. From core-analysis data, average water saturation is 46.2 percent and average residual oil saturation is 12.5 percent.

### *Lobe Facies*

Lobe facies occur in broad sheets at the mouths of channels and are deposited by unconfined high-density turbidity currents (fig. 22, 24). Lobe facies are characterized by massive sandstones and graded sandstones with dewatering features such as dish structures, flame structures, and vertical pipes—features that indicate rapid deposition and fluid escape (fig. 28). They were deposited at high suspended-load fallout rates. In a prograding system such as the Ramsey sandstone, lobe facies would have prograded into the Ford Geraldine area first, then been overlain and partly eroded by the narrower prograding channel-levee system (figs. 26, 27). Thus, lobe deposits are found at the distal ends of the Ramsey 1 and 2 sandstone channels and also under and laterally adjacent to the Ramsey 1 and 2 channels and levees (fig. 22, 24, 26, 27). Deposition of lobe sandstones was periodic, and laminated siltstones are interbedded with the lobe sandstone sheets. Some lobe deposits show an upward coarsening log pattern (fig. 26, well 22; fig. 27, well 184), but many have a massive log response (fig. 27, well 222). The average porosity in 310 lobe sandstone samples is 21.3 percent. Geometric mean permeability is 13 md, and median

permeability is 21 md. From core-analysis data, average water saturation is 46.5 percent and average residual oil saturation is 10.5 percent.

### *Laminated Siltstone Facies*

The laminated siltstone facies consists of organic-rich siltstone laminae interbedded on a millimeter scale with organic-poor siltstone laminae. The depositional origin of the laminated siltstones is uncertain. The pattern of upward coarsening into the Ramsey sandstone and upward fining above it suggests that the laminated siltstones are part of the progradation and retrogradation of the channel-levee and lobe system; the siltstones may represent the most distal part of the lobe. Alternatively, the siltstones may represent windblown silt from the shelf margins. Periods of relative sea-level fall may have exposed increasingly larger areas on the shelf and allowed the wind to carry away greater volumes of silt, resulting in thicker, organic-poor siltstone layers. The relatively uniform thickness of the Ford and Trap siltstone intervals (fig. 21, 25) could be explained as either from deposition of widespread windblown silt or from deposition as the distal part of a broad lobe that extends beyond the margins of the field (Dutton and others, in press). The average porosity in 214 laminated siltstone samples is 15.7 percent, and geometric mean permeability is 0.54 md. From core-analysis data, average water saturation is 54.3 percent and average residual oil saturation is 7.1 percent.

### *Lutite Facies*

These organic-rich siltstones are interpreted as condensed sections that formed in the Ford and Trap intervals during times of very slow siltstone deposition. They contain abundant organic matter, including spores. The organic matter is probably derived from settling from suspension of planktonic organisms. Other lutites interfinger with the levee deposits and represent interchannel deposits. The average porosity in 8 lutite samples is 13.1 percent, and geometric mean permeability

is 0.12 md. From core-analysis data, average water saturation is 40.9 percent and average residual oil saturation is 15.6 percent.

#### Proposed Depositional Model for Ford Geraldine Unit

On the basis of core descriptions and study of the outcrop analog, Ramsey sandstones at the Ford Geraldine unit are interpreted to have been deposited by sandy high- and low-density turbidity currents that carried a narrow range of sediment size, mostly very fine sand to coarse silt. The sands were deposited in a basin-floor setting by a channel-levee system with attached lobes (fig. 29). Channel facies are approximately 1,200 ft wide and 15 to 35 ft deep. They consist of massive and crossbedded sandstones interpreted to have been deposited from high-density turbidity currents (Lowe, 1982). Channel margins are characterized by rippled and convoluted sandstones interbedded with minor siltstones. Channel-margin deposits are interpreted as channel levees formed by overbanking of low-density turbidity currents. Levee deposits are composed of ripple-laminated and convoluted sandstones interbedded with minor siltstones. Lobe sandstones are interpreted as being deposited at the mouth of the channel by high-density turbidity currents. They are identified by massive and graded sandstones with load and dewatering structures such as dish structures, flame structures, and vertical pipes—features that indicate rapid deposition and fluid escape.

The narrow range of sediment size in the Ramsey sandstones, mostly very fine sand, supports the conclusions of Fischer and Sarnthein (1988) and Gardner (1992), of an eolian sediment source for sandstones of the Delaware Mountain Group. In their model, fine sand was transported from source areas in the ancestral Rockies by migration of eolian ergs, and silt and clay were transported by the wind as dust (Fischer and Sarnthein, 1988). Clay was carried by the wind beyond the Delaware Basin, thus accounting for the lack of clay-sized sediment in the Delaware Mountain Group deposits. Silt-sized dust was deposited in the basin by fallout from the wind and settling through the water column, forming topography-mantling laminated siltstones. During low-stands of sea level, dune sands were driven across the exposed shelf to the shelf edge, where they

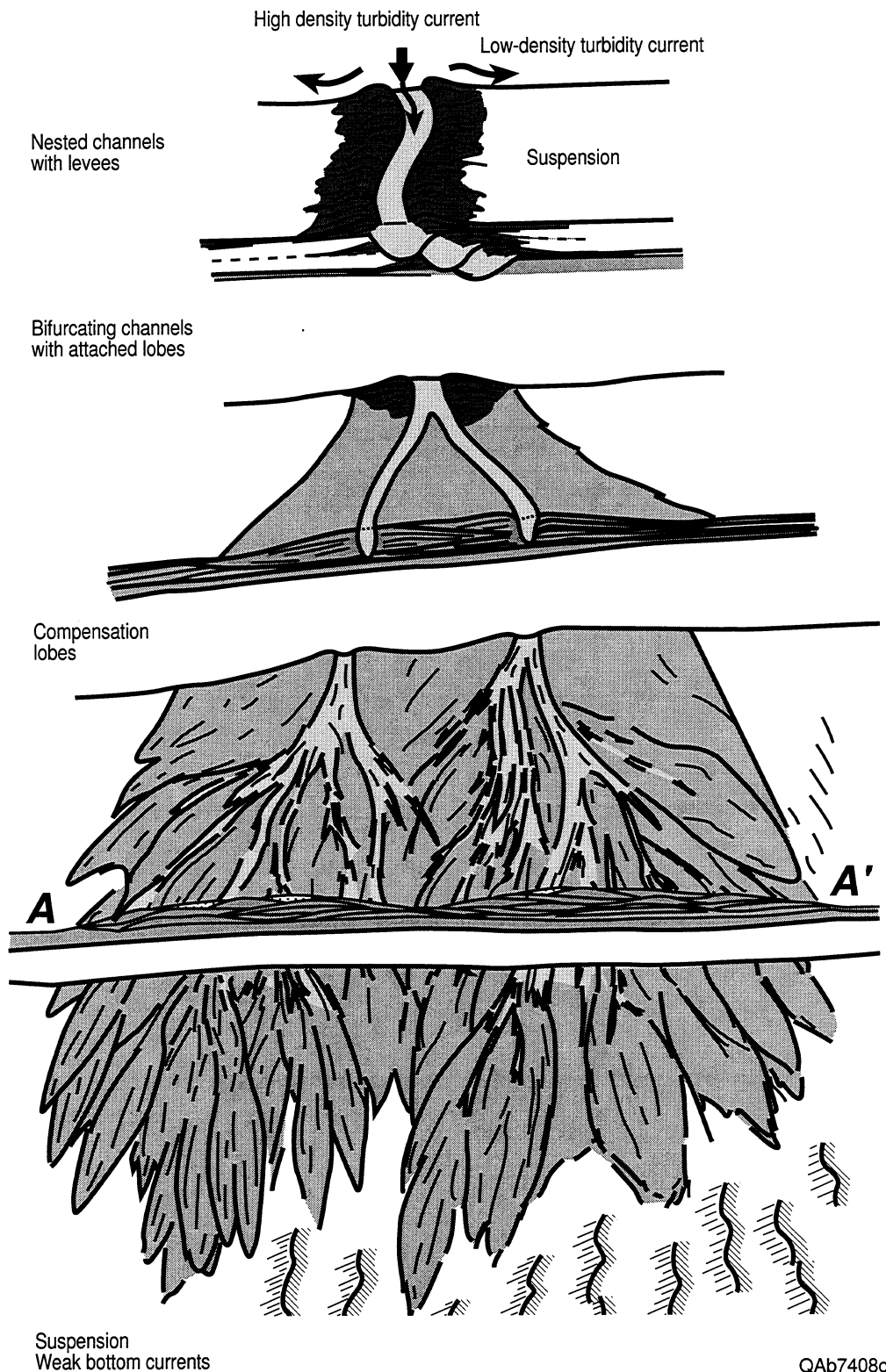


Figure 29. Diagram illustrating depositional model for upper Bell Canyon Formation. Bell Canyon sandstones are interpreted to have been deposited in submarine channels with levees and attached lobes (from Barton, 1997; Dutton and others, 1997).

fed unstable, shallow-water sand wedges. Slumping of the sand wedges gave rise to turbidity currents that carved channels and filled them with well-sorted sandstone. During highstands in sea level, the platform was flooded and the dunes were prevented from migrating to the shelf edge.

Mapping of Ramsey 1 and Ramsey 2 sandstone distribution shows that the younger Ramsey 2 sandstone does not prograde as far basinward as does the older Ramsey 1 sandstone. Kerans and others (1992) interpreted this to have been a time of relative rise in sea level, during which progressively less sand would be allowed into the basin, consistent with landward stepping of the Ramsey 2 sandstone.

Instead of filling a large channel, as suggested by the saline-density current model (Ruggiero, 1985, 1993), Ramsey sandstones were probably deposited on the basin floor (Barton, 1997). Younger sandstones were deposited in topographically low areas created by deposition of the preceding bed, resulting in offset stacking of lobes, called “compensation lobes” by Mutti and Normark (1987). The confinement of sandstones within narrow linear trends may in part result from reef topography on the highly aggradational carbonate platform (Williamson, 1978; Gardner, 1997).

#### Characterization of Diagenetic Heterogeneity

Diagenesis commonly influences sandstone reservoir quality by overprinting and modifying depositional permeability distribution. In many sandstones, the original depositional features, particularly grain size, sorting, and volume of ductile grains, remain the most important predictors of permeability in a sandstone even after burial diagenesis. However, in some sandstones diagenesis is so extensive that it becomes the dominant control on permeability. In the Ramsey sandstones, diagenesis is not unusually extensive. Because detrital grain size is so constant in the sandstone facies, however, the main control on reservoir quality in these sandstones is the volume of authigenic cement.

## *Petrography of Ramsey Sandstones*

The composition of Ramsey sandstones at the Ford Geraldine unit was determined from 32 thin sections from sandstones with a wide range of permeability in order to quantify the petrographic characteristics of grain size, detrital mineralogy, authigenic cements, and porosity.

Ramsey sandstones at Geraldine Ford field are arkoses having an average composition of Q<sub>63</sub>F<sub>32</sub>R<sub>5</sub> (fig. 30). Detrital quartz composes an average of 42 percent of the total rock volume. Orthoclase and other potassium feldspars have an average volume of 11 percent; plagioclase also has an average volume of 11 percent. Many plagioclase grains have been partly vacuolized, sericitized, and chloritized. Rock fragments, including plutonic and metamorphic rock fragments and chert, average 4 percent of the whole-rock volume. Fossil fragments and carbonate rock fragments (<1 percent) occur in several sandstone samples, particularly in the calcite-cemented zones.

Cements and replacive minerals constitute between 4 and 30 percent of the sandstone volume in Ramsey sandstones, with calcite and chlorite being the most abundant. Calcite cement (average = 7 percent, range 1 to 29 percent) occurs both in primary pores and in secondary pores, where it has replaced feldspar grains. On the basis of thin-section staining, some of the calcite cement apparently contains minor iron. Some calcite shows evidence of dissolution. Chlorite (average = 3 percent) forms rims around detrital grains, extending into pores and pore throats. Authigenic quartz, anhydrite, leucoxene, siderite, ankerite, illite or mixed-layer illite-smectite (probably mixed-layer illite-smectite based on X-ray analyses by Williamson, 1978), pyrite, and feldspar overgrowths (both K-feldspar and Na-feldspar) also occur in the Ramsey sandstones, generally in volumes of <1 percent. Quartz occurs as small crystals on quartz grain surfaces, as isolated euhedral crystals, and as syntaxial overgrowths on detrital quartz grains. Quartz generally appears to have overgrown and included authigenic clay. On the basis of petrographic evidence, the relative order of occurrence of the major events in the diagenetic history of the Ramsey sandstones is

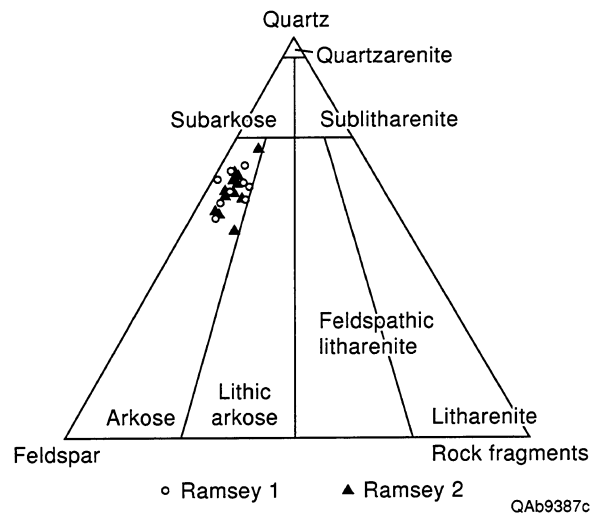


Figure 30. Ramsey sandstones at Geraldine Ford field are arkoses having an average composition of  $Q_{63}F_{32}R_5$ . Sandstone classification of Folk (1974).

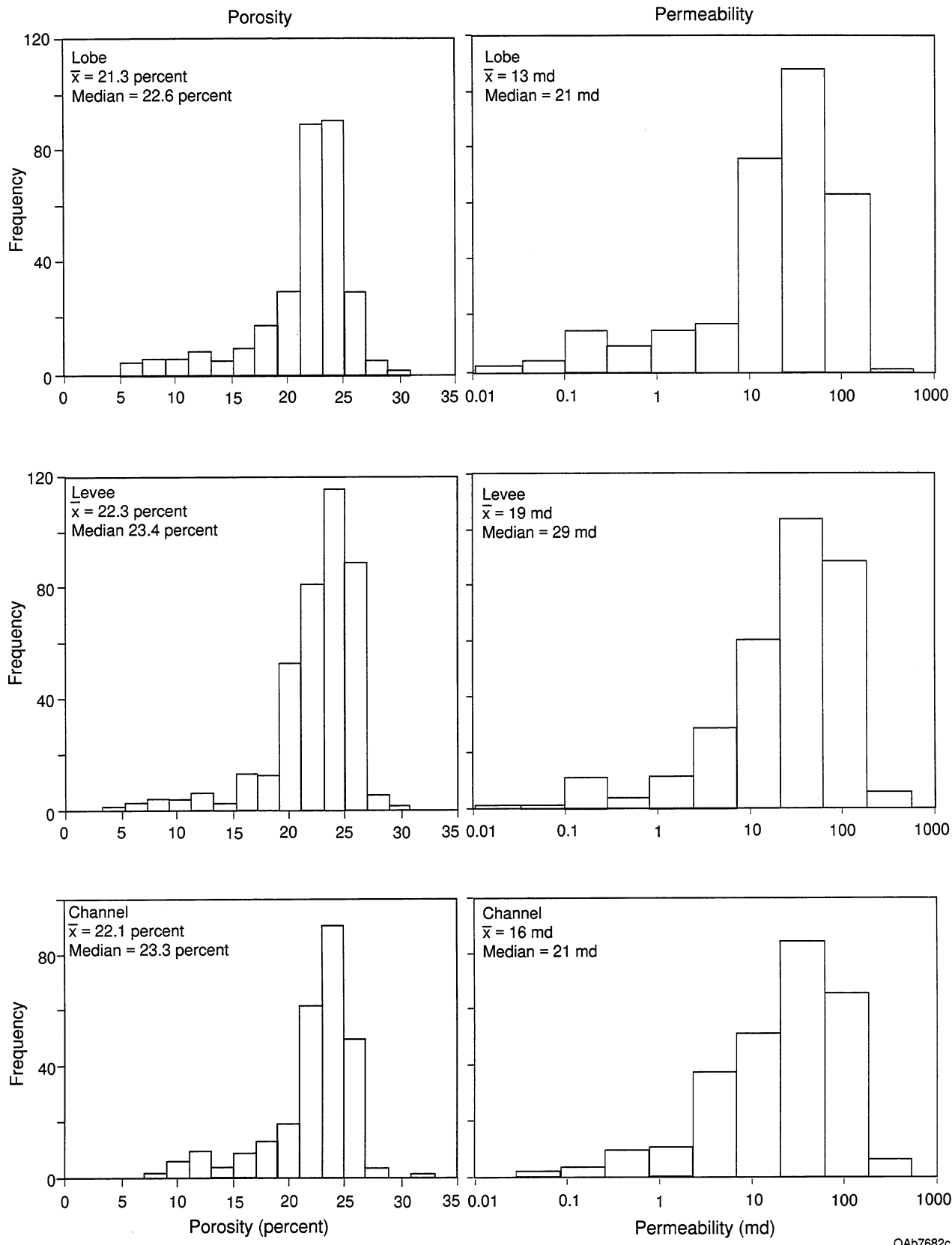
interpreted to be (1) precipitation of chlorite rims, (2) quartz and feldspar overgrowths, and (3) precipitation of calcite cement and minor replacement of framework grains.

Average porosimeter porosity in the petrographic samples is 20.6 percent, and average porosity, determined by point counts of the thin sections, is 18.6 percent. On the basis of thin-section identification, average primary porosity has been found to be 16.4 percent, and average secondary porosity, 2.2 percent. The difference of 2 percent between porosimeter porosity and thin-section porosity provides an estimate of the volume of microporosity.

#### *Diagenetic Controls on Reservoir Quality*

The influence of parameters such as grain size, detrital mineralogy, and volume of authigenic cements on porosity and permeability were analyzed by comparing core analyses with point-count data from thin sections. No statistically significant correlation exists between porosity or permeability and depositional properties such as grain size, percent sand-size grains, sorting, or ductile grain volume. This is unusual for a sandstone, but probably is a result of the narrow range of detrital grain sizes available in the eolian source area. Whereas most sandstones contain ranges of grain size and volumes of detrital clay matrix in different facies, little variation among facies exists in the Ramsey sandstones. As a result, porosity and permeability have very similar distributions in channel, levee, and lobe facies (fig. 31). Porosity and log permeability distributions are negatively skewed, and the low values represent sandstones that have been cemented by calcite.

There is a statistically significant relationship between volume of cement and both porosity (fig. 32) and permeability. Calcite is the most important component of total cement, and it has the greatest impact on reservoir quality. In samples with more than 10 percent calcite cement, geometric mean permeability is reduced to 1.3 md and average porosity to 14.4 percent. Sandstones having less than 10 percent calcite cement have geometric mean permeability of 46 md and average porosity of 23.1 percent. Thus, the main controls on porosity and permeability in the Ramsey sandstones are authigenic cements, particularly calcite, and, to a lesser extent, chlorite.



QAb7682c

Figure 31. Distribution of porosity and permeability in channel, levee, and lobe facies. Porosity and permeability in the three facies are similar because of the narrow range of grain sizes in the system. The low values represent sandstones that have been cemented by calcite.

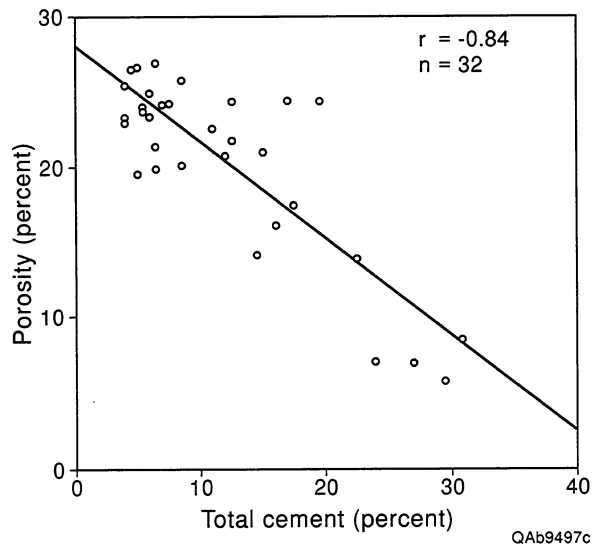


Figure 32. The main controls on porosity and permeability in the Ramsey sandstones are authigenic cements, particularly calcite, and, to a lesser extent, chlorite.

The distribution of calcite cement in Geraldine Ford field can to some extent be determined from the cores because highly calcite-cemented zones have a distinct white color. Calcite-cemented intervals have been noted and described along with other sedimentary features in the core and therefore can be mapped on cross sections (figs. 26, 27). Highly calcite-cemented sandstones occur in all three sandstone facies—channel, levee, and lobe. Most cemented zones in the core are approximately 0.5 to 1 ft thick; their dimensions are unknown, but we assume they are not laterally extensive or continuous. Although they can occur anywhere within the vertical Ramsey sandstone section, they are more common near the tops and bases of sandstones (figs. 26, 27). The source of some of the calcite may be from the adjacent siltstones, which would explain the greater abundance of calcite near the sandstone-siltstone contacts. There may also have been at least a partial internal source of calcite in the sandstones: the detrital carbonate rock fragments and fossils.

Although calcite-cemented zones commonly occur near the top of the Ramsey sandstone, high-permeability values are also common near the top of the sandstone (Dutton and others, 1996). In the Ramsey 2 sandstone, the highest permeability values occur at the top of the unit, with lowest average permeability immediately ( $\approx 1$  ft) below. The high permeability values at the top of the sandstone might indicate permeability enhancement as a result of leaching of calcite cement (Dutton and others, 1996).

No significant difference exists in the porosity versus permeability relationship in channel, levee, and lobe facies (fig. 33). Extensively calcite-cemented sandstones ( $>20$  percent), which have permeabilities  $<1$  md, occur in all three facies. Sandstones with intermediate permeabilities between 1 and 10 md are interpreted to contain moderate amounts of calcite (10 to 20 percent) (fig. 33). High-permeability sandstones occur in all facies but have small volumes of calcite cement.

#### Evaluation of Reservoir Heterogeneity

Microscopic heterogeneity of Ramsey sandstones is controlled primarily by diagenesis. Precipitation of calcite and chlorite have the greatest effect on pore-throat-size distribution.

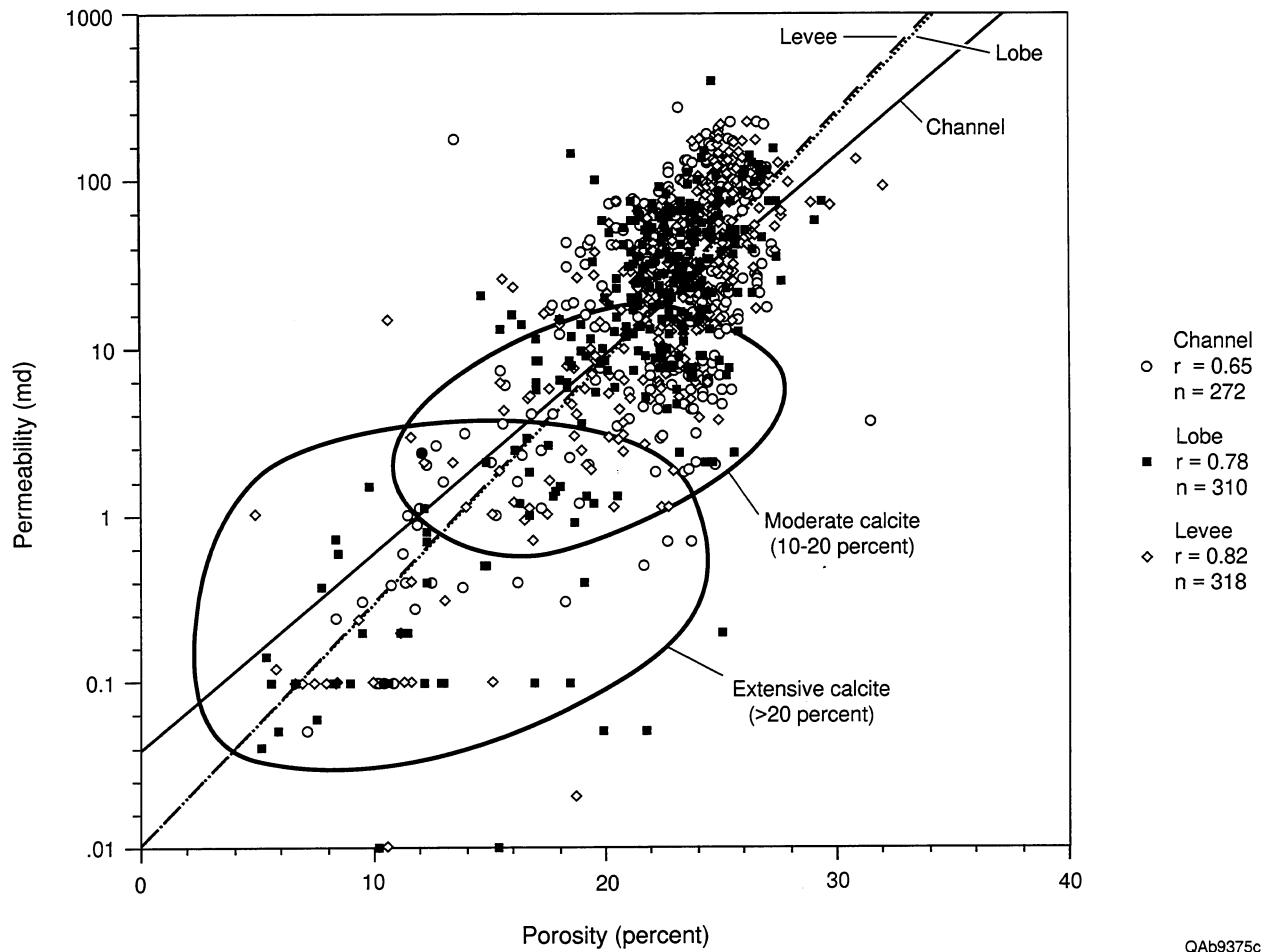


Figure 33. No significant differences exist in the porosity versus permeability relationship in channel, levee, and lobe facies. Calcite-cemented sandstones occur in all three facies.

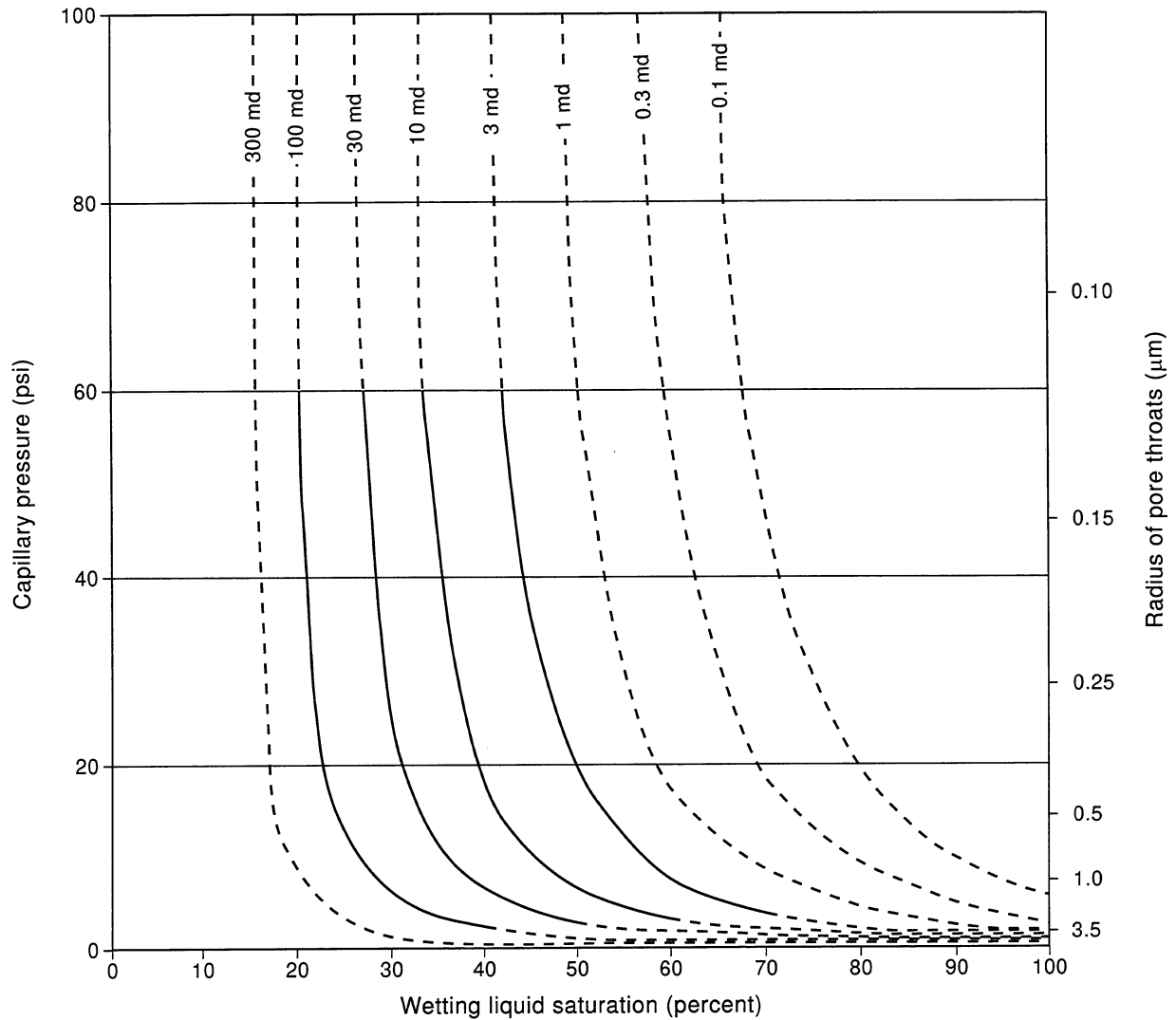
Capillary pressure curves show that in uncemented sandstones, which have permeabilities in the 30 to 300 md range, 60 to 80 percent of pore-throat radii are greater than 1.0  $\mu\text{m}$  (fig. 34). In cemented sandstones having permeabilities of 0.1 to 3 md, only 4 to 40 percent of pore-throat radii are greater than 1.0  $\mu\text{m}$ .

The proposed channel-levee and lobe model for Ramsey sandstone deposition suggests that greater macroscopic (interwell-scale) heterogeneity of reservoir sandstones exists at the Ford Geraldine unit than previously thought (Ruggiero, 1985). Progradation, aggradation, and retrogradation of the system resulted in lateral and vertical offset of channel, levee, and lobe facies (fig. 26, 27). Laminated siltstones and lutites provide the greatest amount of depositional heterogeneity because of the grain size and permeability contrast between sandstone and siltstone facies. The sandstone facies all have similar grain sizes, and thus there may not be much permeability contrast and inhibition of flow at sandstone-on-sandstone contacts, for example where channels incise into lobe facies.

Megascale (field-scale) heterogeneity results from the subdivision of the reservoir into the Ramsey 1 and 2 sandstones. In the northern part of the Ford Geraldine unit, the Ramsey 1 and Ramsey 2 sandstones are separated by a 1- to 3-ft-thick laminated siltstone (SH1) (Ruggiero, 1985), but in the southern part of the Ford Geraldine unit, only the Ramsey 1 sandstone is present (fig. 20).

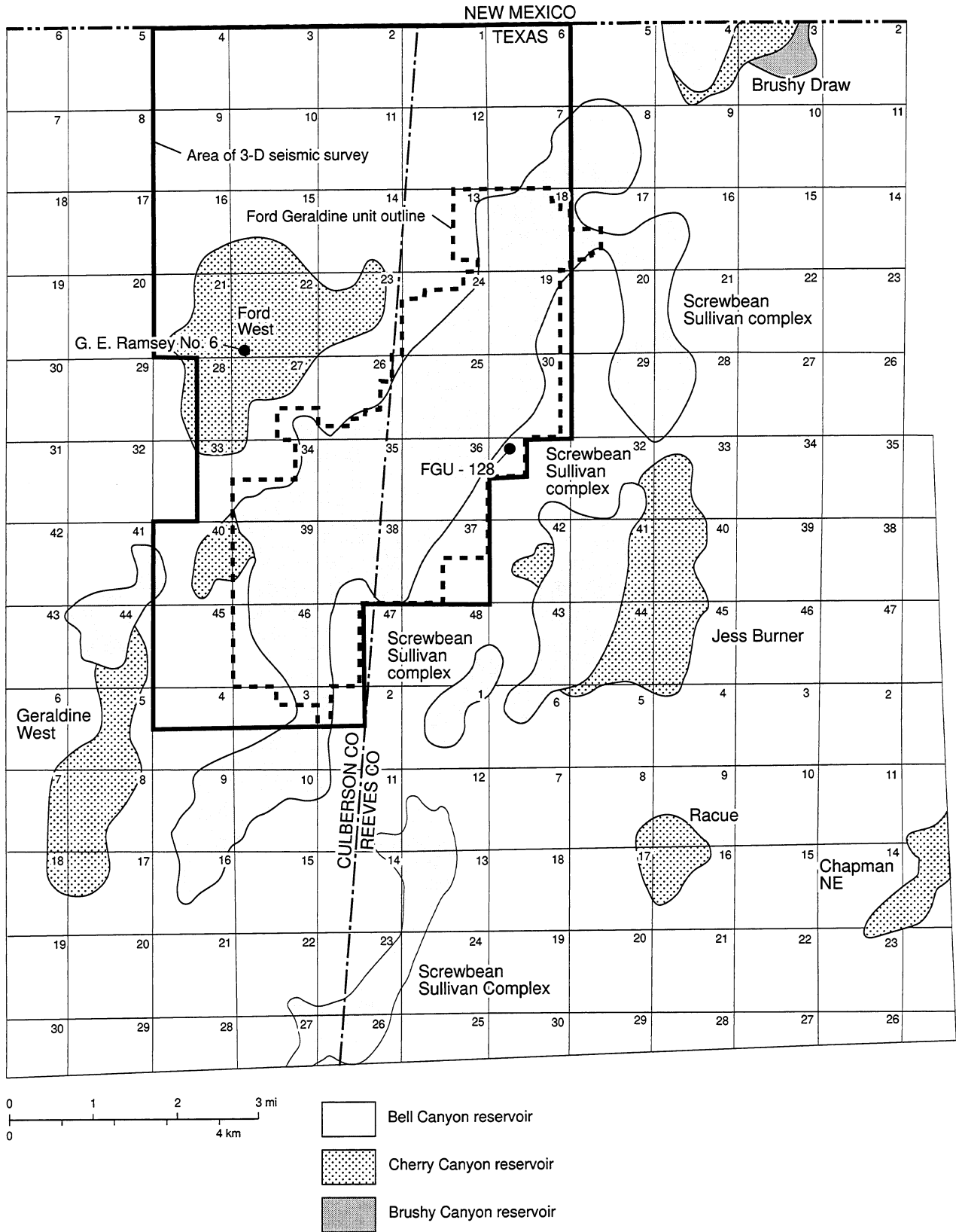
#### Geophysical Interpretation of the Ramsey Reservoir Using 3-D Seismic Data

The upper Bell Canyon Formation Ramsey sandstone was evaluated using 3-D reflection seismic data from a 36-square mile area (fig. 35). These data were acquired over the Geraldine Ford complex, which includes Bell Canyon and Cherry Canyon producing fields, to determine if large-scale heterogeneities in the Delaware Mountain Group could be imaged using 3-D seismic data. This section summarizes the seismic interpretation of the Bell Canyon Ramsey sandstone and the relationship of the seismic data with the reservoir properties data.



QAb9388c

Figure 34. Capillary pressure curves and calculated radii of pore throats for Ramsey sandstones. Curves are based on analyses of 6 samples having permeability ranging from 1.1 to 116 md. Dashed lines indicate extrapolated data. The analyses were done using the centrifuge method with air and kerosene.



QA9374c

Figure 35. Outline of the area in which the 3-D seismic survey was acquired. Also shown are the locations of the Ford Geraldine unit, West Ford field, and other nearby Bell and Cherry Canyon reservoirs, and location of the wells with synthetic seismograms (Conoco G.E. Ramsey No. 6 and FGU-128).

## Synthetic Seismograms and Wavelet Extraction

Synthetic seismograms were generated using the FGU-128 and Conoco G. E. Ramsey No. 6 wells (fig. 35) to correlate the seismic reflection character with the formation tops interpreted from well logs. Both wells penetrate the Ramsey interval, with Ramsey sandstone present in the FGU-128 and absent in the Conoco G. E. Ramsey No. 6.

The FGU-128 well is located on the east side of the Ford Geraldine unit. The synthetic seismogram shows that the base of the Castile Formation salt and the top of the Lamar Limestone produce a peak response that is referred to as the Lamar peak. The trough below the Lamar peak was also picked to help characterize the Ramsey reservoir. This trough, which is referred to as the Ramsey trough, is related to the base of the Ramsey and the top of the Ford siltstone.

The FGU-128 well has 37 feet of Ramsey sandstone in an area of the field associated with 21 percent average porosity (fig. 8); the well has a cumulative production of approximately 45,000 bbl of oil. Measured by a wavelet derived from the seismic data, the Ramsey sandstone in this well is less than 1/4 wavelength thick. This wavelet was derived from the data set between 250 and 1500 milliseconds and was used to derive the seismograms. The wavelet has moderated side-lobe energy but is quite low frequency for imaging the Delaware Mountain Group. Ormsby or Ricker theoretical wavelets (8-14-50-60 Hz and 28 HZ, respectively) approximate the derived wavelet. The maximum thickness of the Ramsey sandstone in the field is 61 feet, which would be approximately 1/4 of a wavelength thick. Therefore the Ramsey sandstone is always below the tuning thickness of this seismic data and is considered a thin bed.

The Conoco G. E. Ramsey No. 6 well is located on the west side of the survey (fig. 35) and has no Ramsey sandstone present. This allows a comparison of the seismic response of a well with Ramsey sandstone to a well without Ramsey sandstone. The peak amplitude at the top of the Lamar is 5 percent greater in the Conoco G. E. Ramsey No. 6 well's synthetic than that of the FGU-128 well. The Ramsey trough is a single broad trough in the well without sandstone and a doublet in the well with sandstone. The amplitude of the Ramsey trough is also 10 percent greater

in the well without sandstone. Due to the shallow depth and lack of recovering high-frequency data in the area the actual seismic data are too noisy to detect accurately the scale of amplitude differences needed to see between these synthetic models. The seismic data are probably too noisy to differentiate accurately the shape of the trough from areas with sandstone and areas without sandstone. However, on a representative seismic line, the amplitudes of the Lamar peak and Ramsey trough are slightly greater at the Ramsey No. 6 location (well with Ramsey sandstone absent) than at the FGU-128 location (well with Ramsey sandstone present).

### Structure, Amplitude, and Coherency Cube Maps

A structure map of the top of the Lamar was made by depth-converting the Lamar time horizon using an average velocity gradient calculated to be between the seismic datum and the Lamar. All wells were used to calculate the structure map, which shows a gentle northeast dip into the deeper portion of the Delaware Basin. A structure map of the top of Ramsey sandstone was created in the same manner, using the Ramsey time horizon. A residual map of the Lamar peak was generated by filtering the Lamar peak horizon with a  $60 \times 60$  filter, then subtracting the resulting smoothed horizon from the original horizon. The residual map shows localized highs and lows. The residual accentuated the subtle high ridge in the structure map that is related to differential compaction over the main Ramsey 1 channel (figs. 15, 22). Another residual high is present in the Stage 5 area where the Ramsey 1 and Ramsey 2 channels stack.

The amplitude map of the Ramsey trough is simply an amplitude extraction on that seismic marker. The Ford Geraldine Unit produces from the area of higher negative amplitudes. One of the best parts of the field, the stage 5 (demonstration) area, is located in the area of the highest amplitude to the north. A trend of slightly lower amplitudes extending though the axis of the field corresponds to a Ramsey sandstone thick (fig. 22).

The seismic volume was processed using the coherency cube transform to identify channels, compartmentalization, or fracturing in the Delaware Mountain Group. Coherency cubes were derived using three, five, and seven trace windows. It was determined that the five-trace window

was best for imaging the upper Delaware section. The coherence extraction on the Lamar shows a crude outline of the productive wells in Ford Geraldine Unit but is not of high enough resolution to determine compartmentalization and does not indicate faulting in the Ramsey sandstone.

#### Correlation Coefficients and Cross Plots

Twenty seven different seismic attributes were generated and cross plotted with various rock properties (such as porosity and permeability), production, and initial potentials over the entire field. Table 3 lists the top 24 correlation coefficients of the more than 300 calculated. The best correlation coefficient (0.49) was calculated using wells only in the Stage 5 area. The other correlation coefficients were calculated using the wells from the entire field. Consistently higher correlation coefficients were derived from cross plots of an amplitude attribute and porosity  $\times$  thickness or average porosity. Attributes derived from the Ramsey trough had consistently higher correlation coefficients than those calculated from the Lamar peak, a composite amplitude, or a window encompassing both the trough and the peak.

The plot of Ramsey root-mean-square (RMS) amplitude (RMS amplitude extracted over a 10-millisecond window centered on the Ramsey trough) versus average porosity, using the well data set from the entire field, exhibits the best correlation. The cross plot shows a wide scatter of points related to the low correlation coefficient of  $-0.39$ . In this case a high amplitude could correlate to either a low or high porosity value and a low amplitude could correlate to either a moderate or high porosity value. The porosity values from the field are limited in range, and a larger range of porosity samples might produce a higher correlation coefficient between the seismic amplitudes and porosity. The cross plot of Ramsey RMS amplitude against waterflood cumulative production to 1991 in the stage 5 area shows the best correlation coefficient of 0.49. This shows that limiting the data to the 45 wells in the Stage 5 area increased the correlation coefficient.

Table 3. Highest correlation coefficients calculated from the data set of seismic attributes cross plotted with various rock properties. Note highest correlation coefficient is 0.49.

	<b>Well log data</b>	<b>Seismic data</b>	<b>Correlation coefficient</b>
1	Waterflood cum 91	ramsey amp	0.49483
2	PHI avg	ramsey rms amp	-0.385492
3	PHI*h	ramsey rms amp	-0.3789
4	PHI*h	ramsey avg refl str	-0.377348
5	PHI*h	ramsey avg abs amp	-0.373124
6	PHI*h	ramsey avg trough	-0.370042
7	net pay >20%	ramsey rms amp	-0.36707
8	PHI avg	ramsey avg abs amp	-0.366438
9	PHI avg	ramsey avg trough	-0.365114
10	PHI avg	ramsey avg refl str	-0.36059
11	PHI*h	ramsey amp	0.360253
12	net pay >15%	ramsey comp	-0.351354
13	average perm	ramsey comp	-0.351354
14	net pay >15%	ramsey avg refl str	-0.349957
15	average perm	ramsey avg refl str	-0.349957
16	net pay >20%	ramsey avg abs amp	-0.34856
17	net pay >20%	ramsey avg refl str	-0.345852
18	net pay >15%	ramsey avg trough	-0.345775
19	average perm	ramsey avg trough	-0.345775
20	net pay >15%	ramsey rms amp	-0.345281
21	average perm	ramsey rms amp	-0.345281
22	net pay >15%	ramsey avg abs amp	-0.341708
23	average perm	ramsey avg abs amp	-0.341708
24	net pay >15%	ramsey amp	0.337709

## Conclusions

Accurately characterizing the Ramsey sandstone is difficult because Ramsey sandstone thickness is always  $\leq 1/4$  wavelength of the seismic data. This puts the Ramsey sandstone into the thin bed category. Nonuniqueness becomes likely since other factors such as velocity and thickness of the Lamar limestone and composition of the Ford siltstone affect the seismic interval that is being used to characterize the Ramsey.

The coherency cube data are effective in delineating the field outline, but probably not as effective in detecting reservoir compartmentalization. Residual mapping of the Lamar assisted in visualizing thick sandstones associated with the Ramsey 1 sandstone near the center of the field. Slight ridges can be seen in the structure map, but the residual maps make these ridges more obvious. Amplitude attributes were also effective in identifying the outline of the field. It was observed, however, that although high amplitudes identify the outline of the field, they are also associated with little or no sandstone, whereas low amplitudes are associated with the residual high and thick sandstone area in the center of the field.

Twenty-seven seismic attributes were calculated and cross plotted with various rock properties such as porosity and permeability, production, and initial potentials over the entire field. The amplitude family of attributes consistently correlated best to reservoir properties. In addition, the rock properties of average porosity and porosity x thickness consistently correlated best to the seismic attributes. The cross plots of the best relationships between rock properties and seismic attributes exhibit significant scatter and have correlation coefficients less than 0.4.

## Fluid Characteristics

Fluid characteristics of the Geraldine Ford field are summarized in tables 4 and 5. Initial pressure in the field was 1493 psi. Pressure declined in the reservoir during primary production to 400 psi by June, 1969 (fig. 36). Oil gravity is 40° API. Reservoir temperature is 83°F, and the original bubble point pressure was 1,383 psi.

Table 4. Fluid characteristics of reservoir.

Initial reservoir pressure	1,493 psi
Reservoir temperature	83°F
Oil gravity	40°
Oil viscosity	1.4 cp
Oil viscosity at in-situ reservoir condition	0.77 cp at 82° F and 1,380 psi
Initial oil formation volume factor ( $B_o$ )	1.287 at bubblepoint
Bubble point pressure	1,383 psi
Initial gas in solution ( $R_s$ )	575 solution GOR, scf/bbl
Fluid composition (sample from FGU-157)	$CO_2 = 0.01$ $N_2 = 0.04$ $H_2S = Nil$ Hydrocarbons = 99.95
Gas gravity	1.135
Gas viscosity	0.07 cp
Initial gas formation volume factor ( $B_g$ )	0.001522 bbl/scf at bubblepoint pressure
Water density	62.4 lbs/ft <sup>3</sup>
Water viscosity	0.95 cp
Water salinity	72,200 to 105,000 ppm total dissolved solids

Table 5. Reservoir pressure and fluid properties.

Pressure (psig)	Fluid Properties		
	Formation volume factor		Initial gas in solution Rs (SCF/STB)
	Oil Bo (bbl/STB)	Gas Bg (bbl/SCF)	
1383 (bubblepoint)	1.278	0.001522	574
1181	1.253	0.001875	512
1076	1.241	0.002083	480
1008	1.232	0.002254	460
878	1.216	0.002619	419
771	1.204	0.003019	386
692	1.192	0.003392	360
524	1.170	0.004509	306

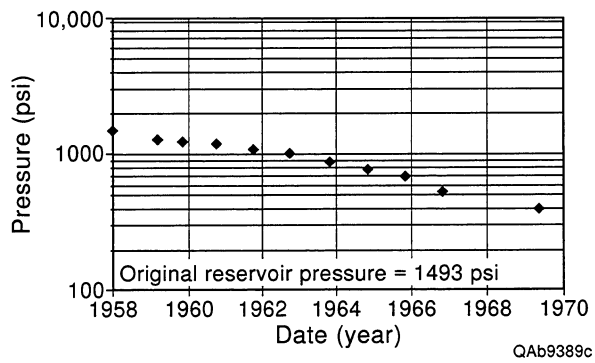


Figure 36. Plot of average reservoir pressure through time for Geraldine Ford field during the period of primary recovery.

## FIELD DEVELOPMENT HISTORY

### Primary Recovery

Primary recovery in the field began 1956 and continued until June 1969. A total of 301 wells were drilled for primary production. Primary cumulative production was 13.2 MMbbl (figs. 37, 38), or 13.3 percent of the 99 MMbbl of original oil in place.

### Secondary Recovery

The Ford Geraldine unit was formed in November 1968, and a pilot waterflood project started in June 1969 (Pittaway and Rosato, 1991). The waterflood was expanded throughout the southern part of the unit in stages between 1972 and 1980 (fig. 4), but the Stage 5 area received only a short, low-volume waterflood. Eighteen new producing wells and 6 new water-injection wells were drilled for the waterflood, and 67 old wells were converted for water injection.

The best response was from the same area that had exhibited high primary production (fig. 39). An additional 6.8 MMbbl of oil was produced after unitization, but only 3.5 MMbbl was attributed to the waterflood (fig. 37), significantly less than predicted from reservoir simulation. By the end of secondary development, recovery efficiency had increased to only 22.5 percent. Of that, 18 percent is attributed to primary recovery and 4.5 percent to secondary recovery (Pittaway and Rosato, 1991).

### Tertiary Recovery

Tertiary recovery by CO<sub>2</sub> injection began in March, 1981, in the entire unit except for the Stage 5 area (fig. 4), but CO<sub>2</sub> supply was erratic until December 1985. Production response occurred in 1986 after higher and constant CO<sub>2</sub> injection began in December, 1985 (fig. 37) (Pittaway and Rosato, 1991). Six new producing wells and 4 new CO<sub>2</sub>-injection wells were drilled for the flood, and 97 old wells were converted for CO<sub>2</sub>-injection, including some water-injection

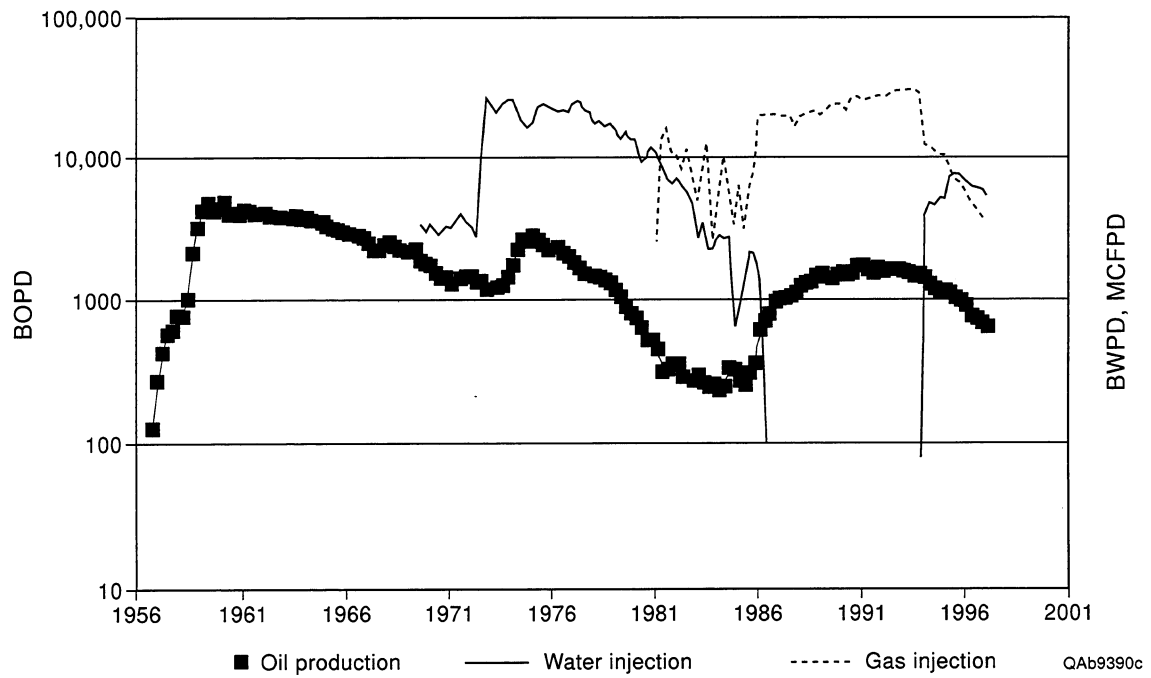
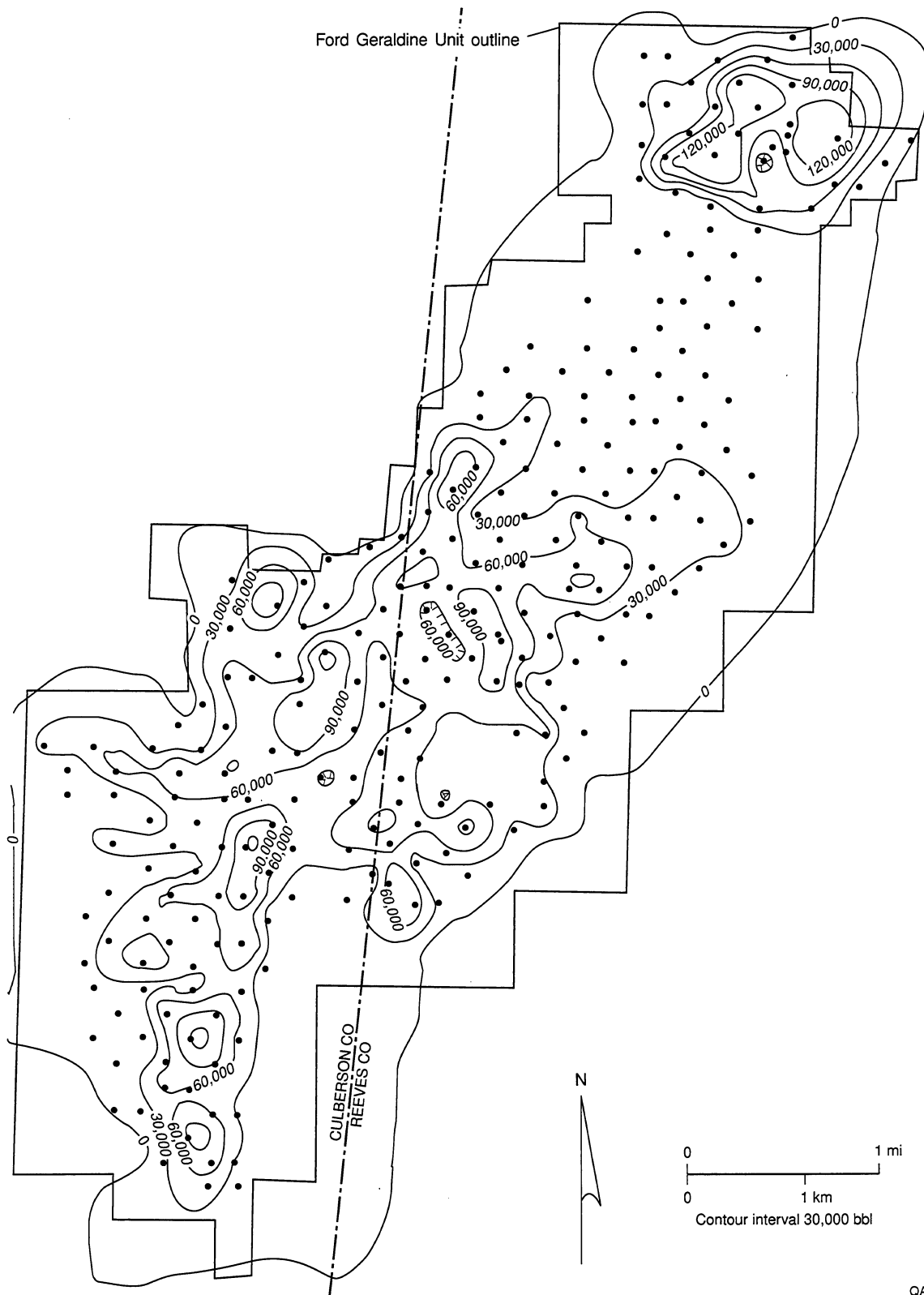


Figure 37. Plots of primary, secondary, and tertiary production in the Ford Geraldine unit, and volumes of water and CO<sub>2</sub> injected.



QA8060c

Figure 38. Map of primary recovery for the Ramsey sandstone in the Ford Geraldine unit, Reeves and Culberson Counties, Texas. The highest oil recovery is in the southwest part of the unit. To the northeast (structurally downdip) there is an isolated area of high oil recovery. The high recoveries to the southwest are from the Ramsey 1 sandstone, and the high recoveries to the northeast are from the Ramsey 1 sandstone and the overlying Ramsey 2 sandstone. The Ramsey 2 sandstone is not developed to the southwest; therefore the Ramsey 2 sandstone represents a separate trap.

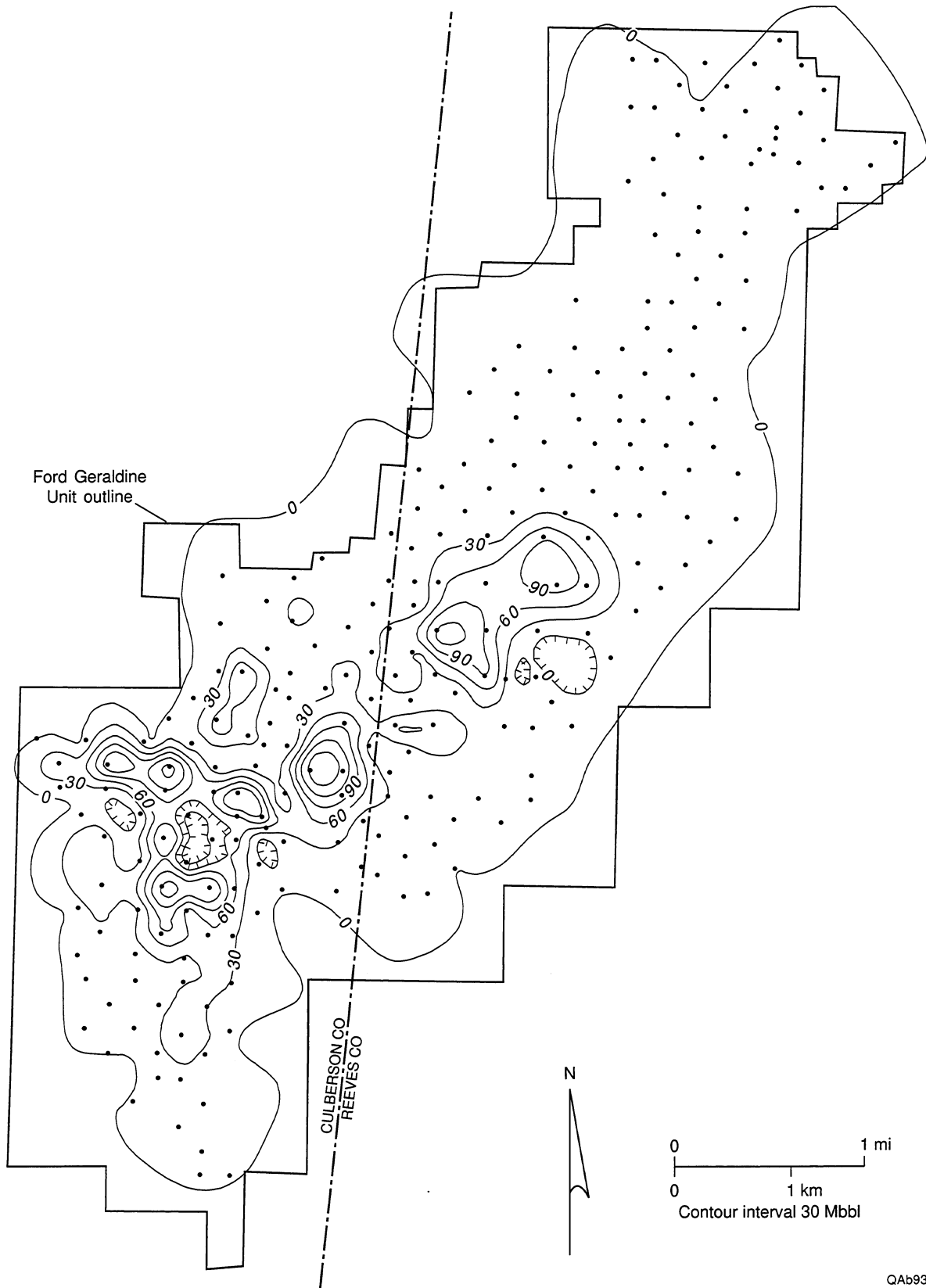


Figure 39. Map of secondary production resulting from the waterflood conducted from 1969 to 1980. Only minor water injection was done in the Stage 5 area (shown in fig. 4) at the northern end of the field.

wells. Cumulative tertiary production to date has been 5.7 million barrels (fig. 40), and tertiary recovery efficiency is 5.8 percent. Estimated ultimate tertiary recovery is 9.0 percent (K. R. Pittaway, written communication, 1997).

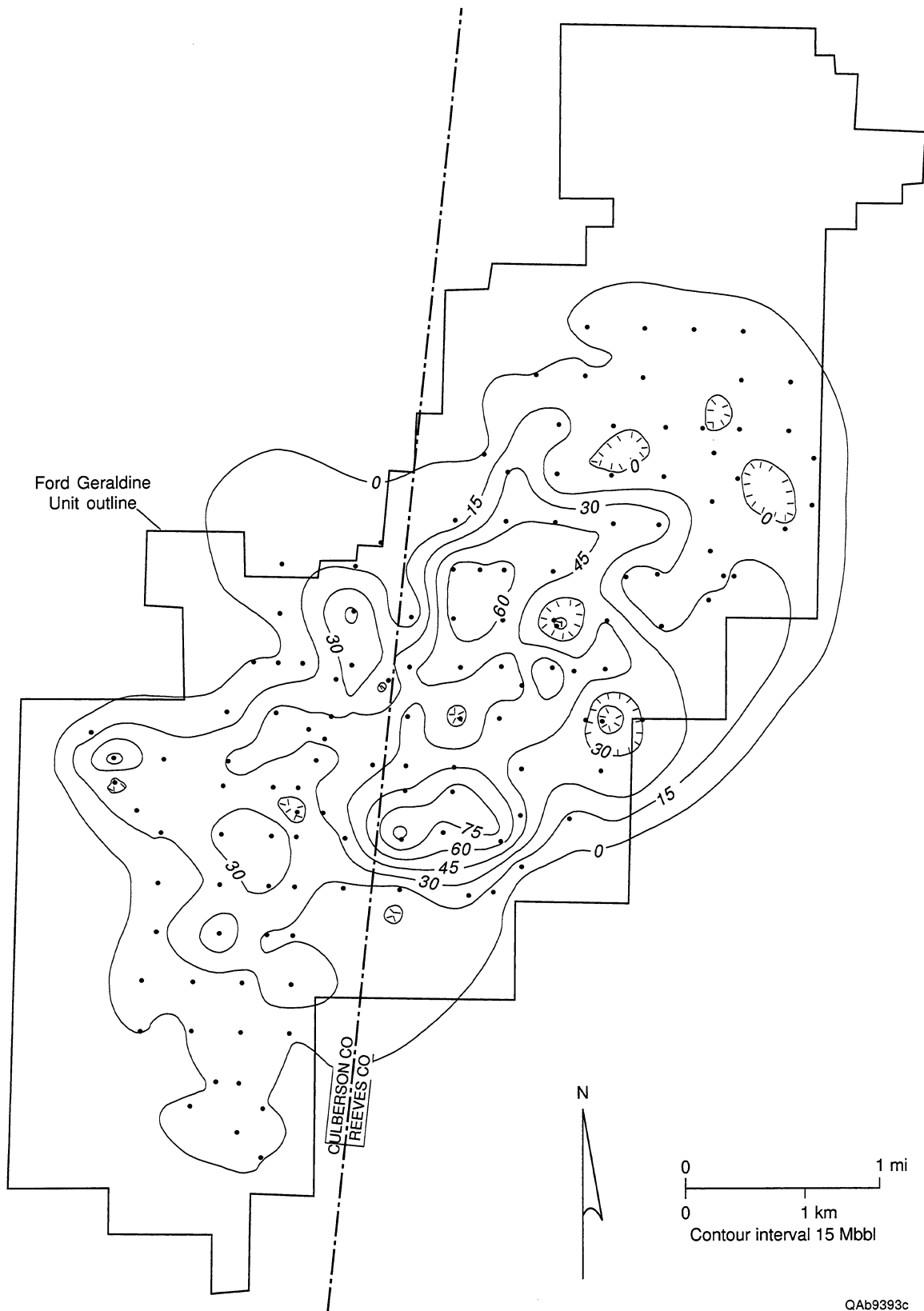
## FIELD PRODUCTION CONSTRAINTS AND DESIGN LOGIC

### Review of Reservoir Description and Development History

The proposed channel-levee and lobe model for Ramsey sandstone deposition suggests that greater lateral heterogeneity of reservoir sandstones exists at Ford Geraldine unit than previously thought (Ruggiero, 1985). Progradation, aggradation, and retrogradation of the system resulted in lateral and vertical offset of channel, levee, and lobe facies. Laminated siltstones and lutites provide the greatest amount of depositional heterogeneity because of the grain size and permeability contrast between sandstones and siltstone facies. The sandstones facies all have similar grain sizes, and thus there may not be much permeability contrast and inhibition of flow at sandstone-on-sandstone contacts, for example, where channels incise into lobe facies. Localized precipitation of calcite cement increases heterogeneity within the sandstones. Although the cemented zones are not interpreted as being laterally continuous between wells, their presence causes “spiky” vertical permeability trends (fig. 18) in the reservoir. Fluid flow is likely to occur preferentially along the high permeability streaks, leaving poorly swept zones of lower permeability.

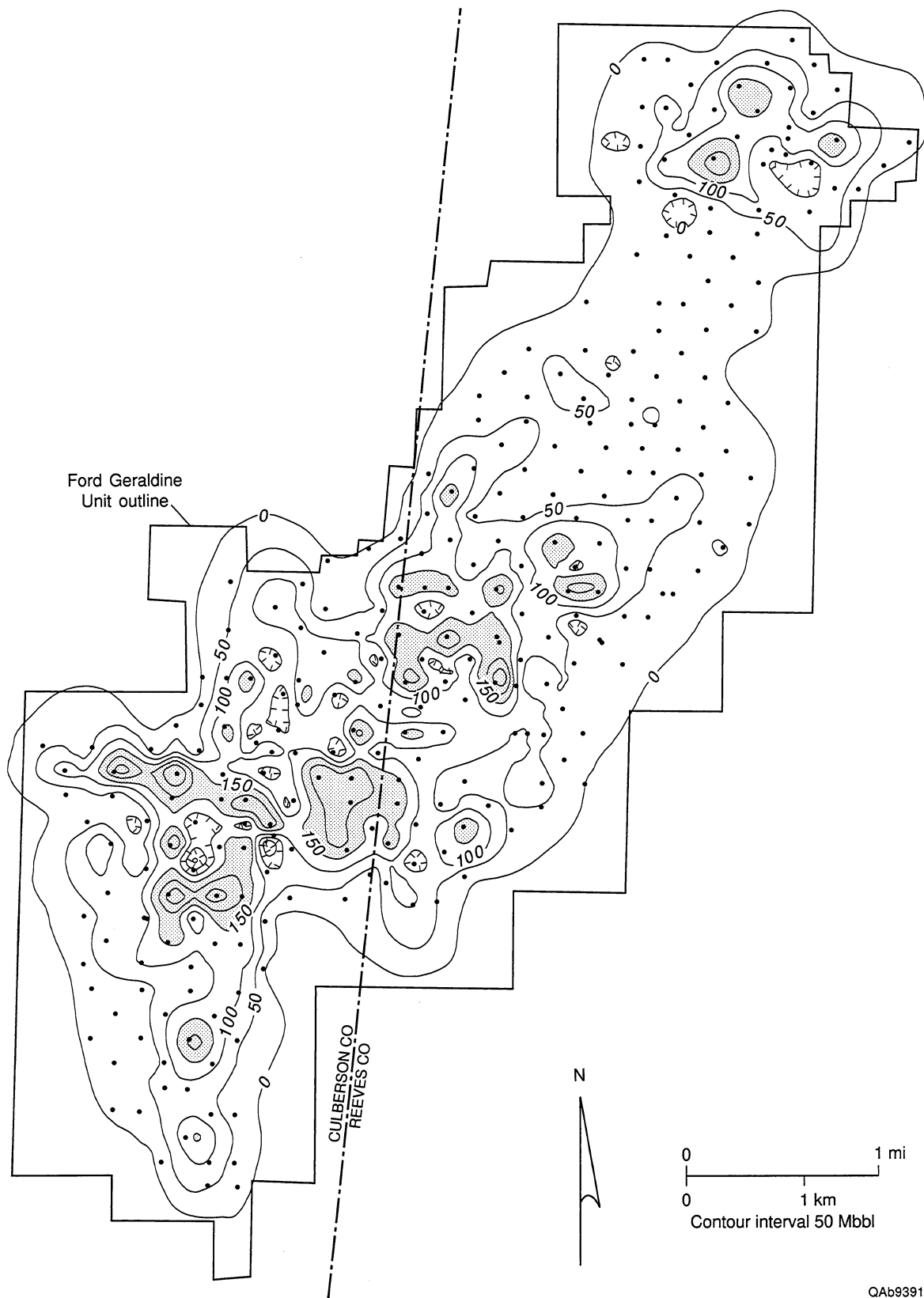
Many of the reservoir properties of the field are not continuous but instead show areas of good porosity and permeability separated by poorer areas (figs. 8, 14), particularly on the margins of the field. These marginal zones of better reservoir quality are interpreted as being levee deposits that formed when low-density turbidity currents overtopped the channel margins and deposited sand in the generally lower-quality interchannel areas. Some of the discontinuity between areas of better reservoir quality may have been enhanced by diagenetic effects as well.

Production from the field generally follows structure, with many, but not all, of the best producing wells occurring along the crest of the compactional anticline (figs. 15, 41). Production



QAb9393c

Figure 40. Map of tertiary production through 1995 resulting from the CO<sub>2</sub> flood that started in 1981. The Stage 5 area (shown in fig. 4) has not been CO<sub>2</sub> flooded.



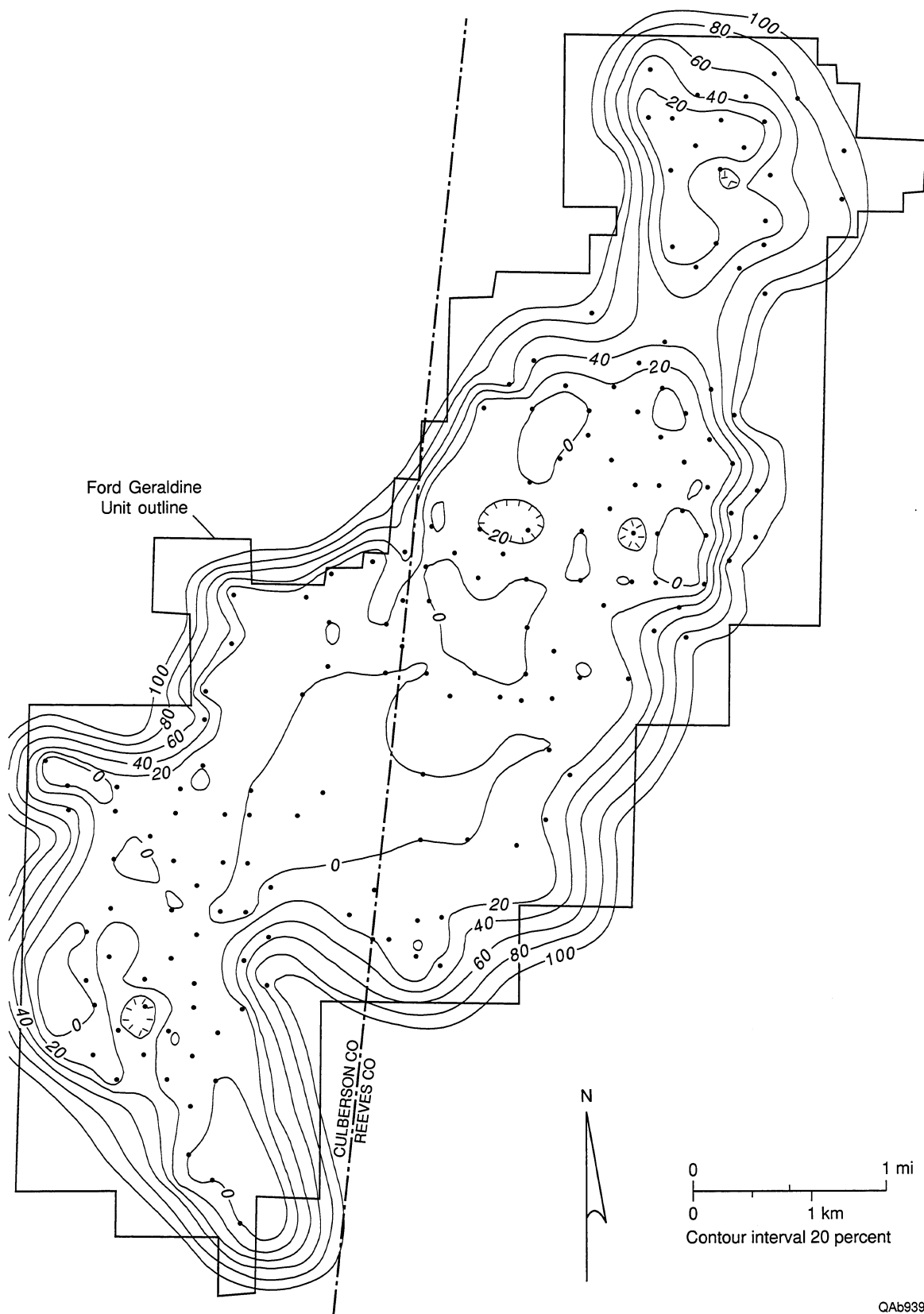
QA9391c

Figure 41. Map of total production from the Ford Geraldine unit through 1995.

from the south part of the field is apparently controlled by a combination of structure and updip porosity pinchout. The best producing wells at the south end of the field are displaced toward the west (up structure) from the trend of thickest Ramsey 1 sandstone (compare figs. 22 and 41). The east-west pattern of good production along the northwestern margin of the field follows a channel trend within the Ramsey 1 sandstone, where the sandstone bifurcates (fig. 22). The trap is primarily stratigraphic, caused by pinchout of the sandstone into low permeability siltstone to the northwest.

There is a distinct separation between production from the northern and southern parts of the field (fig. 41), with a broad area of low total production in between. This separation is not caused simply by sandstone pinchout against a large erosional remnant, as was suggested by Ruggiero (1985), because the Ramsey 2 sandstone pinches out south of the low-producing area (fig. 24). The low-producing zone does include an area where Ramsey 1 sandstone thins markedly over an erosional remnant (fig. 22), but it also includes the thick Ramsey 1 sandstone channel that swings around to the east and south of the remnant. The most likely explanation for low oil production in this area is a combination of (1) high water production, (2) poor reservoir quality, (3) thin Ramsey 1 sandstone in part of the area, and (4) low structural position where the Ramsey 1 sandstone is thick. A zone of high water cut during initial production tests (fig. 42) corresponds to the center of the low-producing zone (fig. 41), and the area of high water cut expanded during primary production. A map of water cut in 1969 (fig. 43), before any water had been injected into the northern part of the field, shows that a wide zone of high water cut (76–100 percent) had extended all the way across the field by this time. In addition to high water production, this same area contains some of the poorer quality reservoir rock in the field, having lower average porosity (fig. 14) and permeability (fig. 8) and a high volume of clay. Finally, as mentioned above, the Ramsey 1 sandstone thins over an erosional remnant in this area, and where sandstones are thick to the east and south of the erosional remnant, they are in a structurally low position (fig. 22).

Total production from Ford Geraldine unit wells shows a statistically significant positive correlation with mobile oil saturation, net pay, and average porosity (table 6) and significant



QAb9392c

Figure 42. Map of the percentage of water (water cut) produced during initial potential (IP) tests.

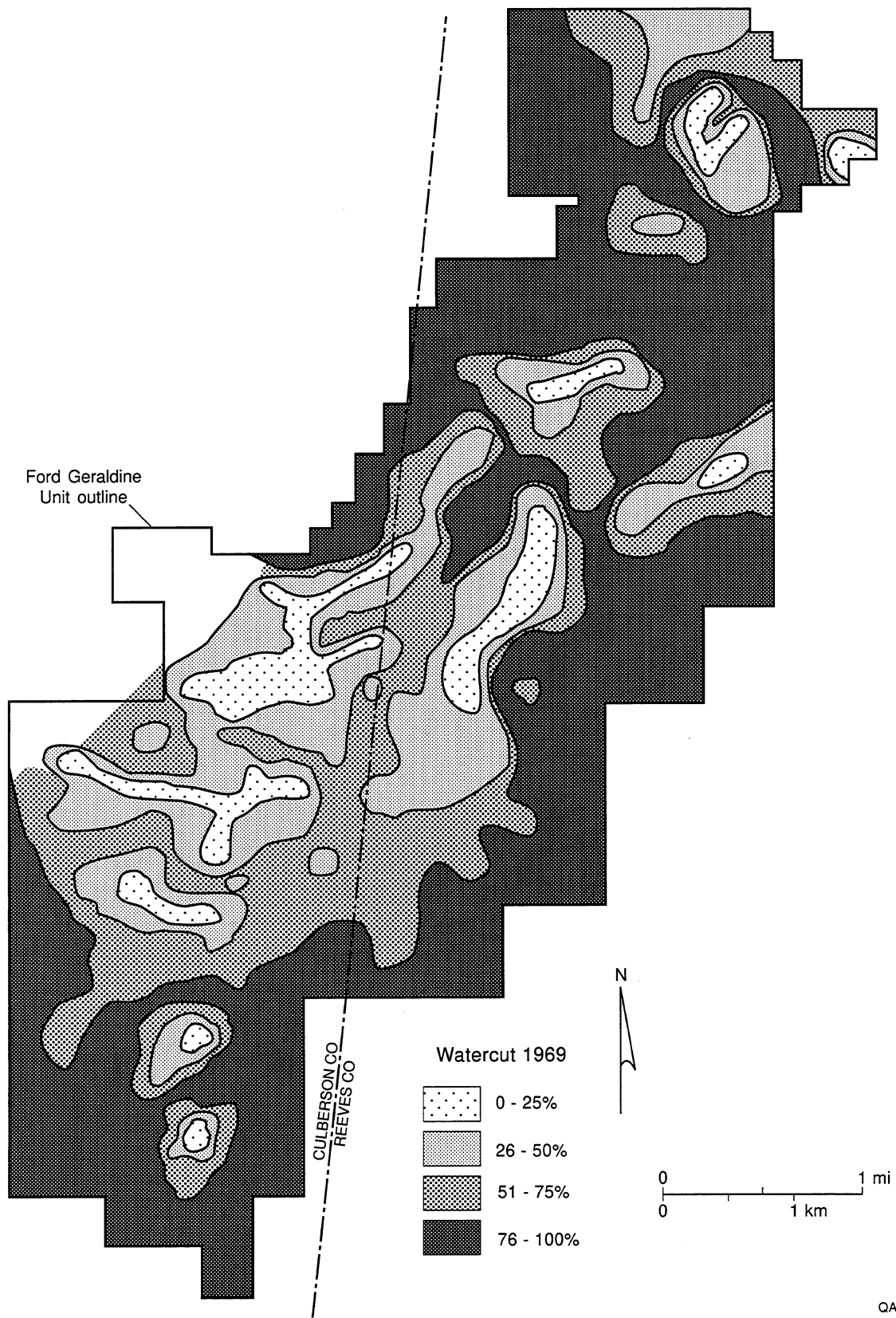


Figure 43. Map of water cut at the end of primary production in 1969 (from Conoco, 1979). The area of good production at the northern end of the field is separated from the rest of the field by an area of high water cut.

Table 6. Highest correlation coefficients calculated from the data set of petrophysical parameters cross plotted with total recovery from Ford Geraldine unit wells through 1995. All the parameters listed are statistically significant at the 95-percent confidence level.

	<b>Parameter</b>	<b>Correlation coefficient</b>
1.	Water cut measured during IP tests	-0.25
2.	Mobile oil saturation	0.24
3.	Volume of clay	-0.23
4.	Net pay (porosity >20 percent)	0.23
5.	Average porosity	0.22
6.	Water saturation (percent)	-0.22
7.	Net pay (porosity >15 percent)	0.22

negative correlation with percent water cut measured during initial potential (IP) tests (fig. 42), volume of clay, and water saturation. The percentage of water produced during IP tests is the single best predictor of eventual total production from a well. The low correlation coefficients indicate that many factors influenced total production. Furthermore, some of the relationships are likely to be non-linear.

### Constraints on Further Producibility

High volumes of water production are a potential constraint on further producibility from the demonstration area at the northern end of the Ford Geraldine unit. This reservoir had a high initial water saturation of 46 percent at discovery. Many wells were fractured during well completion, and some of the fractures may have penetrated the water zone. There is evidence that aquifer water has also encroached into the demonstration area. As a result of all these factors, the produced water-cut toward the end of primary depletion was very high (fig. 43). Therefore, secondary recovery by waterflood was neither effective nor economical in this area. It seems likely that the reservoir can be further produced only through an improved recovery process like a CO<sub>2</sub> flood.

The other main constraint on producibility of the Ford Geraldine unit is the geologic heterogeneity of the reservoir, which is caused by a combination of depositional and diagenetic processes. Laminated siltstone beds and extensively calcite-cemented sandstones are the most important causes of reservoir complexity and reduced sweep efficiency. A laminated siltstone (SH1) that is continuous across the northern part of the unit subdivides the Ramsey reservoir into Ramsey 1 and 2 sandstones. These sandstones are in turn further subdivided by smaller siltstones (fig. 26) that are of sufficient extent to be correlated in several wells. The calcite-cemented zones apparently are not large enough to correlate between wells, but the complexity that they add to the reservoirs probably contributes to reduced sweep efficiency.

## Method of Problem Detection

The problem of water production was apparent because of high water-cut. It was confirmed by the pilot waterflood initiated by Conoco in the demonstration area in 1980 and by simulation studies.

The geologic heterogeneity of the Ramsey sandstone was determined by the detailed characterization of the reservoir that was conducted during Phase 1. Study of outcrop analogs of these reservoirs, description of cores from the reservoir interval, subsurface correlation of logs, petrophysical analysis, and interpretation of the 3-D seismic data all contributed to the understanding of this heterogeneous reservoir.

## Proposed Solution for Reduction of Constraints

In the first phase of this project, detailed geological and engineering characterization of the reservoir provided a better understanding of the reservoir parameters. Oil-bearing portions of the formation were identified, and current fluid saturations were determined. A conditionally simulated permeability model was also generated. Simulation studies were performed under conservative but realistic conditions for CO<sub>2</sub> flood. Results indicated that 10 to 30 percent (1 to 3 MMbbl) of remaining oil in place can be produced by CO<sub>2</sub> injection and that water production will be much lower than during waterflood. To further reduce the potential problem of high water production, it is recommended that the CO<sub>2</sub> flood be confined to the northern part of the Stage 5 area (section 18, fig. 2) to avoid the part of that area in section 19 that has experienced high water cuts (figs. 42, 43) and low productivity (fig. 41).

To minimize the impact of geologic heterogeneity, CO<sub>2</sub> should be injected into both the Ramsey 1 and Ramsey 2 sandstones, above and below the SH1 siltstone. The highest average porosity and permeability in the Ramsey 2 sandstone follows the trend of the channel that cuts through the eastern side of the Stage 5 area (fig. 24). This trend of higher permeability should be taken into account when determining the injection rates in wells that penetrate the channel so that

lower injection rates could be used where a line of injectors crosses the channel trend (Ruggiero, 1985). The goal is to avoid rapid breakthrough of CO<sub>2</sub> along high permeability pathways.

### Evaluation

Results of field performance under CO<sub>2</sub> flood will be monitored and evaluated, and any differences in actual recovery from the ones predicted by simulation studies will be interpreted for future application of this recovery process in other, similar reservoirs.

## EVALUATION OF COST-SHARE PROJECT RESULTS

### Type of Project

This report summarizes the results of reservoir characterization of the Ford Geraldine unit. The demonstration for this project will be a tertiary CO<sub>2</sub> flood at the northern end of the field (Stage 5 area, fig. 4), which will be conducted during Phase 2 of the project.

### Simulation Study

To make reliable predictions of tertiary recovery from the demonstration area, fluid-flow simulations of CO<sub>2</sub> flooding were conducted as the final task of the reservoir characterization phase. These simulations were based on stochastic permeability distributions and geologic characterization of the reservoir. The first step to simulate the pilot area was to generate interwell permeability distributions using geostatistical techniques. Production and other reservoir data were used to make preliminary estimates of tertiary recovery from the demonstration area with a CO<sub>2</sub> flood.

## Geostatistical Permeability Modeling

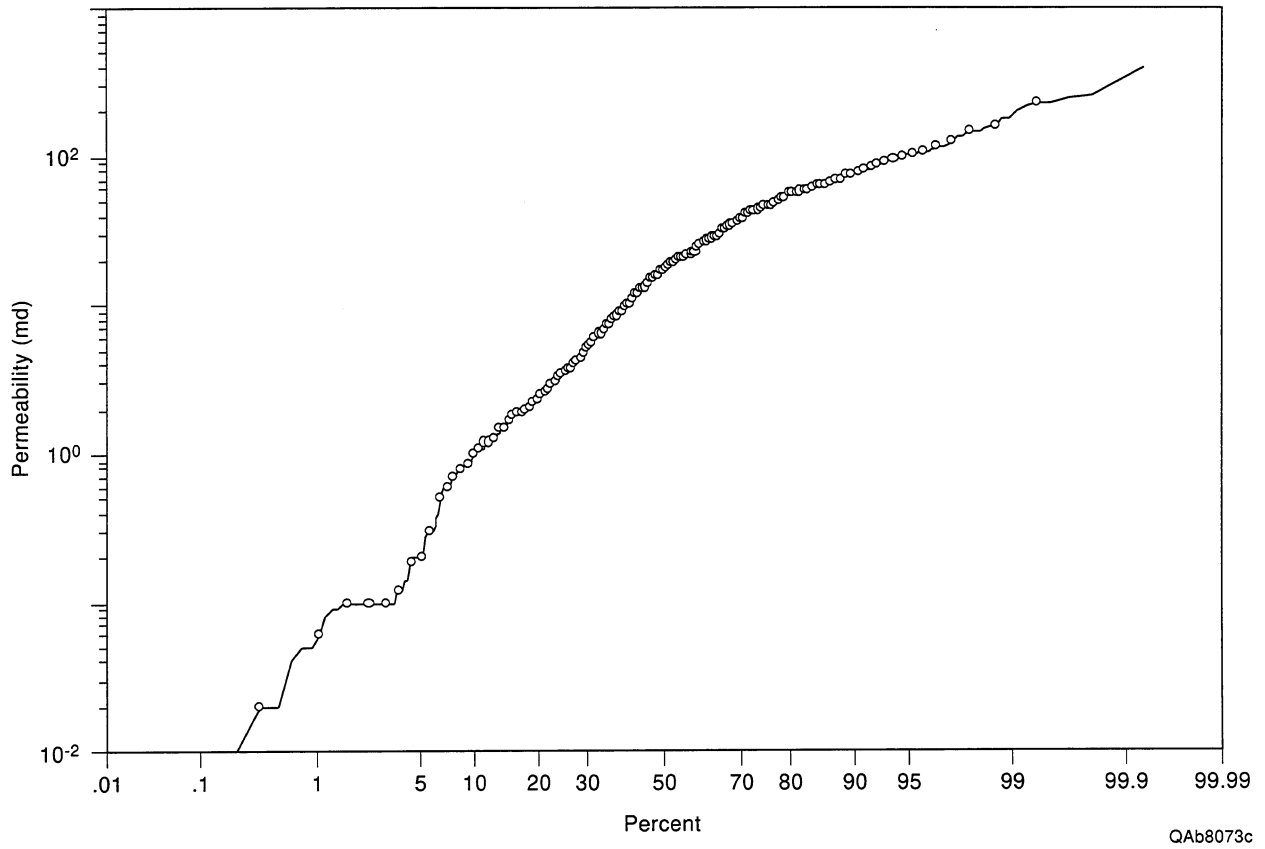
Heterogeneity must be adequately represented to model subsurface reservoirs reliably. It is especially challenging to represent permeability heterogeneity because it cannot be directly mapped by any existing techniques. Geostatistical methods are commonly used to generate interwell permeability distributions. In the technique called conditional simulation, the generated field honors the measured data, follows a desired correlation structure, and maintains reasonable heterogeneity (Journel and Huijbregts, 1978; Hewett, 1986; Lake and Malik, 1993; Malik, 1996).

### *Data Evaluation*

For conditional simulation, the available permeability data have to be examined to determine their distribution. The cumulative distribution function (CDF) is a convenient tool for this purpose. The CDF of a data set with a normal distribution plots as a straight line on a probability plot with a linear scale. Similarly, the CDF of a data set with a log-normal distribution plots as a straight line on a probability plot with a logarithmic scale. In the demonstration area, core permeability data are available for 21 wells with a total of 722 measured permeability values. The CDF of the permeability data plot as an almost straight line on log-probability coordinates (fig. 44), an indication that the permeability data in this field have an approximately log normal distribution. The mean and standard deviation of log permeability are 1.036 and 0.805, respectively. The resulting coefficient of variation (0.776) indicates that heterogeneity is of moderate degree (Jensen and Lake, 1988).

### *Autocorrelation*

To determine the autocorrelation structure, vertical semivariograms (Jensen and others, 1997) of permeability and log permeability were plotted for the cored wells. Rescaled range (R/S) plots (Hewett, 1986; Malik, 1996) were also made to investigate the possibility of a power-law or fractal

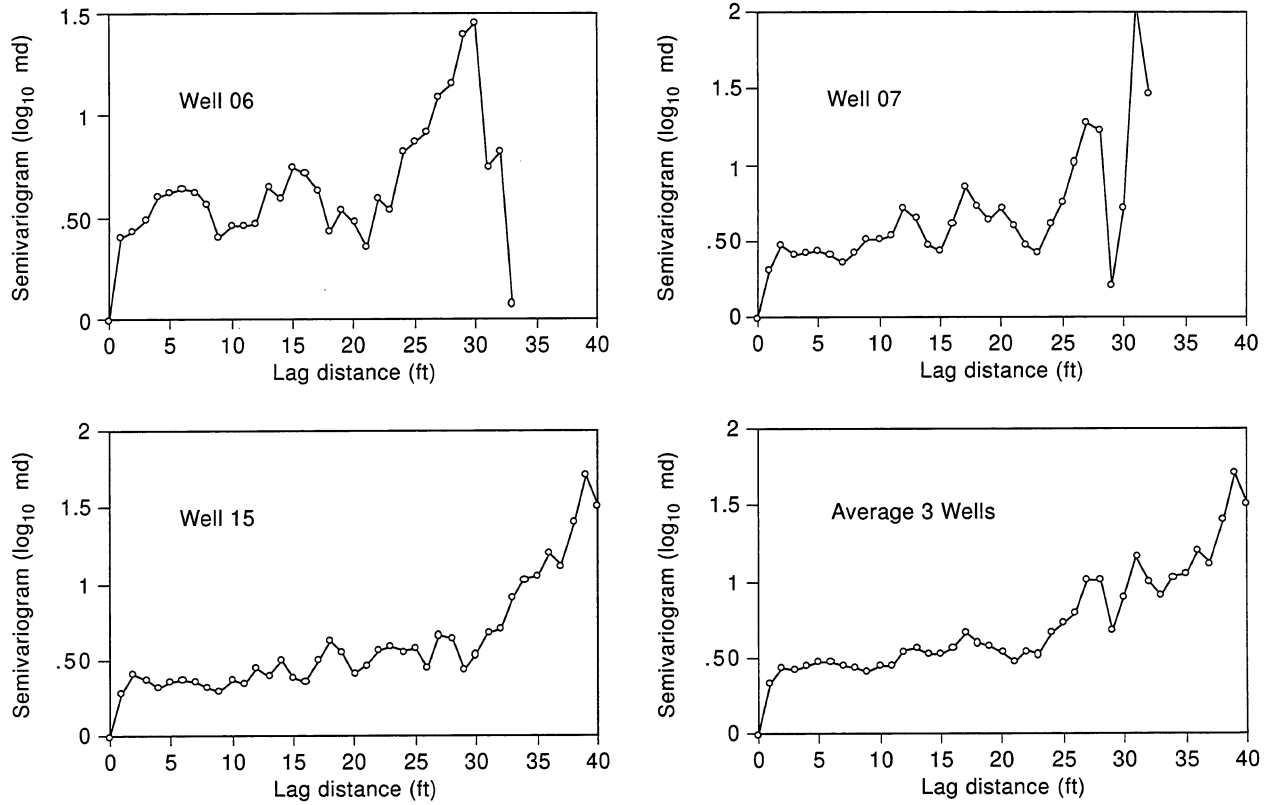


QAb8073c

Figure 44. Cumulative distribution function of core-analysis permeability for 21 wells in the demonstration area.

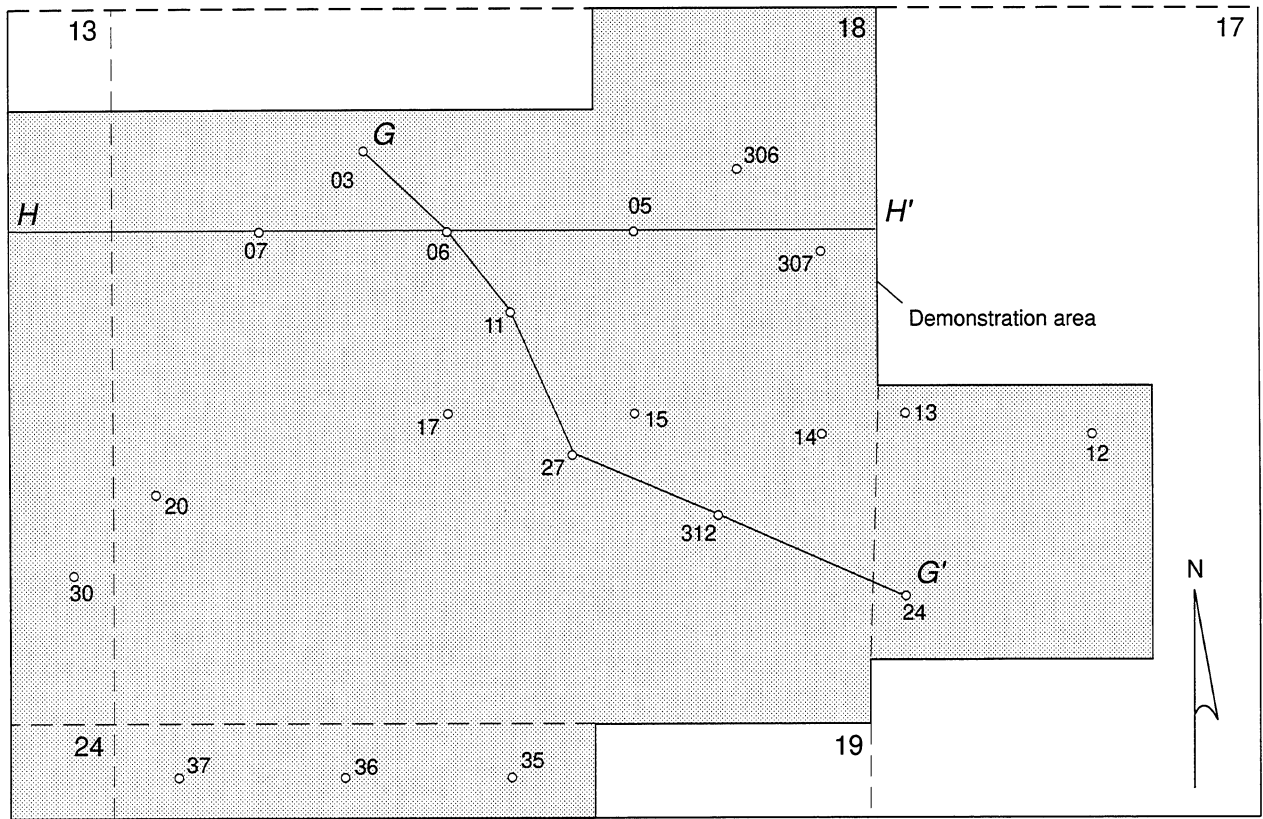
autocorrelation structure. Data in many wells indicated a spherical semivariogram, whereas a few wells appeared to support the possibility of a fractal or power-law semivariogram. The semivariograms of log permeability and their averages for three wells (FGU 6, 7, and 15) are shown in figure 45. These are some of the semivariograms with good structure. For wells FGU 6 and 7 the semivariograms can be interpreted to have approximately spherical autocorrelation structure with a dimensionless range of 0.3. The semivariogram for well FGU 15 has a continuously increasing trend, which is an indication of long-range autocorrelation typical of fractal or power-law semivariograms.

Because the semivariogram analysis did not indicate a well-defined autocorrelation structure, both types of semivariograms were tested in two vertical cross sections, and the resulting permeability distributions were compared with the geologic model of the reservoir. Dimensionless ranges of 0.3 and 0.5 were used for the spherical semivariogram, and intermittency or Hurst coefficients of  $H = 0.16$  fGn and 0.7 fBm (derived from data from two different wells) were used for the power-law semivariogram in these cross sections. Two realizations of cross section G-G' (fig. 46) were generated, one using a spherical semivariogram with a dimensionless range of 0.3, the other with a power-law semivariogram with  $H = 0.7$  fBm. These realizations are log-normal, conditioned by data from wells FGU 3, 6, 11, 27, 312 and 24 (fig. 46). Both realizations are equally probable statistically, but they have to be evaluated with respect to the geology of the reservoir. Both Ramsey 1 and Ramsey 2 sandstones are present in the demonstration area, and between them is the low-permeability SH1 siltstone, which is continuous in the demonstration area. The realization generated with a power-law semivariogram, although quite heterogeneous, is self similar everywhere and does not appear to mimic the dominant geological features. In the realization generated using a spherical semivariogram, however, the low-permeability laminated siltstone within the reservoir is reasonably represented by continuous low permeabilities in the middle horizontal portion. Above and below this unit, the heterogeneity is realistic and extreme values are not predominant. These features are consistent with the characteristics of the two Ramsey sandstones. These observations indicate that a spherical semivariogram with a



QAb8074c

Figure 45. Vertical semivariograms for core-analysis permeability for wells FGU 6, 7, and 15 in the demonstration area, and the average for all three wells. Location of wells shown in figure 46.



○<sup>20</sup> Ford Geraldine unit well number  
 13 Section number

— — Section line

0 ————— 2000 ft  
 0 ————— 609 m

QAb8076c

Figure 46. Map of demonstration area and location of wells used to generate the 3-D permeability distribution. The demonstration area occurs at the northern end of the Ford Geraldine unit.

dimensionless correlation length of 0.3 is the preferable model for geostatistical permeability distribution in this field.

The demonstration area of the field (fig. 46) required 64,720 blocks for 3-D permeability distribution based on a 150 ft block size in each of the two areal directions (x and y) and 1 ft in the vertical (z) direction. A program based on the matrix decomposition method (MDM) (Yang, 1990; Fogg and others, 1991) was used to generate the 3-D permeabilities. This method involves the inversion of a full matrix, which is computationally intensive and time consuming. Therefore, the permeability distributions were generated in separate parts, each consisting of about 10,000 blocks.

#### *Permeability Scale-Up*

Although a block size of  $150 \times 150 \times 1$  ft. is quite gross considering the subcentimeter-scale heterogeneity observed in sandstones, a total of 64,720 blocks is still too large for reservoir flow simulations to be performed economically. The generated permeabilities therefore had to be scaled-up to bring the total number of blocks close to 10,000 for use in fluid-flow simulations.

Several permeability scale-up approaches are mentioned in the literature. They range from simple methods like geometric averaging to more involved techniques such as electrical network analogs (King, 1989). In a comparative study (Malik and Lake, 1997), it has been demonstrated that, with a steady-state flow assumption, direct fine-scale simulation is accurate, flexible, and economical for permeability scale-up. A 2-D code available for this method was adapted for 3-D cases to perform scale-up of the permeabilities generated for the demonstration area. In this method the coarse block is treated as a core and the initial conditions are set to irreducible water saturation in every fine-scale block. Buffer blocks are used at upstream and downstream ends of a coarse block for injection and production. A predetermined pressure drop is imposed to inject oil. Fluid-flow equations are numerically solved for only one time step to determine the single-phase flow rate with steady-state flow assumptions. Effective permeability of the coarse block is determined

from Darcy's law, using the imposed pressure drop, flow rate, flowing phase viscosity, and the length and cross sectional area of the coarse block.

The CDFs of scaled-up permeability and the corresponding fine-scale permeability are compared in figure 47 for a  $40 \times 4 \times 40$  fine-scale block portion of the reservoir along section G–G' (fig. 46). The CDF of core permeability data is also shown for comparison. Although the fine-scale permeabilities have been generated in parts, the CDFs of fine-scale permeabilities compare very well with the core-analysis data. The scaled-up permeability also follows the trend of the fine-scale permeability distribution. The averaging effect of scale-up noticeably affects the permeability values in only a small percentage of coarse blocks at the extreme ends.

Permeability images of scaled-up cross sections retain reasonable heterogeneity after scale-up. The fine-scale vertical cross section is more heterogeneous than the horizontal cross sections. This is consistent with the geology because the reservoirs are generally more heterogeneous vertically than laterally. Overall, the conditionally simulated stochastic permeabilities generated for the demonstration area appear to be in reasonable conformity with the main geologic features of the reservoir.

#### Estimate of Tertiary Recovery from Production Data

To make reliable predictions of tertiary recovery from the demonstration area, fluid-flow simulations of CO<sub>2</sub> flooding were conducted (see section Simulations of Tertiary Recovery). These simulations were based on stochastic permeability distributions and geologic characterization of the reservoir. In addition to the simulations, independent estimates of tertiary recovery from the demonstration area could be made from the available production data and other information about the reservoir.

Original oil in place (OOIP) for areas 1 through 5 (Fig. 4) is plotted in figure 48. Total OOIP is estimated for this analysis to be 83.5 MMbbl (Conoco, 1987). This is a conservative figure because OOIP has been estimated as high as 99 to 110 MMbbl (Conoco, 1987; Pittaway and Rosato, 1991). Figure 49 shows primary, secondary, tertiary, and cumulative recovery

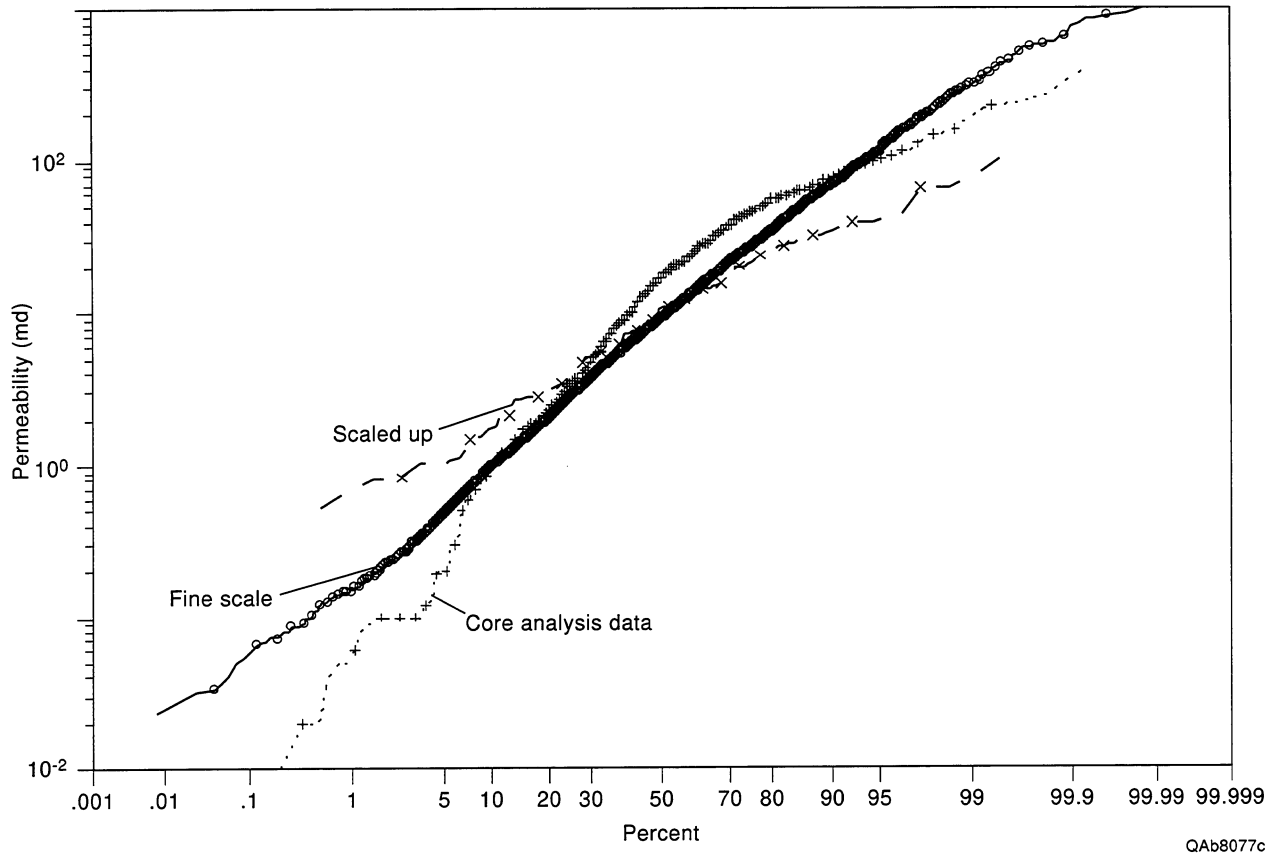


Figure 47. Cumulative distribution functions of permeability from (1) fine-scale permeability distribution, (2) scaled-up permeability distribution, and (3) permeability data from core analyses.

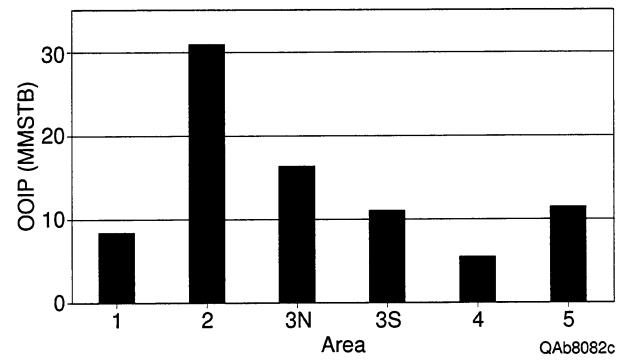


Figure 48. Original oil in place (OOIP) in waterflood areas 1 through 5. Areas are shown in figure 4.

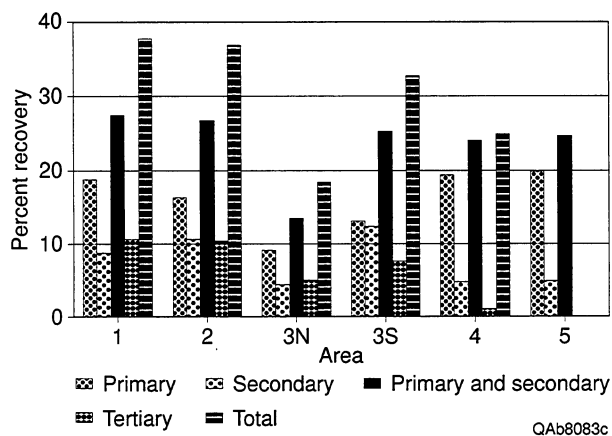


Figure 49. Primary, secondary, primary + secondary, tertiary, and total recovery through December, 1995 as a percentage of original oil in place in areas 1 through 5. Areas are shown in figure 4.

(primary+secondary or primary+secondary+tertiary) by area as a percentage of OOIP, assuming the conservative value of 83.5 MMbbl OOIP. Area 5, the demonstration area, has only primary and minor secondary recovery. Area 3N is the only area with below-average production (fig. 49). The poor performance of this area is probably a result of the anomalous geologic and petrophysical features observed there. The 3N area includes the area of thin Ramsey 1 sandstone (fig. 22), low average porosity (fig. 8) and net pay (fig. 16), and high IP water cut (fig. 42). The primary and secondary recovery performance of the demonstration area is comparable to the other, better producing areas of the reservoir. Post-waterflood oil saturations in the whole reservoir are expected to be similar. Therefore, it is reasonable to assume that the demonstration area will perform similarly to the other areas in tertiary recovery.

Figure 50 shows the overall primary, secondary, and tertiary recovery to December, 1995 in the reservoir as a percentage of the 83.5 MMbbl OOIP. Tertiary recovery does not include the demonstration area. Using the average 7.9-percent tertiary performance of the rest of the reservoir, it is estimated that 904,000 bbl of oil can be recovered from the demonstration area by means of a CO<sub>2</sub> flood (fig. 51). This is probably a conservative estimate; the results of the flow simulations exceed it.

### Simulations of Tertiary Recovery

To estimate the tertiary recovery potential of the demonstration area by another technique, flow simulations were performed for a CO<sub>2</sub> flood. A quarter of a five-spot injection pattern in the demonstration area was selected for flow simulations, and two cases of permeability distribution were considered. In the first case, stochastic permeabilities generated by conditional simulation (Dutton and others, 1997) were used. The simulation grid for this case was  $6 \times 5 \times 8$  (x, y, and z directions, respectively). The second case had layered permeabilities with a  $6 \times 5 \times 6$  grid. The block size was 150 ft in the areal (x and y) directions in both cases. In the vertical (z) direction, the block size was 4 ft for the stochastic case and 5.33 ft for the layered case. In the simulation area, both Ramsey 1 and 2 units are present with an average total thickness of 40 feet. To exclude the

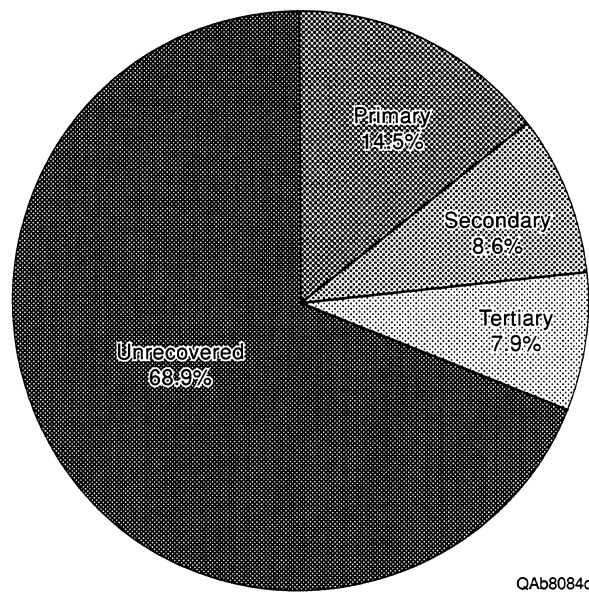


Figure 50. Primary, secondary, and tertiary recovery for all Ford Geraldine unit except area 5.

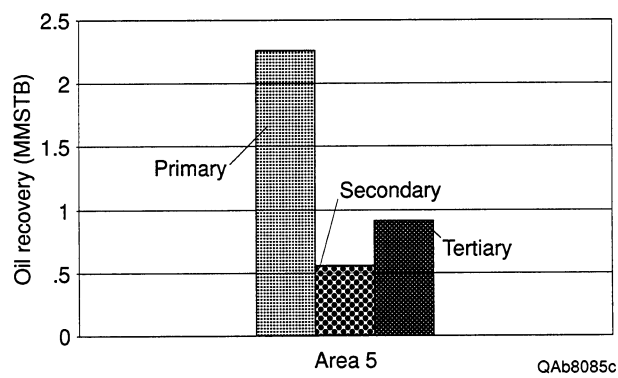


Figure 51. Primary and secondary recovery and project tertiary recovery for area 5.

intermediate silt unit and other smaller shales and silt streaks, total thickness of productive sandstone was assumed to be 32 ft. The stochastic permeabilities were scaled-up to reduce the number of blocks in the z direction from 40 to 8. A permeability cut-off of 5 md was used to exclude the non-producing zones. Maximum permeability was limited to 200 md. The rock compressibility factor used was  $7.499 \times 10^{-6}/\text{psi}$ , and the water compressibility was  $3.15 \times 10^{-6}/\text{psi}$ .

Flow simulations were performed using UTCOMP, an isothermal, three-dimensional, compositional simulator for miscible gas flooding developed at the Department of Petroleum Engineering at The University of Texas at Austin (Chang, 1990). The solution scheme is analogous to IMPES (Implicit Pressure, Explicit Saturations). The equation of state (EOS) is used for flash calculations, phase identification, and fluid property calculations. We have performed three-phase simulations for a CO<sub>2</sub> flood.

Post-waterflood oil saturations in the demonstration area were estimated to be from 35 to 39 percent. An average oil saturation of 37 percent was used for these simulations. An exponential relative permeability model for water, oil, and gas flow was fitted to the measured relative permeability data.

In these simulations, five hydrocarbon components were used. Reservoir hydrocarbons were characterized as four pseudocomponents (Khan, 1992), and their properties were calculated from the PVT (pressure, volume, temperature) data provided by Conoco. The fifth component is CO<sub>2</sub>. Injection pressure is limited to 2000 psia, and production wells have a flowing bottomhole pressure of 600 psia.

### *Simulation Results*

Figure 52a is a plot of oil recovery (fraction of OIP) as a function of time for the two cases. This figure shows breakthrough oil recovery of 28 percent for stochastic permeabilities and 10 percent for layered permeabilities. Unlike a waterflood, these simulations indicate that CO<sub>2</sub> injection results in a gradual increase in recovery even after breakthrough in both cases. Ultimate

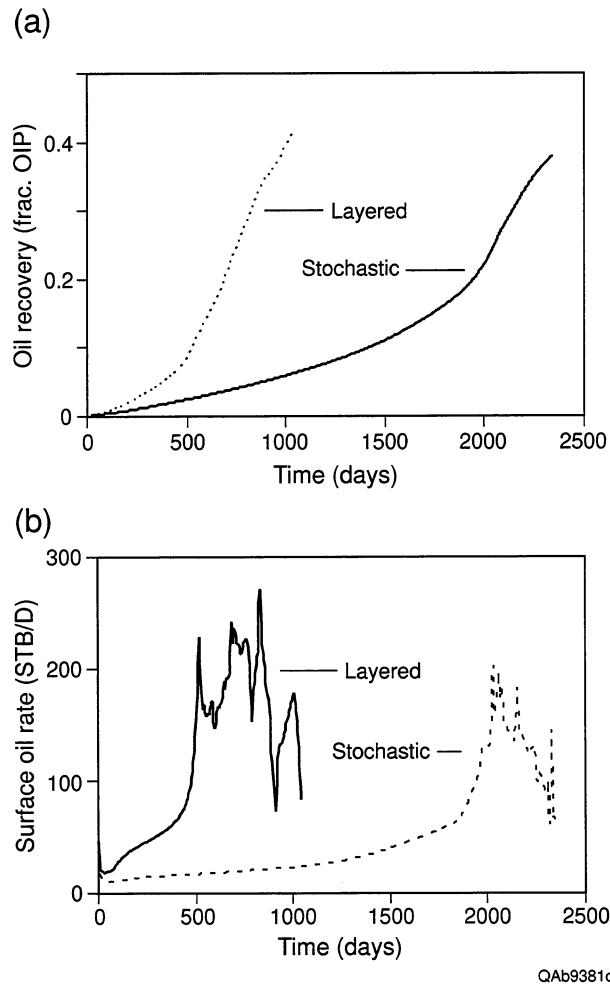


Figure 52. Results of simulation of a CO<sub>2</sub> flood in a quarter five-spot injection pattern in the demonstration area. (a) Oil recovery as a fraction of remaining oil in place. (b) Surface oil production rates.

recovery can exceed 38 percent of OIP. Oil production rates are shown in Fig. 52b. This figure shows a gradual increase in the oil rate until breakthrough. At the time of breakthrough, the oil rate sharply rises to its peak value and gradually declines thereafter. Water-oil ratio (WOR) and gas-oil ratio (GOR) are shown in figure 53. WOR gradually decreases with the progress of the flood and remains low even after breakthrough, but GOR increases sharply after breakthrough. Although the oil rates are quite high for some time after breakthrough (Fig. 52a), the limiting factor in a CO<sub>2</sub> flood may be the excessive gas production.

Depending on various cut-off criteria, estimates of original oil in place (OOIP) in the demonstration area vary from 12.9 to 18.67 MMbbl (Conoco, 1987). Approximately 2.83 MMbbl of oil has been produced through primary depletion and secondary waterflood in this area. Based on the most conservative estimate of OOIP (12.9 MMbbl), post-waterflood OIP in the demonstration area is in excess of 10 MMbbl. Results of the simulations indicate that a minimum of 10 percent of the remaining OIP (1.0 MMbbl) is recoverable through CO<sub>2</sub> flood. This more conservative estimate is based on the breakthrough recovery of a layered model. The stochastic permeability model shows a breakthrough recovery of more than twice this estimate (fig. 53a). If the increased gas production after breakthrough can be handled economically, ultimate CO<sub>2</sub> flood recovery may exceed 30 percent of remaining OIP.

## ENVIRONMENTAL INFORMATION

Surface elevation of the Ford Geraldine unit varies from 2,867 to 3,154 ft above sea level. The surface consists of dry plains with scrubby vegetation. The site is more than 5 mi from navigable surface water and more than 20 mi from air quality non-attainment areas. The Cenozoic Pecos Aquifer crops out in the western part of Reeves County, and has a maximum thickness of 200 to 300 ft. Water from this aquifer contains dissolved-solids concentrations ranging from less than 300 mg/L to more than 5,000 mg/L (Ashworth and Hopkins, 1995). The Rustler Aquifer crops out in eastern Culberson and westernmost Reeves Counties; it has maximum thickness of about 520 ft. Water from the Rustler is used for irrigation, livestock, and oil-field water-flooding

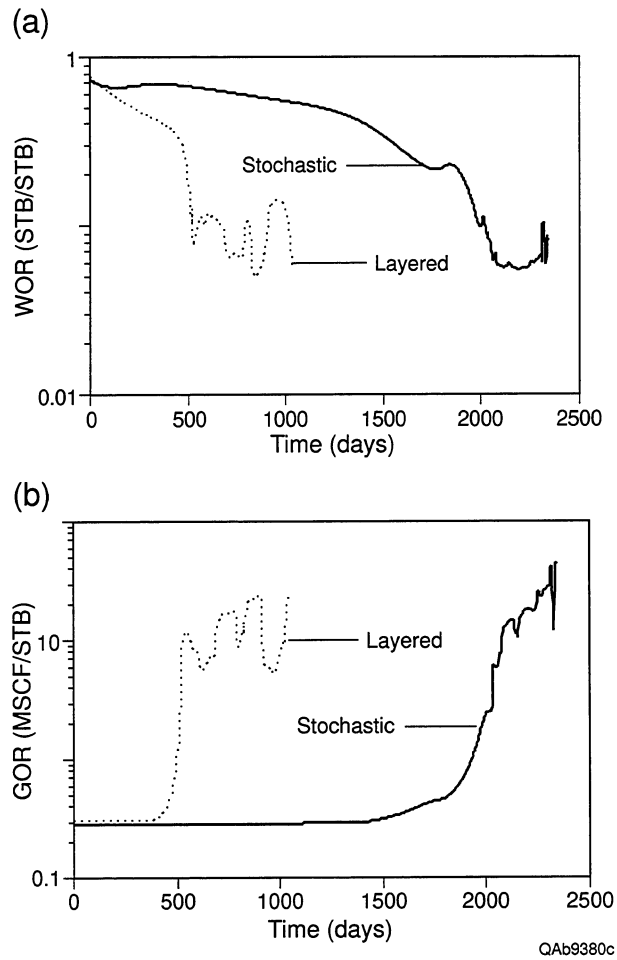


Figure 53. Results of simulation of a CO<sub>2</sub> flood in a quarter five-spot injection pattern in the demonstration area. (a) Surface water/oil ratio (WOR). (b) Surface gas/oil ratio (GOR).

operations, but it is not used for human consumption because of high dissolved-solids concentrations (Ashworth and Hopkins, 1995). Depth of surface casing in Ford Geraldine unit varies from 200 to 400 ft. A total of 117,505,854 barrels of water have been produced from Geraldine Ford field since October, 1960. The water is reinjected at a depth of 2,600 ft, back into the Ramsey.

## CONCLUSIONS

Flow simulations were performed using UTCOMP, an isothermal, three-dimensional, compositional simulator for miscible gas flooding. Results indicate that 10 to 30 percent (1 to 3 MMbbl) of remaining oil in place can be produced by CO<sub>2</sub> injection. High volumes of water production are a potential constraint on further producibility from the demonstration area at the northern end of the Ford Geraldine unit. This reservoir had a high initial water saturation of 46 percent at discovery. Many wells were fractured during well completion, and some of the fractures may have penetrated the water zone. There is evidence that aquifer water has also encroached into the demonstration area. As a result of these factors, the produced water-cut toward the end of primary depletion was very high in the demonstration area, and secondary recovery by waterflood was neither effective nor economical. It is likely that the reservoir can only be further produced by an improved recovery process like a CO<sub>2</sub> flood.

The other main constraint on producibility of the Ford Geraldine unit is the geologic heterogeneity of the reservoir, which is caused by a combination of depositional and diagenetic processes. Laminated siltstone beds and extensively calcite-cemented sandstones are the most important causes of reservoir complexity and reduced sweep efficiency. A laminated siltstone that is continuous across the northern part of the unit subdivides the Ramsey reservoir into two sandstones. These sandstones are in turn further subdivided by smaller siltstones that are of sufficient extent to be correlated in several wells. The calcite-cemented zones apparently are not large enough to correlate between wells, but the complexity that they add to the reservoirs probably contributes to reduced sweep efficiency.

In the first phase of this project, detailed geological and engineering characterization of the reservoir was completed and provided a better understanding of the reservoir parameters. Oil-bearing portions of the formation were identified, and current fluid saturations were determined. A conditionally simulated permeability model was also generated. Simulation studies were performed under conservative but realistic conditions for CO<sub>2</sub> flood. Results indicate that 10 to 30 percent (1 to 3 MMbbl) of remaining oil in place can be produced by CO<sub>2</sub> injection. The simulation also indicates that water production will be much lower than during waterflood. To further reduce the potential problem of high water production, it is recommended that the CO<sub>2</sub> flood be confined to the northern part of the Stage 5 area to avoid the part of the area in section 19 that has experienced high water cuts and low productivity.

To minimize the impact of geologic heterogeneity, CO<sub>2</sub> should be injected into both of the Ramsey sandstones, above and below the widespread siltstone. The highest average porosity and permeability in the Ramsey 2 sandstone follows the trend of the channel that cuts through the eastern side of the Stage 5 area. This trend of higher permeability should be taken into account when determining the injection rates in wells that penetrate the channel so that lower injection rates may be used where a line of injectors crosses the channel trend. The goal is to avoid rapid breakthrough of CO<sub>2</sub> along high permeability pathways.

#### ACKNOWLEDGMENTS

This research was funded by the U. S. Department of Energy under contract no. DE-FC22-95BC14936, by Conoco, Inc., and by the State of Texas under State Match Pool Project 4201 and as part of the State of Texas Advanced Resource Recovery project. The Bureau of Economic Geology acknowledges support of this research by Landmark Graphics Corporation via the Landmark University Grant Program. Susan Hovorka and Edgar Guevara contributed to the early stages of this project. Research was assisted by Carlos Amaya, Radu Boghici, Janaka Paulus, and Mohammad Razi, whose hard work is gratefully acknowledged. Earlier studies of Bell Canyon reservoirs by M. H. Gardner, R. W. Ruggiero, and C. R. Williamson provided the foundation for

the present study. Drafting was by the Graphics staff of the Bureau of Economic Geology under the direction of Joel L. Lardon. Others contributing to the publication of this report were Susan Lloyd, word processing and pasteup, and Christopher LeCluyse, editing.

## REFERENCES

- Ashworth, J. B., and Hopkins, J., 1995, Aquifers of Texas: Texas Water Development Board Report No. 345, 69 p.
- Asquith, G. B., in press, Petrophysics of the Ramsey sandstone, Ford Geraldine Unit, Reeves and Culberson Counties, Texas, *in* 1997 West Texas Geological Society Fall Symposium.
- Asquith, G. B., Thomerson, M. D., and Arnold, M. D., 1995, The recognition of possible oil and water wettability changes in the Permian Delaware Mountain Group sandstones from petrophysical well logs, *in* R. L. Martin, ed., In Search of New Permian Basin Oil and Gas Fields: West Texas Geological Society Fall Symposium, Publication No. 95-98, p. 39-50.
- Barton, M. D., 1997, Basin floor fan and channel-levee complexes, Permian Bell Canyon Formation: 1997 AAPG Annual Convention, Dallas, Texas, Official Program, v. 6, p. A9.
- Berg, R. R., 1979, Reservoir sandstones of the Delaware Mountain Group, southeast New Mexico, *in* Sullivan, N. M., ed., Guadalupian Delaware Mountain Group of west Texas and southeast New Mexico, 1979, Symposium and Field Trip Conference Guidebook: SEPM (Permian Basin Sec.) Pub. 79-18, p. 75-95.
- Chang, Yih-Bor, 1990, Development and application of an equation of state compositional simulator: The University of Texas at Austin, Ph.D. dissertation, 502 p.
- Conoco, 1979, Ford Geraldine CO<sub>2</sub> Project, Internal Report, variously paginated.

- Conoco, 1987, Revised reservoir description for the Ford-Geraldine unit, Culberson and Reeves Counties, Texas, Internal Report, variously paginated.
- Dewan, J. T., 1984, Essentials of Modern Open-Hole Log Interpretation: Tulsa, Oklahoma, PennWell Publishing Co., 345 p.
- Dutton, S. P., Asquith, G. B., Barton, M. D., Cole, A. G., Gogas, J., Malik, M. A., Clift, S. J., and Guzman, J. I., 1997, Application of advanced reservoir characterization, simulation, and production optimization strategies to maximize recovery in slope and basin clastic reservoirs, West Texas (Delaware Basin): The University of Texas at Austin, Bureau of Economic Geology, draft annual report prepared for the U.S. Department of Energy under contract no. DE-FC22-95BC14936, 187 p.
- Dutton, S. P., Barton, M. D., Clift, S. J., Guzman, J. I., and Cole, A. G., in press, Depositional history of Ramsey sandstone channel-levee and lobe deposits, Bell Canyon Formation, Ford Geraldine Unit, West Texas (Delaware Basin), *in* West Texas Geological Society Fall Symposium.
- Dutton, S. P., Hovorka, S. D., and Cole, A. G., 1996, Application of advanced reservoir characterization, simulation, and production optimization strategies to maximize recovery in slope and basin clastic reservoirs, West Texas (Delaware Basin): The University of Texas at Austin, Bureau of Economic Geology, annual report prepared for the U.S. Department of Energy under contract no. DOE-BC14936-5, 81 p.
- Fischer, A. G., and Sarnthein, M., 1988, Airborne silts and dune-derived sands in the Permian of the Delaware Basin: *Journal of Sedimentary Petrology*, v. 58, p. 637-643.
- Fogg, G. E., Lucia, F. J., and Senger, R. K., 1991, Stochastic simulation of interwell-scale heterogeneity for improved prediction of sweep efficiency in a carbonate reservoir, *in* Lake,

- L. W., Carroll, H. B., Jr., and Wesson, T. C., eds., Reservoir characterization II: San Diego, Academic Press, p. 355–381.
- Folk, R. L., 1974, Petrology of sedimentary rocks: Austin, Texas, Hemphill, 182 p.
- Gardner, M. H., 1992, Sequence stratigraphy of eolian-derived turbidites: patterns of deep water sedimentation along an arid carbonate platform, Permian (Guadalupian) Delaware Mountain Group, West Texas, *in* Mruk, D. H., and Curran, B. C., eds., Permian Basin exploration and production strategies: applications of sequence stratigraphic and reservoir characterization concepts: West Texas Geological Society Publication No. 92-91, p. 7-12.
- Gardner, M. H., 1997, Reservoir characterization of deep-water siliciclastic reservoirs in the upper Bell Canyon and Cherry Canyon Formations of the northern Delaware Basin, West Texas, *in* Major, R. P., ed., Oil and gas on Texas State Lands: an assessment of the resource and characterization of type reservoirs: The University of Texas at Austin, Bureau of Economic Geology Report of Investigations No. 241, p. 137-146.
- Green, K. M., Frailey, S. M., and Asquith, G. B., 1996, Laboratory analysis of the clays within the Brushy Canyon Formation and their reservoir and petrophysical implications: Red Tank Field, Lea County, New Mexico, *in* DeMis, W. D., and Cole, A. G., eds., The Brushy Canyon Play in Outcrop and Subsurface: Concepts and Examples: Permian Basin Section SEPM, Publication No. 96-38, p. 165-171.
- Hewett, T. A., 1986, Fractal distributions of reservoir heterogeneity and their influence on fluid transport: SPE Annual Fall Meeting, New Orleans, LA, Paper SPE 15386.
- Hills, J. M., 1984, Sedimentation, tectonism, and hydrocarbon generation in Delaware Basin, west Texas and southeastern New Mexico: American Association of Petroleum Geologists Bulletin, v. 68, p. 250-267.

- Hills, J. M., and Kottowski, F. E., 1983, Southwest/southwest mid-continent region correlation chart: American Association of Petroleum Geologists Correlation Chart Series.
- Hiss, W. L., 1975, Stratigraphy and groundwater hydrology of the Capitan aquifer, southeastern New Mexico and western Texas: University of Colorado, Ph.D. dissertation, 396 p.
- Jensen, J. L. and Lake, L. W., 1988, The influence of sample size and permeability distribution upon heterogeneity measures: SPE Reservoir Engineering, v. 3, p. 629-637.
- Jensen, J. L., Lake, L. W., Corbett, P. W. M., and Goggin, D. J., 1997, Statistics for petroleum engineers and geoscientists: Upper Saddle River, New Jersey, Prentice Hall, 390 p.
- Journel, A. G. and Huijbregts, C. J., 1978, Mining Geostatistics, Academic Press, San Diego, CA., 600 p.
- Kerans, C., Fitchen, W. M., Gardner, M. H., Sonnenfeld, M. D., Tinker, S. W., and Wardlaw, B. R., 1992, Styles of sequence development within uppermost Leonardian through Guadalupian strata of the Guadalupe Mountains, Texas and New Mexico, *in* Mruk, D. H., and Curran, B. C., eds., Permian Basin exploration and production strategies: applications of sequence stratigraphic and reservoir characterization concepts: West Texas Geological Society Publication No. 92-91, p. 1-6.
- Khan, S. A., 1992, An expert system to aid in compositional simulation of miscible gas flooding: The University of Texas at Austin, Ph.D. dissertation.
- King, P. R., 1989, The use of renormalization for calculating effective permeability: Transport in Porous Media, v. 4, p. 37-58.
- Kneller, B., 1996, When is a turbidity current not a turbidity current? A question of mobility? (abs.): AAPG Annual Convention, San Diego, Official Program, v. 5, p. A76.

- Lake, L. W. and Malik, M. A., 1993, Modeling fluid flow through geologically realistic media, *in* North, C. P., and Prosser, D. J., eds., *Characterization of Fluvial and Aeolian Reservoirs*, Geological Society Special Publication, The University of Aberdeen, p. 367–375.
- Lowe, D. R., 1982, Sediment gravity flows: II. Depositional models with special reference to the deposits of high-density turbidity currents: *Journal of Sedimentary Research*, v. 52, p. 279-297.
- Malik, M. A., 1996, Geostatistical reservoir characterization and scale-up of permeability and relative permeabilities: The University of Texas at Austin, Ph.D. dissertation, 174 p.
- Malik, M. A., and Lake, L. W., 1997, A practical approach to scaling-up permeability and relative permeabilities in heterogeneous permeable media: Society of Petroleum Engineers, Proceedings, SPE Western Regional Meeting, Paper SPE 38310, p. 485-500.
- Mutti, E., and Normark, W. R., 1987, Comparing examples of modern and ancient turbidite systems: problems and concepts, *in* Leggett, J. K., and Zuffa, G. G., eds., *Marine Clastic Sedimentology: Concepts and Case Studies*: London, Graham and Trotman, p. 1-38.
- Pittaway, K. R., and Rosato, R. J., 1991, The Ford Geraldine unit CO<sub>2</sub> flood—update 1990: Society of Petroleum Engineers Reservoir Engineering, v. 6, no. 4, p. 410-414.
- Ruggiero, R. W., 1985, Depositional history and performance of a Bell Canyon sandstone reservoir, Ford-Geraldine field, west Texas: The University of Texas at Austin, Master's thesis, 242 p.
- Ruggiero, R. W., 1993, Depositional history and performance of a Permian Bell Canyon sandstone reservoir, Ford-Geraldine field, West Texas, *in* Rhodes, E. G., and Moslow, T. F., eds., *Marine Clastic Reservoirs*: New York, Springer-Verlag, p. 201-229.

- Thomerson, M. D., 1992, Petrophysical Analysis of the Brushy Canyon Formation, Hat Mesa Delaware Field, Lea County, New Mexico: Texas Tech University, Master's thesis, 124 p.
- Walling, S. D., 1992, Authigenic clay minerals in sandstones of the Delaware Mountain Group: Bell Canyon and Cherry Canyon Formations, Waha Field, West Texas: Texas A & M University, Master's thesis, 63 p.
- Williamson, C. R., 1978, Depositional processes, diagenesis and reservoir properties of Permian deep-sea sandstones: Bell Canyon Formation, Texas-New Mexico: The University of Texas at Austin, Ph.D. Dissertation, 262 p.
- Yang, An-Ping, 1990, Stochastic heterogeneity and dispersion: The University of Texas at Austin, Ph.D. Dissertation, 241 p.

## APPENDIX A

The information in this report is supplemented by electronic and hard-copy data. Electronic data have been transferred to:

Mr. Jerry Casteel  
National Petroleum Technology Office  
U.S. Department of Energy  
P.O. Box 3628  
Tulsa, OK 74101

The electronic data consist of the following:

1. Well-history data

Well depth  
Perforated zones  
Completion type  
Completion date  
Stimulation type  
Cored intervals  
Status (water injector, oil producer, etc.)

2. Cumulative production per well

Status  
Water saturation  
Primary oil recovery  
Secondary oil recovery  
Tertiary recovery  
Total recovery through December, 1995  
Estimated pattern pore volume  
Estimated original oil in place  
Date of initial potential (IP) test  
IP barrels oil per day  
IP gas/oil ratio  
Ramsey sandstone thickness

3. Well conversion dates

Core depths

Timing of new wells drilled

Producers

Water injection

CO<sub>2</sub> injection

Timing of old wells converted

Water injection

CO<sub>2</sub> injection

Disposal wells

Status

4. Latitude and longitude for each well

5. Stratigraphic tops

Kelly bushing

Top Lamar limestone

Top Lamar condensed section

Top Trap siltstone

Top Trap condensed section

Top Ramsey 2 sandstone

Top SH1 siltstone

Top Ramsey 1 sandstone

Top Ford siltstone

Top Ford condensed section

Top Olds sandstone

6. Digitized logs for all wells

7. Core-analysis data

Well

Depth

Permeability

Porosity

Water saturation

Oil saturation

Hard-copy data has been transferred to:

Mr. Jerry Casteel  
National Petroleum Technology Office  
U.S. Department of Energy  
P. O. Box 3628  
Tulsa, OK 74101

The hard-copy data consist of the following:

1. Core descriptions
2. Special core-analysis data

Electrical properties  
Drilling mud resistivity measurements  
Capillary pressure curves  
Injectivity tests  
Laboratory waterflood summary  
Oil-water relative permeability data  
Oil-gas relative permeability data

3. Analysis of reservoir fluids

Hydrocarbon analyses  
PVT data  
Viscosity data  
Solubility and swelling test data  
Miscibility-displacement-test data

4. Representative seismic section
5. Seismic interpretations



